AN EXPERIMENTAL AND ANALYTICAL STUDY OF HEAT TRANSFER TO POLYMER SOLUTIONS IN TURBULENT PIPE FLOWS UNDER CONSTANT WALL HEAT FLUX

By

HYUNG KEE YOON
Bachelor of Engineering
Korea University
Seoul, Korea
1980

Master of Science
Oklahoma State University
Stillwater, Oklahoma
1982

Submitted to the Faculty of the Graduate College
of the Oklahoma State University
in partial fulfillment of the requirements
for the Degree of
DOCTOR OF PHILOSOPHY
December, 1986

AN EXPERIMENTAL AND ANALYTICAL STUDY OF HEAT TRANSFER TO POLYMER SOLUTIONS IN TURBULENT PIPE FLOWS UNDER CONSTANT WALL HEAT FLUX

Thesis Approved:

A. J. Ghajar

Thesis Adviser

F. O. Thomas

Mayis Seapan

Robert W. Morrell

Norman N. Durham

Dean of the Graduate College

ACKNOWLEDGMENTS

I would like to thank my adviser, Dr. A. J. Ghajar, for his advice, encouragement, and guidance throughout this study. I would also like to thank Dr. P. M. Moretti, Dr. F. O. Thomas, and Dr. M. Seapan for their valuable comments and discussion.

This study was supported by the School of Mechanical and Aerospace Engineering and University Center for Energy Research (UCER) at Oklahoma State University. I would appreciate Mr. K. Toh and Mr. M. Azar for their helpfulness in the technical and experimental phases of this project. I would like to express my compliment to Daleene Caldwell for typing the final manuscript.

I would like to express my sincere gratitude to Mr. and Mrs. Hyung Bok Yoon, and Mr. and Mrs. Chong Sun Cha for their financial support and encouragement. I am most grateful to Mr. and Mrs. In Shik Yoon, my loving daughters, Susan and Hanna, and my wife, Moonsook, for their love and prayer. This work is dedicated to them.

TABLE OF CONTENTS

LIST OF TABLES

LIST OF FIGURES

Figure Page

NOMENCLATURE

English Letters

A^+	constant that characterizes thickness of wall layer
C_p	specific heat of fluid
D	tube diameter or diffusion coefficient
DR	drag reduction ratio, DR = f_p/f_s
F	turbine meter frequency
f	Fanning friction factor, $f = \tau_w/\frac{1}{2}\rho U^2$
f_p	friction factor for polymer
f_s	friction factor for solvent
FR	friction drag reduction ratio, FR = $(f_s - f_p)/f_s$
h	heat transfer coefficient
H	difference in elevation of two-fluid manometer interface
HR	heat transfer reduction ratio, HR = $j_{h,p}/j_{h,s}$
j_h	Colburn j-factor, $j_h = St\ Pr_a^{2/3}$
$j_{h,p}$	Colburn j-factor for polymer
$j_{h,s}$	Colburn j-factor for solvent
K	von Karman constant
K_f	thermal conductivity of fluid
K_s	thermal conductivity of tube
L	tube length
L_h	heated tube length
L_p	distance between pressure taps

Nu	Nusselt number, $Nu = hD/K_f$
P	pressure
Pr_a	Prandtl number based on the apparent viscosity, $Pr_a = \eta_a C_p/K_f$
$\dot{Q}$	volume flow rate
$\dot{q}$	heat flow rate
r	radial distance from the centerline
R	radius or electrical resistance of tube
r^+	dimensionless radius, $r^+ = ru_\tau/\nu$
Re_a	Reynolds number based on the apparent viscosity, $Re_a = \rho UD/\eta_a$
Sc	Schmidt number, $Sc = \nu/D$
St	Stanton number, $St = Nu/(Pr_a Re_a)$
T	temperature
T_b	local fluid bulk temperature
T_e	bulk exit temperature
T_i	bulk inlet temperature
T_w	local wall temperature
u	local time-mean axial velocity
$u+$	dimensionless mean velocity, $u+ = u/u_\tau$
u'	axial fluctuating velocity
U	local bulk axial velocity
u_τ	shear velocity, $u_\tau = (\tau_w/\rho)^{1/2}$
v'	radial fluctuating velocity
Ws	Weissenberg number, $Ws = \lambda U/D$
Ws_{cf}	critical Weissenberg number for momentum transfer
Ws_{ch}	critical Weissenberg number for heat transfer
x	local axial distance
y	radial distance from the wall

y^+	dimensionless radial distance from the wall, $y^+ = yu_\tau/\nu$
y_1^+	dimensionless thickness of the laminar sublayer
y_2^+	dimensionless thickness of the transition zone

Greek Letters

$\dot{\gamma}$	shear rate
ε_h	eddy diffusivity of heat
ε_m	eddy diffusivity of momentum
η	steady shear viscosity
η_a	apparent viscosity at the wall
η_0	zero shear rate viscosity
η_∞	infinite shear rate viscosity
θ	dimensionless temperature difference, $\theta = (T_w - T_b)x/D/(T_w - T_b)exit$
λ	fluid time scale
ρ	density of fluid
τ	shear stress
ν	kinematic viscosity
Ω	characteristic frequency, $\Omega = U/D \cdot Re_a^{0.75}$

Subscripts

a	based on apparent viscosity
b	bulk
c	centerline
cr	critical
e	exit
exp.	experimental

f	related to fluid
h	heat transfer
L	evaluated at the edge of the viscous sublayer
i	inlet or inside
m	momentum transfer
o	outside
p	polymer
pred.	predicted
s	solvent
w	evaluated at the wall
wi	inside of the wall
wo	outside of the wall

CHAPTER I

INTRODUCTION

It has been recognized that small addition of certain polymers to a turbulent flow can produce a very significant reduction in friction drag and heat transfer. Since the resulting fluids possess both viscous and elastic characteristics, they are classified into viscoelastic fluids. Numerous studies have been conducted to clarify this phenomenon, but no solid theory that can fully explain it and accurately predict its characteristics has been established [1, 2]. The current study is aimed to elucidate the effects of polymers on water flowing turbulently in circular pipes under the constant wall heat flux condition via carefully designed experiments and numerical analyses. This chapter is devoted to the descriptions of the background, the specific areas in need of research, and the objectives and method of approach of the work.

1.1 Background

There is high interest in the possible use of polymer additives in the liquid natural resource transport systems; in liquid and solid transport in pipe-lines; in hydraulic fracturing processes for petroleum industries; in fire fighting systems; on the surfaces of torpedoes and ships; and on rotating surfaces of hydraulic machines. Viscoelastic fluids also play a role in the chemical, biochemical and food processing industries since many of the industrial chemicals and fluids are

viscoelastic in nature. Furthermore, they often undergo heat exchange processes during preparation or in their application. An understanding of the fluid mechanics and heat transfer behavior of such fluids is necessary if engineering systems are designed to accommodate their unique characteristics.

Many attempts have been made to illuminate the effects of polymers on the behaviors of momentum and heat transfer. However, recent major reviews of the relevant works [1, 2] suggested that most of the previous experimental studies have been carried out without taking into account all of the following important factors: 1) thermal entrance length [3-6], 2) pipe diameter [6, 7], 3) solvent chemistry [8-11], 4) polymer degradation [11-15], 5) temperature dependent fluid properties [1, 2], and 6) polymer rheology [16-22]. Table I summarizes the experimental conditions of the previous experiments. These experimental deficiencies resulted in unreliable data bases which have been used to interpret the flow mechanisms for viscoelastic turbulent flows. Subsequently, the experimental investigators supplied the analytical investigators incorrect information, causing them to develop inadequate heat transfer models for drag reducing turbulent pipe flows. The existing heat transfer models do not have general predictive capability for various polymer solutions with wide ranges of concentrations throughout the flow field [23-26]. These models generally fall into two categories: 1) models that use a direct analogy to correlate heat and momentum transfer phenomena (see Table II); and 2) models that are valid only for a particular polymer concentration, mostly for the maximum heat transfer reduction asymptotic case. New analytical studies should be conducted to remedy the inadequacy of the existing heat transfer models for

TABLE I

EXPERIMENTAL STUDIES OF HEAT TRANSFER IN DRAG REDUCING TURBULENT PIPE FLOWS

Year	Investigator(s)	Polymer concentration (ppm)	Pipe diameter (in.)	Reynolds numbers	Prandtl numbers	T_w (°F)	T_b (°F)	L/D	Heat transfer mode[a]	Friction mode[b]
1966 1967	Marrucci & Astarita[c] Astarita & Marrucci[c]	ET 597: 600, 1000	0.472	$Re=6x10^3$ - $6x10^4$	?	?	?	100	CT	ZHF
1966 1967	Gupta[c] Gupta, et al.[c]	ET 597: 100, 500, 4500	0.745	$Re=7x10^2$ - $9.2x10^4$	Pr_b=7-12: 80-90	103-182	75-95	2-40	CF	ZHF
1968	McNally[c]	WSR 301: 2, 10, 20	0.78	$Re_f=2.5x10^4$ - $2.5x10^5$	Pr_f=2.5-2.8	190-199	~140	52	CT	ZHF
1969	Smith, et al.[c]	WSR 301: 10 WSR N3000: 10,100, 1000	0.117	$Re_b=5x10^2$ - $2.5x10^4$	Pr_b=6-9	98-102	78-80	18	CF	SIM
1970	Corman[c]	Guar Gum: 50, 100, 200, 300, 600, 1200, 2400	0.62 0.92	$Re'=7x10^3$ - $9x10^4$	?	?	70-90	78, 116	CF	SIM
1970 1973	Khabakhpasheva, et al[c]	Polyox: 70 Polyacrylamide: 120	0.39	$Re_b=10^3$ - $3.1x10^4$	Pr_b=6.5-9.0	~93	~84	60	CF	?
1971	Howard [12]	Polyox WSR301: 5, 12.5,50,100,200,500 Polyhall M295: 5, 12.5,50,100,200,500	0.5	$Re=10^4$ - 10^5	?	?	65	60	CF	ZHF
1972	Monti[c]	ET 597: 250, 750, 1000,2000,4000,6000	0.423	$Re'=6x10^3$ - $6x10^4$	?	?	?	~40	CF	?

TABLE I (Continued)

1974	Debrule [27]	Polyox: 10, 50	0.377	$Re_b=2x10^4-2x10^5$	$Pr_b=4.4-10$	T_b+5	48 - 103	40	CF	ZHF
1974	Yoo [28]	Separan AP-30: 100, 500, 1000, 1500 WSR 301: 1000, 2000 Polyhall-654: 1000, 1500	0.87	$Re_a=3x10^3-10^4$	$Pr_a=6-80$	75 - 80	105 - 115[d]	5 - 110[d]	CF	ZHF
1975	Yoo & Hartnett [3]	Separan AP-30: 1000	0.87	$Re_a=4.87x10^4-8.18x10^4$	$Pr_a=11.1-17.7$	82 - 125	70 - 80	110	CF	ZHF
1975	Mizushina, et al [4]	P.E.O.: 5, 20, 50, 100, 200	1.0	$Re=3x10^3-3.5x10^4$	Pr=6-10	?	?	160	CF	?
1978	Tung, et al[29]	Separan AP-273: 2500	0.886	$Re'=3x10^2-1.5x10^4$	?	?	75 ± 2	?	CF	ZHF
1979	Ng & Hartnett [30]	Separan AP-273: 1500	0.886	$Re'=1.5x10^4-1.9x10^4$	?	?	75 ± 2	285	CF	SIM
1980	Cho, et al [31]	Separan AP-273: 1500, 2000 WSR-301: 3500, 4500, 5000 FRA: 3000	0.386 0.512 0.886	$Re'=10^3-4x10^4$	$Pr_a=40$	?	71-75	450	CF	SIM
1981	Kwack, et al [6]	Separan AP-273: 5,10, 20,30,100,500,1000	0.384 0.512	$Re_a=2x10^3-10^5$	$Pr_a=6.25-13.68$	78-81	71-75	430	CF	SIM
1982	Ng [25]	Separan AP-273: 1500, 2000 WSR-301: 3500, 4500, 5000 FRA: 3000	0.386 0.512 0.886	$Re'=10^3-4x10^4$	$Pr_a=25-40$	T_b+8 $-T_b+15$	73-104	282-648	CF	SIM
1983	Kwack [26]	Separan AP-273: 5, 10, 20, 30, 50, 100, 300, 500, 1000	0.386 0.512	$Re_a=7x10^3-10^5$	$Pr_a=6.5-25$	?	?	280-620	CF	SIM

[a] CT, constant wall temperature mode; CF, constant wall heat flux mode.

[b] ZHF, SIM friction is measured at zero heat flux (ZHF) or simultaneously with St (SIM).

[c] Taken from reference [1].

[d] Reported only for measurements in the entrance region.

TABLE II

ANALYTICAL STUDIES OF HEAT TRANSFER IN DRAG REDUCING TURBULENT PIPE FLOWS

Year	Investigator(s)	Heat Transfer Mode[a]	Momentum Eddy Diffusivity Model	Basic Hypothesis: Reynolds Analogy	Basic Hypothesis: Constant Property	Other Approach
1967	Poreh and Paz [13]	CF		X	X	$u^+ = y^+$ $0 < y^+ < y_1^+$ $u^+ = y_1^+ \ln(y^+/y_1^+) + y_1^+$ $y_1^+ < y^+ < y_2^+$ $u^+ = 2.5 \ln(y^+/y_j^+) + y_j^+$ $y_2^+ < y^+ < r_0^+$
1968	Wells, Jr. [32]			X	X	$St = \dfrac{f/2}{\frac{U_L}{U_\tau}1.02(f/2)^{1/2}(Pr-1)Pr^{-1/3}+1.2}$
1971	Hughmark [14]		$\varepsilon_m/\nu = 0.000067y^{+3}$	X	X	
1973	Debrule and Sabersky [27]	CF	$\varepsilon_m/\nu = n^2 u^+ y^+[1 - \exp(-n^2 u^+ y^+)]$	X	X	
1975 1977	Mizushina, et al [33] Mizushina, et al [4]		$\varepsilon_m/\nu = f(y^+, R^+)^2 D f_m^2 \dfrac{du^+}{dy^+}$		X	$\varepsilon_h/\varepsilon_m = 1.5\{1 - \exp[-y^+(42 + 120/Pr^{1/2})^{-1}\} \times [1 - \exp(-y^+/26)]^{-1}$
1975	Ghajar [83]	CF	$\varepsilon_m/\nu = \frac{1}{2}\{1 + \frac{k^2 r_o^{+2}}{9}[1 - (\frac{r}{r_o})^2]^2[1 + (\frac{r}{r_o})^2]^2[1 - \exp(\frac{-(1 - r/r_o)}{A^+/r^+})]^2\}^{1/2} - 1/2$	X	X	
1975	Dimant and Poreh [1]	CF,CT	$\ell^+ = ky^+[1 - \exp(-y^+/A^+)]$	X		

TABLE II (Continued)

1977	Kale [35]	CT	$\varepsilon_m/\nu = n^2u^+y^+[1 - \exp(-n^2u^+y^+)]$	X	X	
1980	Cho, et al [31]	CF			X	$St_x Pr'^{2/3} = a(x/D)^b (Re')^c$
1980	Smith and Edwards [15]	CF, CT	$\varepsilon_m/\nu = by^{+3}$ for $0 \le y^+ \le y_1^+$ $\varepsilon_m/\nu = (y^+/A^+)(1 - y^+/A^+) - 1$ for $y_1^+ \le y^+ \le y_2^+$ $\varepsilon_m/\nu = 0.07\,R^+$ for $y_2^+ \le y^+ \le r_0^+$	X		
1981	Hanna, et al [36]	CF	$\ell^+ = ky^+\frac{[1 - \exp(-y^+/A^+)]}{[1 - \exp(-B^+y^+)]^{1/2}}$ and $\varepsilon_m/\nu = k_3y^{+3} + k_4y^{+4} + k_5y^{+5}$	X	X	
1984	Yoon and Ghajar [23]	CF	$\varepsilon_m/\nu = \frac{1}{2}\{1 + \frac{k^2r_o^{+2}}{9}[1 - (\frac{r}{r_o})^2]^2[1 + (\frac{r}{r_o})^2]^2[1 - \exp(\frac{-(1 - r/r_o)}{A^+/r^+})]^2\}^{1/2} - \frac{1}{2}$		X	$\varepsilon_h/\varepsilon_m = 1$ for $Pr_a < 6.25$ $\varepsilon_h/\varepsilon_m = 1.5\{1 - \exp[-y^+(42 + 120/Pr^{1/2})^{-1}]\}$ $\times [1 - \exp(-y^+/26)]^{-1}$ for $6.25 \le Pr_a < 8.0$ $\varepsilon_h/\nu = Cy^{+3}$ for $Pr_a \ge 8.0$

[a] CT, constant wall temperature mode; CF, constant wall heat flux mode.

viscoelastic turbulent pipe flows. Since the characteristics of viscoelastic turbulent flows can be affected by the several factors described earlier, predictions based solely on first principles are not likely to exist in the near future. The current analytical study focuses on the development of a general semi-empirical equation of heat eddy diffusivity in terms of pertinent dimensionless parameters for viscoelastic fluids, which can be determined directly from experimental measurements of pressure drop and rheological properties. Since the mathematical modeling and its verification as well as the interpretation of the flow mechanisms for viscoelastic fluids are feasible only based on experimental results, there is a definite need to conduct new experimental studies, free from the above described experimental deficiencies, which can provide a detailed and reliable data base.

1.2 Specific Areas in Need of Research

Even though a great number of studies have been conducted to investigate the friction drag and heat transfer characteristics in viscoelastic turbulent pipe flows, the usefulness of their results is questionable (or limited) as discussed in Section 1.1. In experimental and analytical studies of heat transfer in drag reducing turbulent pipe flows, one has to pay particular attention to the following areas:

1.2.1 Thermal Entrance Length

The thermal entrance length for drag reducing turbulent pipe flows is extremely long compared to that for Newtonian flows, which have a thermal entrance length of approximately 10 to 15 diameters. Yoo and Hartnett [3] investigated thermal entrance length effects for non-

Newtonian fluids in turbulent pipe flows with L/D = 100 and found out that this length is shorter than the length necessary to yield a thermally fully developed flow. Kwack et al. [6] confirmed this fact with experiments using L/D = 600 and concluded that thermal entrance length for viscoelastic fluids is a function of the polymer concentration and requires 400 to 500 diameters for the maximum heat transfer reduction case, as shown in Figure 1.1. Unfortunately, most of the previous experimental studies did not represent the thermally fully developed condition they were supposed to represent, as tabulated in Table I. The existing heat transfer correlations [35, 37, 38] based on the short thermal entrance length data could introduce considerable error in the calculation of heat transfer coefficients when compared to the thermally fully developed data. These correlations should be re-evaluated and possibly modified with reliable experimental data obtained for various polymer solutions in the thermally developed region.

1.2.2 Pipe Diameter

A number of experimental studies have suggested that pipe diameter has considerable effect on the behaviors of friction drag and heat transfer for viscoelastic turbulent pipe flows. It is generally interpreted that this diameter effect could be due to the influence of polymer molecules on the boundary layer close to the pipe wall. If the polymers act on the boundary layer, then the effect should be seen in small pipes prior to the larger ones since the boundary layer would form a larger portion of the total flow in a small pipe. In order to improve our ability to predict the behavior of drag reducing polymer additives

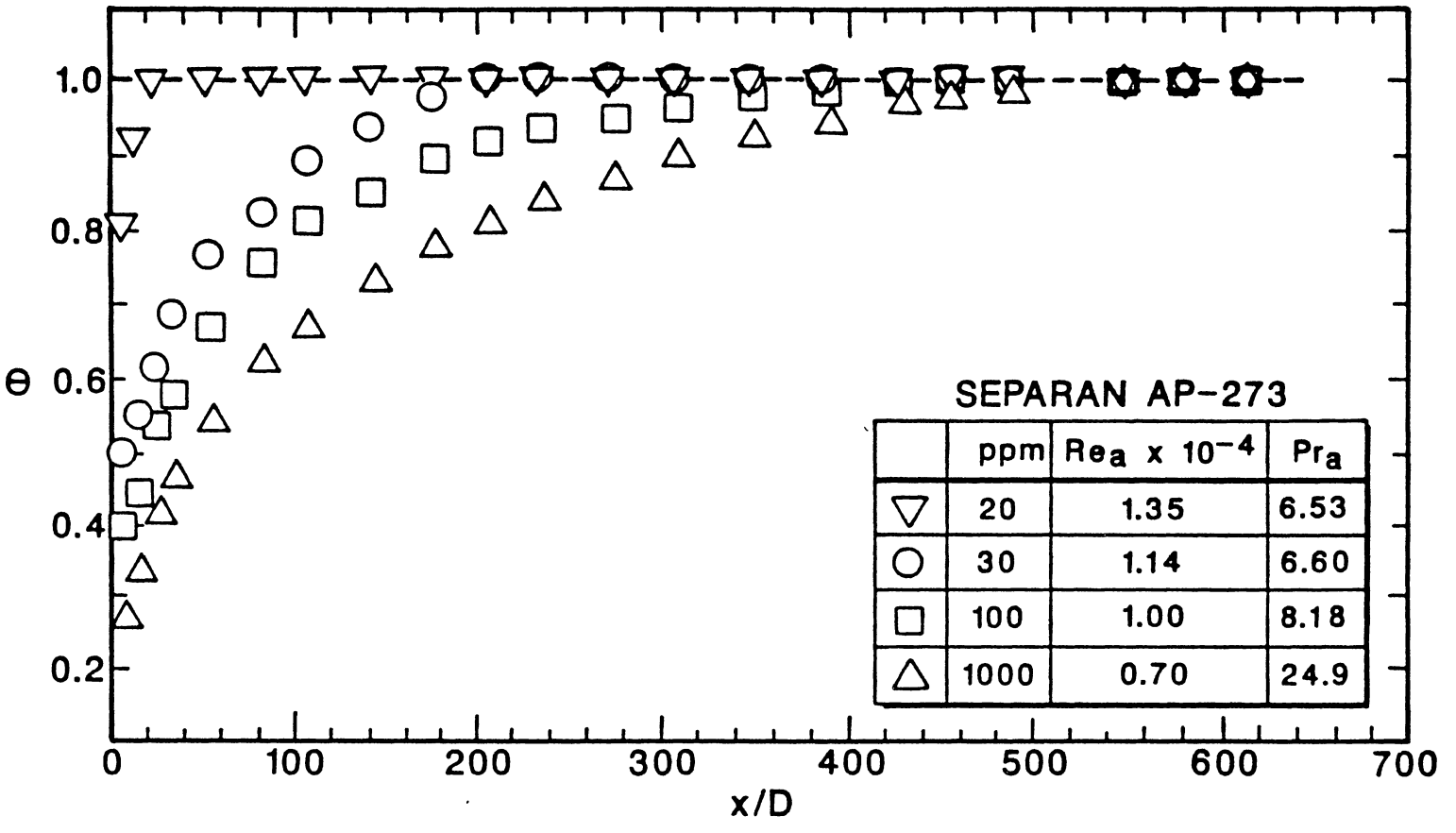

Figure 1.1 Dimensionless Temperature Vs. x/D in the Thermal Entrance Region for Various Concentrations of Separan Solution. Taken From Reference [6]

in industrial applications, a better understanding of the scaling laws for such fluids is required. Few attempts [39-42] have been made to develop a scaling law for friction factor. However, no conclusive results have been achieved. Especially, the scaling law for heat transfer coefficient is not available as yet. The existing scaling laws for friction factors should be evaluated with the experimental data obtained by independent studies. The possible extension of these laws to the case of heat transfer should be studied.

1.2.3 Temperature Dependent Fluid Properties

As shown in Table II, most of the analytical studies assumed constant fluid properties. In order to assume constant fluid properties in drag reducing flows, the wall-to-bulk temperature difference should be small. It is recommended that $T_w(°F)/T_b(°F)$ be kept less than 1.1 [1, 2].

Table I shows that most of the previous experiments were conducted at large wall-to-bulk temperature differences. In those cases, it is necessary to apply certain correction factor to the experimental data in order to account for variations of fluid properties due to temperature differences. There are two kinds of methods generally used, reference temperature method and property ratio method. The property ratio method is more commonly adopted. In this method, all variables are evaluated at the bulk temperature, and the effects of the variable liquid properties are lumped into a function of the viscosity ratio.

In such a scheme, the following power laws offer an excellent approximation for flows at given Reynolds and Prandtl numbers:

$$Nu_{vp} = Nu_{cp}(\eta_w/\eta_b)^n \qquad (1.1)$$

and

$$f_{vp} = f_{cp} \, (\eta_w/\eta_b)^m \qquad (1.2)$$

Thus, for large wall-to-bulk temperature differences, the effects of the temperature dependent fluid properties on polymer solution flows should be studied further for practical engineering applications. However, since this effort was expected to result in much extra work without significant contribution to the main objectives of the current study, these effects were minimized by maintaining $T_w(°F)/T_b(°F)$ less than 1.1.

1.2.4 Weissenberg Number

In addition to the concentration of polymer, there are several other factors which affect the characteristics of momentum and heat transfer in drag reducing turbulent pipe flows, such as pipe diameter, solvent chemistry, solute effects, and mechanical degradation. According to Kwack [26], the polymer concentration, the level of mechanical degradation, and the effects of solvent chemistry and solute, influence the fluid time scale, while the flow rate and pipe diameter determine the flow time scale. A dimensionless parameter which is the ratio of the fluid time scale to the flow time scale has been used to characterize the change in the elasticity of a viscoelastic fluid. This dimensionless parameter was defined as either the Weissenberg number [5, 6] or the Deborah number [35, 49, 56]. In this study, this parameter is designated as the Weissenberg number except for direct references of the published literatures. The expression of Weissenberg number depends on the postulated mechanism for viscoelastic fluids. The Weissenberg number employed in this study is defined as

$$Ws = \frac{\lambda}{D/U} \tag{1.3}$$

where λ is the fluid time scale and D/U is the flow time scale.

Successful correlation of polymer characteristics in terms of the Weissenberg number depends on the accurate estimation of the fluid time scale. Several investigators [2, 4, 35] have tried to estimate the fluid time scale from the measurements of intrinsic viscosity. The determination of intrinsic viscosity requires the extrapolation of polymer viscosity data to zero shear rate and zero concentration. It was pointed out by Skelland [44] that such extrapolation for non-Newtonian fluids might result in large uncertainties, especially at very low shear rates. Other estimations of the fluid time scale can be obtained from the measurements of the first normal stress difference or the shear rate dependent viscosity. According to Yoo [28], while it is possible to determine the first normal stress difference with good accuracy for the high concentration polymer solutions, it is not so for the low concentration or highly degraded solutions. The third approach in determination of the fluid time scale is the use of shear rate dependent viscosity data. According to the works of Bird [18] and Elbirli and Shaw [19], a generalized Newtonian model in conjunction with steady shear viscosity data can produce the fluid time scale of a viscoelastic fluid quite accurately. The shear viscosity is a rheological property which can be measured with good accuracy for various concentrations of polymer solutions and well-represent their characteristics. Typical shear viscosity-shear rate relationship for a polymer solution is shown in Figure 1.2. Note that this figure indicates that the zero shear rate viscosity increases with increasing

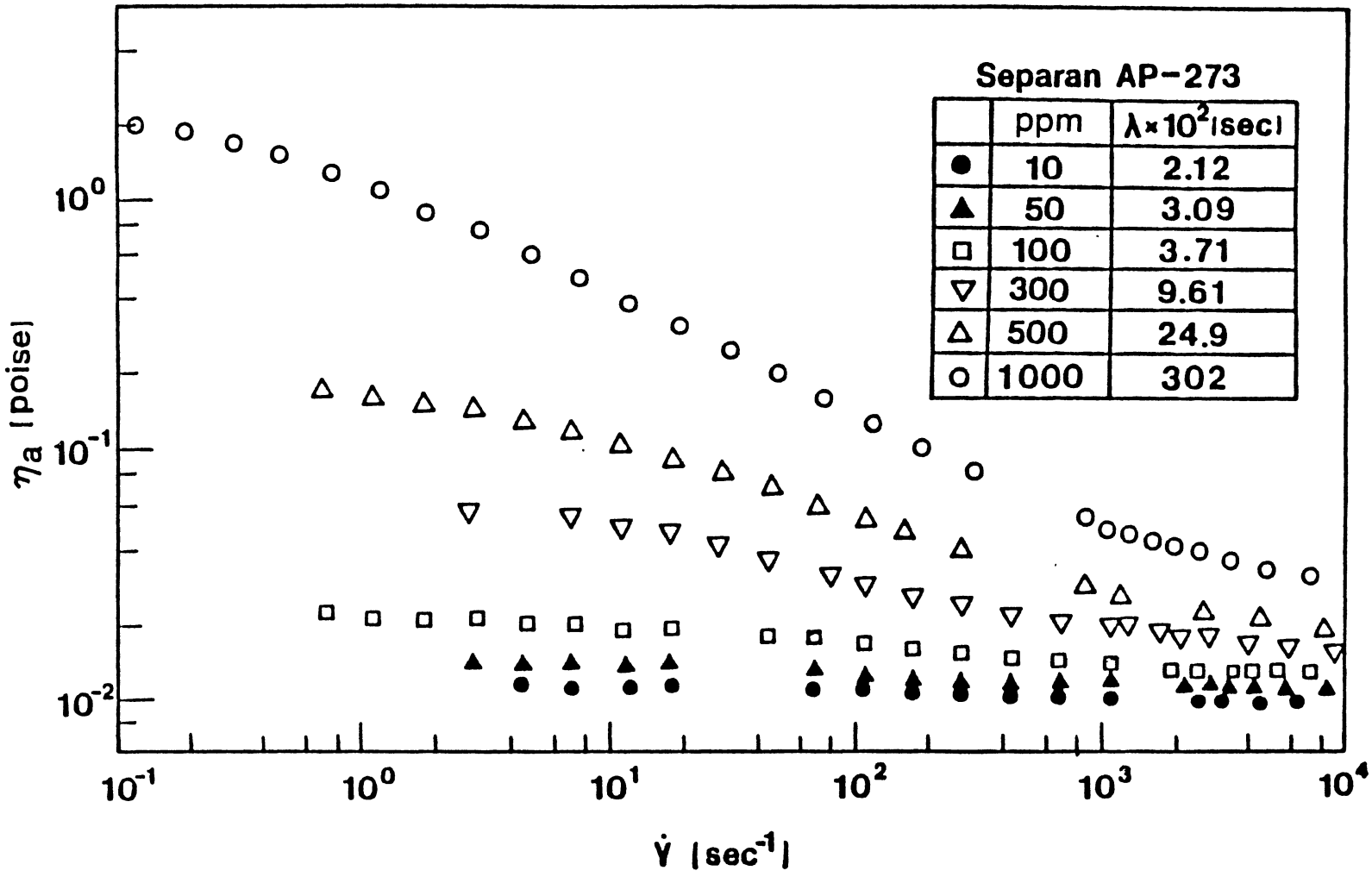

Figure 1.2 Shear Rate Dependent Viscosity of Separan Solutions. Taken from Reference [26]

polymer concentration, which implies an increase in the elasticity of the fluid. So the fluid model which is used to calculate the fluid time scale must well-characterize the pronounced change in the low shear rate viscosity as observed in Figure 1.2. Among generalized Newtonian fluid models published, the Ellis, Eyring, and the Powell-Eyring models (see Table III) are widely used for study of viscoelastic fluids because of their well-representation of fluid elasticity and simplicity of application to analytical studies. Several studies [26, 45-47] have suggested that the Powell-Eyring model appears to be quite accurate and consistent in the calculation of the fluid time scale at various polymer concentrations. In this study, the Powell-Eyring model was employed to estimate the fluid time scale.

The existence of the maximum reduction asymptotic conditions for momentum and heat transfer suggests the feasibility of a threshold value of Weissenberg number beyond which the characteristics of a flow are independent of flow parameters, such as concentration, degradation, pipe diameter, solvent chemistry, and solute. This threshold value, so called the critical Weissenberg number, has been suggested and determined for an aqueous polyacrylamide solution [6, 26, 30, 43]. The critical Weissenberg numbers were estimated to be Ws_{cf} = 5-10 for momentum transfer and Ws_{ch} = 200-250 for heat transfer with the use of the Powell-Eyring model. These estimations were made by Kwack [26] based on the apparent viscosity measurements of Separan AP-273. It may be easily inferred that the comparison of the Weissenberg number for a particular flow to these critical values can result in good estimation of the relative amount of reduction in friction factor or heat transfer coefficient with respect to the well-established maximum reduction

TABLE III

GENERALIZED NEWTONIAN MODELS

Model	Fluid Time Scale
Ellis model $\frac{1}{\eta_a} = \frac{1}{\eta_0}\left[1 + \left(\frac{\tau}{\tau_{1/2}}\right)^{\frac{1-n}{n}}\right]$	$\lambda = \eta_0/\tau^*_{1/2}$
Eyring model $\eta_a = \eta_0\left[\frac{\text{arc sinh } \lambda\dot{\gamma}}{\lambda\dot{\gamma}}\right]$	λ
Powell-Eyring model $\eta_a = \eta_\infty + (\eta_0 - \eta_\infty)\left[\frac{\text{arc sinh } \lambda\dot{\gamma}}{\lambda\dot{\gamma}}\right]$	λ

*$\tau_{1/2}$ is the shearing stress where the viscosity η is equal to the half of η_0.

asymptotes. Subsequently, the critical Weissenberg number for heat transfer is a key parameter of the heat eddy diffusivity equation, which is presented in Section 5.3. Furthermore, since these critical Weissenberg numbers suggest the optimum point compromising performances and economics of a particular polymer additive, there is a definite need for further work to study the general applicability of these critical values to other polymer solutions.

1.2.5 Rheology and Data Presentation

Even though a number of experimental and analytical studies for turbulent polymer solutions have been conducted so far, the inconsistent presentations of the results in the published literature have caused a great deal of confusion to the readers and made the direct comparison of data obtained by various experimenters quite difficult. On the other hand, the specification of the concentration of a given polymer in a given solvent, such as 100 ppm of polyacrylamide in water, as used by most of the investigators, is an inadequate definition of the fluid. It has been demonstrated that minor variations in the molecular weight distribution of polymer or minor changes in the chemistry of the solvent have major effects on the rheological properties and consequently on the heat transfer behavior. It is necessary to determine the rheology of the fluid and to describe the elastic behavior in a dimensionless form. The previous studies [2, 11, 25, 26, 28] have shown that the pronounced changes of the rheological properties with the addition of a polymer to a solvent are observed in the first normal stress difference and shear viscosity with negligible effects on the other properties such as density, specific heat, and thermal conductivity of the fluid. Those

changes in the rheological properties are due to the elasticity of the polymer solutions which can be well-characterized by the fluid time scale. It is possible to obtain an accurate estimation of the fluid time scale with the use of either the first normal stress difference or the shear viscosity, if accurate measurements of these properties can be made. However, Yoo [28] pointed out that the first normal stress difference cannot be measured with good accuracy for low concentration or degraded solutions, an area of concern. The current study focuses only on the changes in the rheology of a solution due to shear viscosity. Furthermore, the following dimensionless groups are proposed for presentation of the results: Reynolds number, Prandtl number, and Weissenberg number.

As tabulated in Table I, several investigators have introduced a variety of definitions for Reynolds and Prandtl numbers for their convenience in presenting their works, which are summarized in Table IV for easy comparison. The merits and demerits of the different definitions specified were discussed in detail by Cho and Hartnett [2]. The results of this study are presented in terms of Reynolds number based on the apparent viscosity at the wall (apparent Reynolds number), because it allows more direct comparisons of experimental results with those predicted from the analytical studies. This results from the fact that most analytical studies of momentum and heat transfer for non-Newtonian fluids have been carried out under the assumption of constant viscosity in the radial direction at a fixed flow rate to avoid mathematical complexity. This is exactly the case for the current analytical study (see Chapter V). Furthermore, the non-Newtonian viscosity is proven experimentally to be almost constant for most

TABLE IV

DEFINITIONS OF REYNOLDS AND PRANDTL NUMBERS

Definition	Shear stress-shear rate	Reynolds number	Prandtl number	Pe(= $\rho C_p UD/K_f$)
1	$\tau_w = K'(8U/D)^n$	$Re' = \rho U^{2-n} D^n / K' 8^{n-1}$	$Pr' = C_p K'(8U/D)^{n-1}/K_f$	$Re'Pr'$
2	$\tau_w = \eta_a \dot{\gamma}_w$, $\dot{\gamma}_w = [(3n+1)/4n]8U/D$	$Re_a = \rho UD/\eta_a$	$Pr_a = \eta_a C_p/K_f$	$Re_a Pr_a$
3	$\tau_{ij} = K(D_{ij})^n$	$Re_{gen} = \rho U^{2-n} D^n / K$	$Pr_{gen} = C_p K(U/D)^{n+1}/K_f$	$Re_{gen} Pr_{gen}$
4	η_s = solvent viscosity	$Re_s = \rho UD/\eta_s$	$Pr_s = \eta_s C_p/K_f$	$Re_s Pr_s$
5	$\tau_w = \eta_{eff} 8U/D$	$Re_{eff} = \rho UD/\eta_{eff}$	$Pr_{eff} = \eta_{eff} C_p/K_f$	$Re_{eff} Pr_{eff}$

Taken from Reference [2]

aqueous polymer solutions in the shear rate range corresponding to turbulent flow conditions. The corresponding Prandtl number is defined such that the product of the Reynolds and Prandtl numbers yield the Peclet number ($\rho C_p UD/K_f$) as shown in Table IV. The third dimensionless group, the Weissenberg number, was discussed in detail in Section 1.2.4.

The Reynolds and Weissenberg numbers defined above play a major role in determining fluid mechanics and heat transfer characteristics of viscoelastic turbulent pipe flows. Additionally, the consistency in presenting the current experimental results in terms of the dimensionless groups described so far will allow easier comparisons with the future experimental works and afford a valuable data basis for future analytical studies.

1.3 Objectives and Method of Approach

The main objectives of the current study were to experimentally determine the momentum and heat transfer characteristics of drag reducing turbulent pipe flows and to develop and establish a semi-empirical equation for heat eddy diffusivity based on the experimental results. The problem analysis included the following phases:

1. The study of the Powell-Eyring fluid model which was used to estimate the fluid time scale. This model includes as key parameters the zero shear rate viscosity and the infinite shear rate viscosity, which are very much dependent on the type of viscometer used. Therefore, it is essential to study the sensitivity of the model to variations in the zero shear rate viscosity and the infinite shear rate viscosity. The performance of the model was also investigated with the comparison to other model. (See Section 4.1).

2. The data collection of friction factors and heat transfer coefficients which were required to interpret the mechanisms of momentum and heat transfer for turbulent viscoelastic flows. The current study involved two different polymers (polyacrylamide, Separan AP-273 and polyox, WSR-301) with wide range of concentrations (10-1000 ppm) flowing in two different pipe diameters (0.436 in. and 0.739 in.) operated by the once-through mode. The measurements of pressure drop and heat transfer were conducted in the thermally fully developed region under the constant wall heat flux condition. Particular attention was paid to the systematization of data presentation in terms of the pertinent dimensionless parameters. (See Section 4.2).

3. The study of a scaling method which can be used to account for the effects of pipe diameter and polymer concentration on the behaviors of momentum and heat transfer for turbulent viscoelastic flows. The scaling law of Astarita et al [42] proposed for the friction factor was applied to the current experimental data for the verification of its general applicability and extended to the case of heat transfer. (See Section 4.3).

4. The study of the critical Weissenberg number for heat transfer which is one of the key parameters in the proposed equation for heat eddy diffusivity. The current study used two different approaches to degrade a highly concentrated polymer solution: recirculation and/or dilution. The test fluids included two polyacrylamide solutions (Separan AP-273 of 1500 ppm and Separan AP-30 of 3000 ppm). The particular purpose of this phase of the study was to establish the general applicability of the critical Weissenberg number for heat transfer suggested by the previous work [26] to other polymer

solutions. (See Section 4.4).

5. The development of a heat transfer correlation in terms of the pertinent dimensionless parameters which can be determined from the measurements of pressure drop and rheological properties of the fluid. (See Section 4.5).

6. The development of an eddy diffusivity expression for heat which can accurately predict the characteristics of heat transfer. This expression should be applicable to various polymer solutions with wide range of concentrations. Furthermore, it should be qualitatively consistent with the experimental observations. The development and establishment of the expression was based on the experimental results of Kwack [26] and this study. (See Section 5.3).

It is anticipated that the results of the current research will:

1) Provide a detailed and reliable data base upon which meaningful comparisons between present and future experimental data can be made. In planning of the experimental studies and in the analysis of the data, careful consideration were given to the effects of thermal entrance length, pipe diameter, mechanical degradation, solvent chemistry, solute, and temperature dependent fluid properties. In addition, the rheological properties of the fluid were measured and analyzed with great care. All of the results were presented in terms of the pertinent non-dimensionalized parameters. Since all of these conditions are rarely met, it follows that there are few meaningful comparisons in the literature.

2) Aid in the development of a general expression for eddy diffusivity of heat capable of predicting heat transfer to drag reducing polymer solutions with wide range of concentrations. The major outcome

of this study would be the ability to characterize and predict heat transfer in turbulent pipe flows with drag reduction.

CHAPTER II

SURVEY OF PREVIOUS WORKS

Extensive studies have been conducted to investigate the characteristics of friction drag and heat transfer in viscoelastic turbulent pipe flows. Excellent reviews for the momentum transfer of viscoelastic fluids were given by Hoyt [39] and Virk [48]. On the other hand, those for the heat transfer can be found in the works of Diamant and Poreh [1], and Cho and Hartnett [2]. In this chapter, the previous studies, which are closely related with the objectives of the current study, are briefly discussed. Included are the experimental works for heat transfer, the momentum transfer correlations, the heat transfer correlations and the numerical methods.

2.1 Experimental Works

Gupta et al. [49] conducted one of the earliest studies on heat transfer in viscoelastic fluids. They presented the measurements of friction factors and heat transfer coefficients in terms of generalized Reynolds number. It was concluded that at a given flow rate the reduction in heat transfer is far greater than that in friction drag. It was also suggested that the drag reduction does not arise as a result of a conservative, as opposed to a dissipative turbulent field, but rather because of a strong depression of turbulent eddies in the flow. An attempt was made to relate the drag reduction to the Deborah number,

which is a dimensionless parameter indicating a direct relationship between the fluid time scale and the turbulent structure. However, no conclusive success was obtained.

McNally [50] attempted to interpret the mechanism responsible for the drag and heat transfer reduction in viscoelastic fluids. He suggested that this mechanism is an interaction between the polymer molecules and the small scale turbulent eddies rather than the stabilization and thickening of the viscous and transition sublayers. It was argued that the drag and heat transfer reduction can be observed at the Reynolds number higher than certain critical value, so called the onset Reynolds number. It was also suggested that the onset Reynolds number for momentum transfer is higher than that for heat transfer. This implied that a normalization of the onset points is needed for meaningful comparisons between momentum transfer and heat transfer. McNally [50] proposed that the Reynolds numbers for heat transfer should be divided by 2.76 and the heat transfer coefficients multiplied by 1.22. Based on the results obtained by the above normalization procedures, he concluded that a direct analogy between heat transfer and momentum transfer is also applicable to viscoelastic fluids. It should be mentioned that this conclusion was drawn based on very limited experimental results up to 40 ppm of WSR-301.

Smith et al. [51] suggested that there is a maximum heat transfer reduction asymptotic condition, which was expressed by

$$St\ Pr_b^{0.6} = 0.184\ Re_b^{-0.54} \tag{2.1}$$

They compared this correlation with that for the maximum friction drag

reduction case obtained in the previous work [52], which was expressed by

$$f/2 = 0.21\ Re^{-0.55} \tag{2.2}$$

They concluded that a Chilton-Colburn type analogy is valid for viscoelastic fluids. Their conclusion is doubtful, because the polymer concentration used was not high enough to reach the maximum heat transfer reduction asymptote and the test section was not long enough to produce the thermally fully developed condition.

Sidahmed and Griskey's work [52] was concerned about the determination of the effect of polymer on mass transfer in drag reducing fluid system using an electrochemical technique. They attempted to correlate the mass transfer with the heat transfer. They suggested that for the fully developed condition, the Wells' correlation [32] adapted for mass transfer

$$St = \frac{f/2}{1.02 \frac{U_L}{U_\tau} (f/2)^{1/2} (Sc - 1)(Sc)^{-1/3} + 1.2} \tag{2.3}$$

can be used to estimate the Stanton number. They also proposed that for short heat transfer entry lengths, the correlation

$$St = 0.06\ Sc^{-2/3}\ Re^{-0.30}\ (x/D)^{1/3} \tag{2.4}$$

should be used.

Monti [11] conducted very extensive studies concerning degradation, temperature dependent properties and chemical effects. All of the data were presented as a function of Re_f or Re' due to the fact that the

apparent viscosity heavily depends on the shear rate. Generally, the drag reduction effect increased with addition of polymer. However, there was an optimum concentration beyond which the friction drag increased with the increase of polymer. In contrast, the heat transfer coefficients reduced consistently with the increase of polymer. He attributed this phenomenon to the fact that for the increased concentration, the viscosity of a fluid has a pronounced increase but the thermal conductivity is almost constant. He postulated from his experimental results that Reynolds analogy is not valid for viscoelastic fluids.

Debrule and Sabersky [27] measured heat transfer and friction coefficients in smooth and rough tubes for dilute polymer solutions. The results obtained for the smooth tube showed that the friction factors were reduced by a factor of 3 and the heat transfer coefficients by a factor of 5. For the rough tube the coefficients were reduced even more drastically. Their interpretation of drag reduction phenomenon was that the long chain molecules reduce the turbulence near the wall and increase the thickness of the effective viscous layer.

Compared with the previous works, Ng et al. [53] used highly concentrated polymer solutions (aqueous Separan AP-273 solutions of 1500, 2000, and 2500 ppm). Even though the test section used had relatively long heated length (L/D = 250), they found that all the experimental data for heat transfer were in the thermal entrance region. They investigated the influence of variable properties on heat transfer due to the bulk-to-wall temperature difference. Their results showed that the heat transfer coefficients at each Reynolds number for the large ΔT (20-37°C) are generally greater than those for the small ΔT

(4.5-8.5°C) with the difference being approximately 10%. They suggested that the general character of this phenomenon, higher heat transfer coupled with unsteady wall temperature readings for the large ΔT, was due to the natural convection. Their subsequent work [5] showed that the thermal entrance region for highly concentrated viscoelastic fluids is greater than 430 pipe diameters. This study also suggested that the heat transfer was influenced by degradation much earlier than the friction factor. The onset of transition for both friction factor and heat transfer coefficients was found to occur simultaneously at a generalized Reynolds number, Re' of approximately 5500.

Cho and Hartnett [24] reviewed the available experimental momentum, heat and mass transfer results to study the validity of analogy for viscoelastic fluids. They used the experimental results obtained at the maximum reduction asymptotic cases. Ng et al. [5] proposed the following empirical expression for the maximum drag reduction case:

$$f = 0.20\ Re_a^{-0.48} \tag{2.5}$$

Virk and Suraiya [54] proposed the maximum mass transfer reduction asymptote for Reynolds number ranging from 5000 to 35000:

$$St\ Sc^{2/3} = 0.022\ Re^{-0.29} \tag{2.6}$$

They compared Equations (2.5) and (2.6) with the experimental heat transfer data of Ng et al. [5] and concluded that for turbulent viscoelastic flows, the eddy diffusivity of mass is much larger than that of momentum, while the eddy diffusivity of heat is much smaller

than that of momentum. They also extensively investigated the entrance region for each transfer and suggested that the entrance length for mass, momentum and heat transfer is 35, 100, and 430 pipe diameters, respectively.

Kwack et al. [55] measured friction factors and heat transfer coefficients using aqueous polyacrylamide solutions of various concentrations ranging from 10 ppm to 1000 ppm. They concluded that the hydrodynamic length and thermal entrance length at the maximum reduction asymptotes for polyacrylamide solutions is 110 and 400-500 pipe diameters, respectively, consistent with the previous work [24]. They proposed that for fully developed flows at the maximum heat transfer reduction asymptotic case,

$$j_h = 0.03\ Re_a^{-0.45} \tag{2.7}$$

and for developing flows

$$j_h = 0.13\ (x/D)^{-0.24}\ Re_a^{-0.45} \tag{2.8}$$

Their results also revealed that the percentage heat transfer reduction is much greater than the percentage drag reduction.

The review of relevant works clearly revealed that most of the previous studies have been conducted with the data base obtained under inadequate experimental conditions: 1) short test section, 2) low polymer concentration, 3) severe polymer degradation, 4) large wall-to-bulk temperature difference. Particularly, the study of rheological properties for each solution has been greatly scant. For the better

understanding of the polymer effects on the characteristics of momentum transfer and heat transfer, there is a definite need to conduct new experiments for various polymers with wide range of concentrations in the fully developed flows. These data base can be also used to develop and verify the theoretical models for viscoelastic fluids.

2.2 Momentum Transfer Correlations

Since the heat transfer of a solution is directly related to the flow motion, it may be easily inferred that the accurate knowledge of momentum transfer is essential to study the heat transfer behavior.

Rodriquez et al. [56] attempted to correlate the friction factors with the rheological properties of the solutions. They assumed the friction factor ratio a fundamental quantity of drag reducing solutions. From the measurements of rheological properties, the fluid time scale for each polymer-solvent was estimated using the Zimm's model [95], which has the following expression:

$$\lambda_k = \frac{M \frac{\eta_{sp}}{c} \eta - \eta_s}{0.586RT \beta_k} \tag{2.9}$$

where M is the viscosity average molecular weight, η_{sp} is the specific viscosity deviation defined as $(\eta - \eta_s)/\eta_s$, and β_k is the Eigen value corresponding to the Kth mode of relaxation. They correlate the friction factor ratio (f_p/f_s) with the modified Deborah number $(\lambda_1 U/D^{0.2})$ for each polymer-solvent system, which was formed to eliminate the diameter effects on friction factors. For different polymer-solvent systems, they proposed a shift factor of the form $1/(4[\eta]-1)$, where $[\eta]$

is the intrinsic viscosity of the solution.

Astarita et al. [42] correlated the drag reduction data with two dimensionless parameters obtained from a phenomenological analysis of the drag reduction mechanism. To account for the diameter effect on drag reduction, the characteristic frequency (flow time scale) was used. The characteristic frequency (Ω) was estimated by the Seyer and Metzner's model [57], which was expressed as

$$\Omega = \frac{U}{D} Re_a^{0.75} \tag{2.10}$$

To correlate the friction factor data for various polymer concentrations and types, an additional parameter was needed. From the dimensional analysis, they suggested that the friction factor should be a function of Reynolds number and Deborah number. To eliminate the influence of Reynolds number on the friction factor, a drag reduction ratio (DR), defined as

$$DR = f_p/f_s = DR\ (\Omega\lambda) \tag{2.11}$$

was assumed to be a function of Deborah number only. They further assumed that for a given polymer solution, the value of λ is constant. This indicated that for a given solution, DR is a unique function of Ω. When different solutions are involved, λ values should be known. Since it was difficult to accurately determine λ values for low concentrations, the following alternative method was proposed. Let $\Omega_{0.5}$ be the frequency corresponding to a drag reduction of 0.5:

$$0.5 = DR\ (\Omega_{0.5}\lambda) = DR\ (K) \tag{2.12}$$

where $K = \Omega_{0.5}\lambda$ is a constant which, if Equation (2.11) is valid, does not depend on the particular solution considered. Equation (2.12) can be written in the equivalent form:

$$DR = DR\ (\frac{\Omega K}{\Omega_{0.5}}) = DR'\ (\frac{\Omega}{\Omega_{0.5}}) \tag{2.13}$$

The above equation was proposed to correlate the friction factors for various concentrations, different diameters, and different polymer types.

Sellin and Ollis [41] conducted a dimensional analysis for friction factor and suggested the following functional relationship for smooth pipes:

$$f = g\ (Re,\ D\sqrt{\lambda\nu},\ C,\ P) \tag{2.14}$$

where P is a parameter defining the state of the polymer species used. Since it was difficult to accurately determine the parameters λ and P, these parameters were replaced by a function of the pipe shear velocity, u_τ and the characteristic polymer molecular length, ℓ. They used the scale-up method proposed by Granville [40] and the three layer model for the velocity profile by Virk [48]. It was assumed that the addition of polymer to turbulent pipe flows causes a parallel shift of the velocity profile by an amount ΔB without change of the slope. Furthermore, the value of ΔB was hypothesized to be a function of the shear velocity and the polymer properties, i.e.

$$\Delta B = g\,(u_\tau \ell/\nu) \tag{2.15}$$

Now

$$\frac{u_\tau \ell}{\nu} = U\sqrt{f/8}\,\frac{\ell}{\nu} = \frac{1}{\sqrt{8}}\left(\frac{\ell}{D}\right)\left(\mathrm{Re}\sqrt{f}\right) \tag{2.16}$$

Therefore, for the same polymer and the same value of $(u_\tau \ell/\nu)$, Equation (2.16) became

$$\left(\mathrm{Re}\sqrt{f}\right)_2 = \left(\mathrm{Re}\sqrt{f}\right)_1 \cdot \left(D_2/D_1\right) \tag{2.17}$$

There were two procedures to scale diameter effects on the friction factors when Equation (2.17) was used. One was the piecewise integration method of the velocity profile across the pipe diameter and the other was the graphical method proposed by Granville [40]. They concluded that either method could give good results for small diameter variances, but both of them failed to result in satisfactory predictions for the maximum drag reduction cases.

The main objective of Darby and Chang's work [58] was to relate the friction loss in turbulent drag reducing solutions to the measurable nonlinear viscoelastic properties. Their correlation could be expressed as a generalized form which is applicable to non-Newtonian viscoelastic as well as Newtonian fluids, in a wide range of tube sizes. The constitutive equations proposed to correlate the rheological properties were

$$\eta = \eta_\infty + \frac{\eta_0 - \eta_\infty}{(1 + \zeta^2\dot{\gamma}^2)^\Omega} \tag{2.18}$$

and

$$\psi_1 = \frac{2(\eta_0 - \eta_\infty)\theta}{(1 + \zeta^2\dot{\gamma}^2)^{2\Omega+\beta}} \tag{2.19}$$

where ψ_1 is the first normal difference, $\Omega = \frac{1-M}{2}$, n the flow index in the power law region and ζ the reciprocal of the shear rate at the point where the power law region of the viscosity curve intersects with η_0. They hypothesized that the energy which is stored by elastic properties would represent a reduction of energy which would otherwise be dissipated by viscous forces, i.e. drag reduction. They solved the mean rate of energy dissipation per unit mass using the Maxwell model, which was expressed as

$$\tau + \lambda\frac{D\tau}{Dt} = \eta_0\dot{\gamma} \tag{2.20}$$

The final correlation between the Newtonian friction factor and the corresponding friction factor of polymer solution at the same flow rate had the following expression:

$$f_p = \frac{f_s}{\sqrt{1 + De^2}} \tag{2.21}$$

Where $De = \omega_p\lambda$ is the characteristic dimensionless eddy frequency (Deborah number) for the system and ω_p the frequency of oscillation for the polymer solutions. To estimate the fluid time scale λ needed for calculation of Deborah number, they solved Equations (2.18) and (2.19)

simultaneously. The following equation was obtained:

$$\lambda = [(1 + \zeta^2\dot{\gamma})^2 - 1]^{1/2} / \dot{\gamma} \tag{2.22}$$

They formulated the Deborah number in terms of directly measurable properties and determined adjustable constants using a linear regression method. The final expression of Deborah number was derived as

$$De = 0.145 \left(\frac{8U\lambda}{D}\right)\left[\frac{Re_s}{1 + \left(\frac{8U\lambda}{D}\right)^2} \frac{\eta_s}{\eta_0}\right]^{0.285} \tag{2.23}$$

The review of previous works indicates that the drag reduction phenomenon is closely associated with the rheological properties of solutions. Especially, the pronounced change in the zero shear rate viscosity caused by the addition of polymer seems to directly reflect the amount of drag reduction. The previous works suggested that the fluid time scale can be estimated with good accuracy from the measurements of rheological properties with the use of a constitutive equation. This time scale was used to form a key dimensionless parameter, i.e. Deborah number (Weissenberg number), controlling drag reduction together with the flow time scale of the system. The future work of drag reduction phenomenon should be directed in this way. Another interesting result of the previous works can be found in the scaling laws for pipe diameter effects [41, 42]. These methods should be carefully studied because of their tremendous importance in practical engineering applications.

2.3 Heat Transfer Correlations

Many attempts have been made to develop a reliable heat transfer

correlation for drag-reducing turbulent pipe flows. In this section, previous studies are scrutinized with the purpose of elucidating key parameters in their proposed expressions.

Pruitt et al. [37] showed that the heat transfer coefficients for viscoelastic fluids could not be well-predicted by the semi-empirical correlation of Metzner and Friend [88] for Newtonian and purely viscous non-Newtonian fluids:

$$St = \frac{f/2}{1.2 + 11.8\,(Pr-1)(Pr)^{-1/3}\sqrt{f/2}} \tag{2.24}$$

They have empirically found that a good correlation with data for viscoelastic fluids was achieved by modifying Equation (2.24) as follows:

$$St = \frac{(f/2)(1-FR)}{1.2 + 11.8(Pr-1)\,(Pr)^{-1/3}\,\sqrt{(f/2)(1-FR)}} \tag{2.25}$$

where FR was defined by the equation

$$FR = (\Delta P_s - \Delta P_p)/\Delta P_s \tag{2.26}$$

in which Δp_s and Δp_p were the pressure drop along the test section for the solvent and for the polymer solution at the same flowrate, respectively. For better predictions, they recommended to use the value of FR measured at the point of the maximum drag reduction asymptote.

Poreh and Paz [13] modified the von Karman's three layer model [89] so that it could be applied to viscoelastic fluids. The modified version of the three layer model has the following expressions:

For a laminar sublayer:

$$u^+ = y^+ \qquad 0 < y^+ < y_1^+ \tag{2.27}$$

For a buffer zone:

$$u^+ = y_1^+ \ln(y^+/y_1^+) + y_1^+ \qquad y_1^+ < y^+ < y_2^+ \tag{2.28}$$

For a turbulent core zone:

$$u^+ = 2.5 \ln(y^+/y_j^+) + y_j^+ \qquad y_2^+ < y^+ < r_0^+ \tag{2.29}$$

where y_j^+ is the intersection of the shifted equation for the turbulent zone with the viscous sublayer equation. For Newtonian fluids, the ratio of y_1^+/y_j^+ was known to be 0.43. They assumed that for the case of polymer solutions, the ratio of y_1^+/y_j^+ might remain the same. The continuity requirement of the velocity profile at y_2^+ resulted in the following expression from Equations (2.28) and (2.29):

$$\ln(y_2^+/y_1^+) = \frac{1.32y_j^+ - 4.9}{y_j^+ - 5.8} \tag{2.30}$$

The above observation suggested that the velocity profile might depend on the parameter y_j^+ only. They related y_j^+ to the velocity shift Δu^+, which Elata et al. [60] expressed with the characteristics of the flow at the wall as follows:

$$\Delta u^+ = 2.5\ C \ln(\tau_w \lambda/\eta) \tag{2.31}$$

where λ is the relaxation time and C is a concentration dependent parameter. With the use of the modified three layer model of velocity, they developed the following expression for heat transfer coefficients in polymer solutions:

$$St = \sqrt{f/2}\ /\{y_1^+ [\ln[Pr - (Pr-1)y_1^+/y_2^+] + (Pr-1)) + \sqrt{(2/f)}\} \tag{2.32}$$

The development of Equation (2.32) was based on the following assumptions: 1) $\varepsilon_m/\varepsilon_h = 1$, 2) constant shear stress and heat flux in the radial direction, and 3) insignificant eddy diffusivity in the laminar sublayer and the buffer zone. The above assumptions should be carefully examined with the recent findings for viscoelastic fluids.

Wells [32] derived a heat transfer correlation using the analogy between energy and momentum transports in turbulent flows, which has the following expression:

$$St = \frac{f/2}{1.2 + 1.02 \frac{u_L}{u_\tau}(f/2)^{1/2}(Pr-1)\ Pr^{-1/3}} \qquad (2.33)$$

where u_L is the local velocity evaluated at the edge of the viscous sublayer. He suggested that the proper expression for u_L/u_τ could account for the increase of viscous sublayer due to addition of polymer. In this study, the Meyer's friction factor correlation [61] was used. This analysis also failed to include the eddy diffusivity in the viscous sublayer.

Corman [38] suggested that the use of the friction factor expression of Elata et al. [60] and the heat transfer correlation of Wells [32] could predict his experimental data quite well. However, the experimental data were unreliable due to the use of short test section and centrifugal pump.

Kale [35] extended to viscoelastic fluids the Reichardt's expression for heat transfer in Newtonian turbulent flows:

$$St = \frac{f/2 \cdot Pr_t \cdot 1/\theta_m}{1/\phi_m + (Pr \cdot Pr_t - 1)(f/2)^{1/2} \int_0^{u_c/u_\tau} \frac{du^+}{1 + Pr \cdot Pr_t \varepsilon_m/\nu}} \qquad (2.34)$$

Where θ_m is the ratio of mean to maximum temperature difference and ϕ_m is the ratio of mean to centerline velocity. Kale used 1.0 and 1.2 for θ_m and $1/\phi_m$ suggested by Metzner and Friend [88] for purely viscous fluids. He further assumed that the turbulent Prandtl number ($Pr_t = \varepsilon_m/\varepsilon_h$) would be equal to 1.0 (incorrectly). The integral part of Equation (2.34) was solved using the Deissler's velocity expression near the wall [59]:

$$u^+ = \int_0^{y^+} \frac{dy^+}{1 + n^2 u^+ y^+ (1 - e^{-n^2 u^+ y^+})} \tag{2.35}$$

The results obtained from such computational scheme were correlated with Prandtl number and Deborah number as follows:

$$\int_0^{u_c/u_\tau} \frac{du^+}{1 + Pr \cdot \varepsilon_m/\nu} = 9.2\ Pr^{-0.258} + 1.2\ De\ Pr^{-0.236} \tag{2.36}$$

The second term in Equation (2.36) corresponds to the shift of velocity due to polymer addition. The final expression for dimensionless heat coefficient was obtained as

$$St = \frac{f/2}{1.2 + (Pr-1)(f/2)^{1/2}\{9.2Pr^{-0.258} + 1.2\ De\ Pr^{-0.236}\}} \tag{2.37}$$

He also suggested that for Deborah numbers ≥ 20, the reduction in friction and heat transfer might approach the maximum reduction asymptotes. For these asymptotic cases, Equation (2.37) became

$$St = \frac{f/2}{1.2 + (Pr-1)(f/2)^{1/2}\{9.2\ Pr^{-0.258} + 24\ Pr^{-0.236}\}} \tag{2.38}$$

Even though the predictions using Equation (2.37) resulted in considerable errors compared with reliable experimental data [5, 25, 26], it is noteworthy that he involved the fluid time scale (Deborah number) in the heat transfer correlation for viscoelastic fluids.

Based on extensive heat transfer data, Cho et al. [31] developed an empirical heat transfer correlation.

$$St\ Pr'^{2/3} = 0.13\ (x/D)^{-0.3}\ Re'^{-0.4} \tag{2.39}$$

However, the application of Equation (2.39) was limited to the undegraded and saturated solutions over the range of Re' from 6000 to 60,000 and of x/D up to 430.

No single correlation available can accurately predict the heat transfer coefficients for various polymer solutions with wide range of concentrations in the thermally fully developed region. The inadequacy of existing heat transfer correlations was due to the fact that these correlations were developed and established using inaccurate experimental data. However, the scrutiny of previous works indicated that key parameters in the heat transfer correlations were the friction drag reduction ratio (FR) and the fluid time scale (λ), which can be determined from the measurements of pressure drop and solution viscosities, respectively. New attempt should be made to develop a reliable heat transfer correlation in terms of these two key parameters based on extensive and reliable experimental data.

2.4 Numerical Methods

Numerous investigators have attempted to determine friction factors

factors and heat transfer coefficients for viscoelastic fluids by solving the conservation equations with the proper account of drag reduction. As mentioned before, since the drag reduction phenomenon is attributed to the interaction of polymer molecules and turbulent eddies, most analytical modelings have been focused on the eddy diffusivity.

Debrule and Sabersky [27] assumed that a direct analogy between heat and momentum is valid for viscoelastic fluids, i.e. $\varepsilon_h = \varepsilon_m$. They used the Deissler's empirical relationship for ε_m in the viscous sublayer [59]:

$$\frac{\varepsilon_m}{\nu} = n^2 \frac{uy}{\nu} [1 - \exp (-n^2 \frac{uy}{\nu})] \qquad (2.40)$$

It was suggested that the value of n for viscoelastic fluids should change according to the level of drag reduction. Their results showed that instead of n = 0.124 for pure water, typical values of n for the polymer solutions are between 0.030 an 0.040 for the 50 ppm solution and between 0.040 and 0.050 for the 10 ppm solution. This conclusion is considered incorrect since different type of polymers can produce different level of drag reduction at the same concentration. They failed to relate the change in n to the rheology of the polymer solutions.

Diamant and Poreh [1, 62] contended that the van Driest's model [63] could produce the velocity profile exceeding the parabolic shape observed in a laminar flow for small value of r_0^+/A^+, which is practically impossible. For the better prediction of the velocity profile which is also essential to the heat transfer calculation, they modified the van Driest's equation as follows:

$$u^+ = u_1^+ + u_2^+ \tag{2.41}$$

where u_1^+ is the solution of the following equation

$$\frac{du_1^+}{dy^+} + \frac{2(1 - y^+/r_0^+)}{1 + \sqrt{1 + 4K^2y^{+2}[1 - \exp(-y^+/A^+)]^2\,(1-y^+/A^+)}} \tag{2.42}$$

and

$$u_2^+ = \frac{0.67}{2K}\,[1 - \cos(\pi y^+/r_0^+)][1 - \exp(-2r_0^+/A^+)] \tag{2.43}$$

They suggested that the value of A^+ should change according to the level of drag reduction. The dependence of A^+ on the polymer properties was approximated by

$$A^+/A_N^+ = 5.0\,[1 + (u_\tau/u_{\tau\ cr})^4]^{\Delta/40} - 4 \tag{2.44}$$

where A_N^+ is the value of A^+ for Newtonian fluids, i.e. $A_N^+ = 26$ and $\Delta = \alpha/\sqrt{32}$ is the Virk's parameter [48]. For solving the energy equation, they assumed that the turbulent Prandtl number is unity. The eddy diffusivity expression used was

$$\varepsilon_m/\nu = \varepsilon_h/\nu = K^2y^{+2}[1 - \exp(-y^+/A^+)]^2\,du^+/dy^+ \tag{2.45}$$

Where A^+ can also be calculated using Equations (2.43) and (2.44). Their results indicated that this model could predict the heat transfer coefficient for low concentrations fairly well. For the relatively high concentration (Polyox solution of 50 ppm), this model failed to give good prediction of heat transfer coefficients. The above result can be

expected since Reynolds analogy, on which this study was based, can be valid for low concentrations, but not for high concentrations (see reference [23]).

Ghajar and Tiederman [34] used the eddy diffusivity expression proposed by Cess [64] for the prediction of heat transfer coefficients in drag reducing turbulent pipe flows. They employed the iterative computation scheme proposed by Tiederman and Reischman [65] for the calculation of A^+. For more details, see Chapter V. They also assumed the validity of Reynolds analogy for viscoelastic fluids. Their prediction scheme could produce considerable errors compared with the recent experimental data [26], especially at the high concentrations.

Mizushina et al. [33] used a damping factor model to analyze the results of drag reduction, which is summarized as

$$\varepsilon_m/\nu = f_m\,(y^+, r_0^+)^2\; DF_m^2\; \frac{du^+}{dy^+} \tag{2.46}$$

where

$$DF_m = 1 - \exp\left[-\frac{y^+}{A^+}\sqrt{-\alpha + \sqrt{\alpha^2+1}}\,\right] \tag{2.47}$$

$$f_m\,(y^+, r_0^+) = 0.4y^+ - 0.44\,y^{+2}/r_0^+ + 0.24\,y^{+3}/r_0^{+2} - 0.06y^{+4}/r_0^{+3} \tag{2.48}$$

$$\alpha = \frac{2\lambda_t}{\nu}\,(u_\tau/A^+)^2 \tag{2.49}$$

and

$$\lambda_t/\lambda_\ell = 3.76 \times 10^8\; Ws^{1.34} \tag{2.50}$$

The fluid time scale for simple laminar flow (λ_ℓ) was calculated using the equation derived by James and Acosta [66]. They extended the concept of a damping factor model for momentum transfer to the heat

transfer. The damping factor for heat transfer was expressed as a function of Prandtl number as follows:

$$DF_h = 1 - \exp[-y^+/(a_0 + a_1\sqrt{Pr})] \tag{2.51}$$

Instead of assuming $\varepsilon_m/\varepsilon_h = 1$, they suggested that the ratio of $\varepsilon_m/\varepsilon_h$ for viscoelastic fluids approaches 1.5 in the turbulent core just as that for Newtonian fluids does. Thus the eddy diffusivity of heat for viscoelastic fluids was obtained as

$$\varepsilon_h/\nu = 1.5\ f_m(y^+, r_0^+)^2\ DF_m^2\ (DF_h/DF_m)\ \frac{du^+}{dy^+} \tag{2.52}$$

The two adjustable constants in Equation (2.51), a_0 and a_1, were evaluated as $a_0 = 42$ and $a_1 = 120$ from the condition that ε_h/ν becomes equal to ε_m/ν for a Newtonian fluid near the wall at $Pr \approx \infty$. The final expression of heat eddy diffusivity for viscoelastic fluids was:

$$\varepsilon_h/\nu = 1.5 f_m(y^+, r_0^+)^2\ [1 - \exp(1 - y^+/A^+\ \sqrt{-\alpha + \sqrt{\alpha^2+1}}\ )]^2$$

$$\times\ \{[1 - \exp\ (\frac{-y^+}{42 + 120\ \sqrt{Pr}})]/[1 - \exp\ (\frac{-y^+}{A^+})]\}\ \frac{du^+}{dy^+} \tag{2.53}$$

The predictions of heat transfer coefficients using Equation (2.53) produce somewhat higher values compared with the recent experimental data [25, 26], especially at high concentrations. This may be due to the fact that the determination of adjustable constants in the proposed equations was based on the experimental data obtained in the thermally developing region.

The work of Hanna et al. [36] had two primary objectives. The first was to develop fundamental asymptotic analytical relationships for heat or mass transfer with drag reduction. The second was to formulate a new eddy diffusivity model leading to these analytical relationships in such a way that the results could be viewed as appropriate asymptotic solutions to the problem for the case of large Prandtl number. The first objective was achieved through the use of an asymptotic expansion of the Lyon equation [36] for large Prandtl number which is valid regardless of the particular eddy diffusivity distribution. The second objective was achieved through a new modification of drag reduction eddy diffusivity model developed by Diamant and Poreh [62]. They proposed the following expression

$$\ell^+ = Ky^+ \frac{[1 - \exp(-y^+/A^+)]}{[1 - \exp(-B^+ y^+)]^{1/2}} \tag{2.54}$$

where ℓ^+ is the dimensionless mixing length $(\frac{\ell u_\tau}{\nu})$. The parameter B^+ was related to the drag reduction by the following equation:

$$B^+ = 0.26 \exp [-2.98 (FR/FR_{max})] \tag{2.55}$$

This model could predict the experimental data of Smith et al. [51], which unfortunately were obtained in the thermally developing region.

Smith and Edwards [15] developed the simplified integral expressions for heat transfer, which were written as

$$St = \sqrt{f/2} \Big/ \int_0^{r_0^+} [(1-y^+/r_0^+)dy^+ \Big/ (\frac{1}{Pr} + \frac{1}{Pr_t}\frac{\varepsilon_m}{\nu})] - \beta \tag{2.56}$$

and

$$St = \sqrt{f/2}/(Pr - Pr_t) \int_0^{u_c^+} [du^+/(1 + \frac{Pr}{Pr_t}\frac{\varepsilon_m}{\nu})] + \frac{Pr_t}{\sqrt{f/2}} [4.07\sqrt{f/2} + 1] - \beta \quad (2.57)$$

for the constant wall heat flux condition and the constant wall temperature condition, respectively. In this study, the turbulent Prandtl number ($\varepsilon_m/\varepsilon_h$) was also assumed to be unity. They tested four different expressions of ε_m for Newtonian fluids proposed by several investigators [63, 67-69]. To account for the drag reduction, the apparent solution viscosity at the wall was used. Their results indicated that the expression of Mizushina and Ogino [69] produced the best predictions of heat transfer coefficients compared with the others. As for comparisons, this study used the experimental data of Gupta [70] which were collected in the short test section.

Most of the previous analytical works employed the direct analogy between momentum transfer and heat transfer, which recent studies have shown to be invalid for viscoelastic fluids. Furthermore, their results have been verified with inadequate experimental data, which were obtained in the thermally developing region under severe mechanical degradation. The existing models should be re-evaluated and possibly modified with the reliable experimental data of recent studies.

The review of previous experimental works clearly illustrated that they have been conducted under inadequate experimental conditions: 1) short test section, 2) severe mechanical degradation, and 3) insufficient study of rheological properties. Subsequently, the interpretation of the flow mechanisms and the development of the flow

models, which were based on those experimental results, were far from accurate. For the better understanding and reliable modeling of the flow mechanisms for viscoelastic fluids, new experimental and analytical study should be carefully designed and conducted free from the inadequacy of the previous works discussed so far.

CHAPTER III

EXPERIMENTAL APPARATUS

The current experimental facilities and procedures were designed so as to minimize the inadequacy of the previous experimental studies. This chapter documents the special features of the present experimental apparatus. Also included are the results of calibration runs which were conducted with tap water to verify the reliability of the experimental facilities and procedures.

3.1 Principle of Apparatus

A convenient method of relating pressure drop to mean flow rate is to use a dimensionless quantity called friction factor. The Fanning friction factor, which was used in this study, is defined as

$$f = \tau_w/(\frac{1}{2}\rho_f U^2) = \frac{D_i \Delta P}{4 L_p}/(\frac{1}{2}\rho_f U^2) \qquad (3.1)$$

Thus, the determination of friction factor requires measurements of the bulk mean velocity (U) and the pressure drop (ΔP) across the distance between two pressure taps (L_p) when the solution density (ρ_f) and the inside diameter of test section (D_i) are known.

In describing the heat transfer characteristics of fluids, the heat transfer coefficient was used to form some dimensionless quantities such as Nusselt number or Stanton number. The heat transfer coefficient (h)

is defined as

$$h = \frac{\dot{q}/(\frac{\pi}{4} D_i^2)}{T_{wi} - T_b} \tag{3.2}$$

The determination of heat transfer coefficient demands measurements of the heat flow rate ($\dot{q}$), the inside wall surface temperature (T_{wi}) and the bulk mean temperature (T_b). The heat flow rate can be measured in two ways: 1) from the enthalpy rise of the fluid determined from measurements of the flow rate and the difference between inlet and outlet bulk temperatures, and 2) from the electrical power supplied across the test section. Since the heat flow rate calculated from measurement of the potential drop across the tube has been proven to be more reliable [25, 26], this method was adapted in this study. The inside wall temperature can be determined using the Fourier's law of conduction [71] from measurement of the outside wall temperature (T_{wo}). For a fluid flowing inside a hollow cylinder with uniform heat generation in the tube wall and negligible heat loss to the surroundings, the following formula is valid:

$$T_{wi} = T_{wo} - \frac{\dot{q}}{2\pi(R_0^2 - R_i^2)K_s L_h} [R_0^2 \ln(R_0/R_i) - (R_0^2 - R_i^2)/2] \tag{3.3}$$

where L_h is the heated pipe length and K_s is the thermal conductivity of the pipe. The local bulk mean temperature (T_b) at the desired location x is determined from measurement of the exit bulk temperature (T_e). Since the heat generation in the tube is considered to be fairly uniform across the tube, the following equation holds:

$$T_b = T_e - (T_e - T_i) \cdot (L_h - x)/L_h \qquad (3.4)$$

where T_i is the inlet bulk temperature. In summary, the determination of heat transfer coefficient requires measurements of the heat flow rate, the inlet and outlet bulk temperatures, and the outside wall temperature when the dimensions of test sections and the properties of solutions are known. Details of the data reduction procedures are given in Appendix A along with the sample calculations and uncertainty analyses of friction factors and heat transfer coefficients for Newtonian and polymer solutions.

3.2 Experimental Facilities

The current experiments were conducted in the Basic Fluid Dynamics Laboratory at Oklahoma State University. The layout of flow circulation system is shown in Figure 3.1. The flow loop was designed to be used either as a once-through circulation system or a recirculation system. The special features of the current experimental facilities are as follows:

The test sections consist of two seamless stainless steel pipes (Type 304), which are 38 feet long. Stainless steel pipe was used in most of the previous experiments of this type and has proven to be effective in producing a uniform heat flux when a current passes through it. In addition, stainless steel is corrosion resistant, which is important for use with polymer solutions. The smaller pipe is 3/8" nominal schedule 80 pipe. The actual inside diameter is 0.436" and the L/D ratio is 1046. The larger pipe is 3/4" nominal schedule 80 with an actual inside diameter of 0.739". The L/D ratio is 617. These ratios

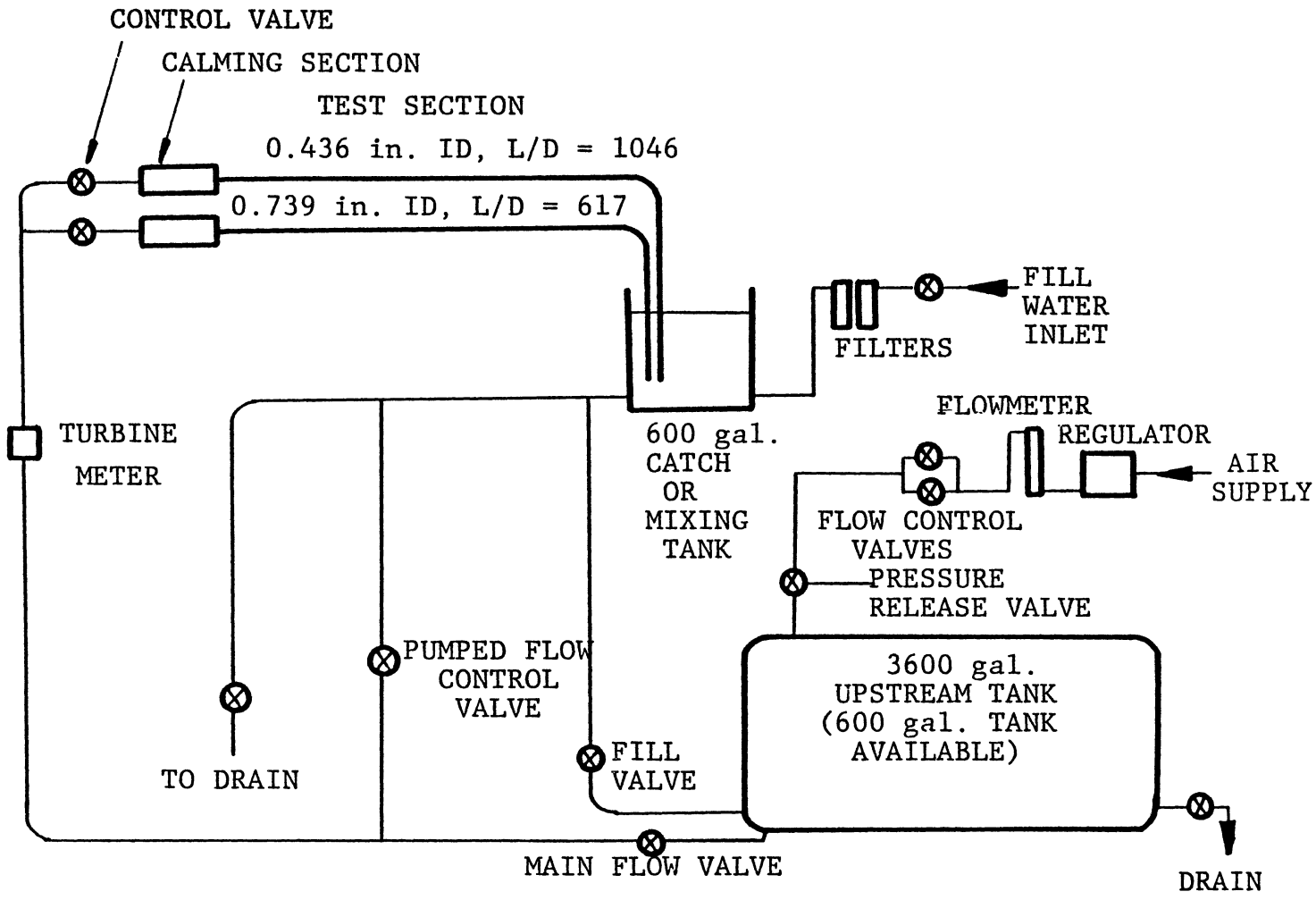

Figure 3.1 Schematic of the Flow Circulation System

are quite adequate for different types of polymers with varying degrees of concentrations to achieve the thermally fully developed condition. The end connections of test sections consist of 10" x 10" x 1/4" copper plates. The end plates were silver-arc soldered to the ends of the test section to secure a well defined electric circuit through the end plates. The upstream and downstream sections were electrically insulated from one another. The two-section arrangement allows the operator to choose the location where he desires the temperature profile to begin developing. A detailed drawing of the test section is shown in Figure 3.2.

The constant wall heat flux boundary condition was maintained by a Lincoln DC-600 welder. This welder is a SCR output controlled by three phase DC power source. It can operate in the constant voltage or constant current (variable voltage) mode, and has a 100% duty cycle rating at 600 amps and 44 volts [72]. It has built-in voltage compensation to hold the output essentially constant even when the input voltage fluctuates between a range of 10%. The test sections were insulated from the environments using the fiberglass pipe insulation and vapor-proof pipe tape. Double wrapping of fiberglass insulation was deemed enough to produce the well-insulated condition.

To determine the hydrodynamic entrance lengths and the friction factors for different types of polymers with wide range of concentrations, numerous pressure taps were drilled into the test section as shown in Figure 3.3. In drilling the pressure taps, one has to ensure that the ratio of tube wall thickness to tap hole diameter be greater than 1.5 and less than 15 for the best results [28]. Following this recommendation, 5/64" holes were drilled in the 3/8" pipe giving a

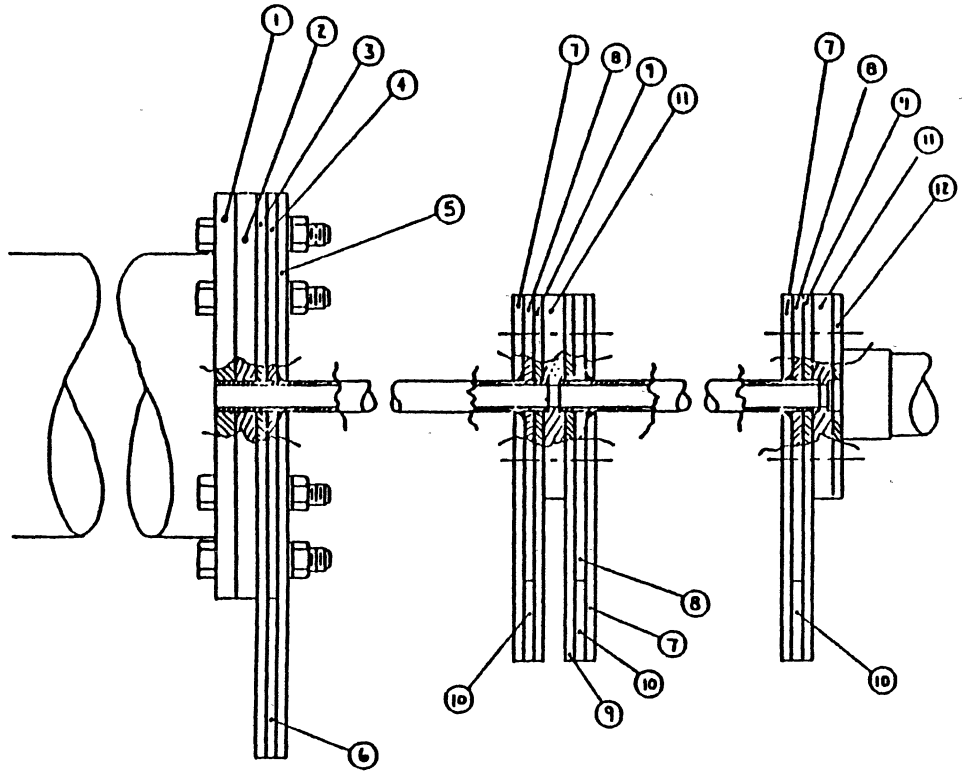

NOTATION

1. Chamber Collar - 3
2. Insulation - 1
3. Cooper Plate - 1
4. Copper Plate - 2
5. Bus Bar - 1
6. Bus Bar - 2
7. Cooper Plate - 3
8. Bus Bar - 3
9. Bus Bar - 4
10. Bus Bar - 5
11. Insulation - 2
12. Collar

Figure 3.2 Test Section Assembly

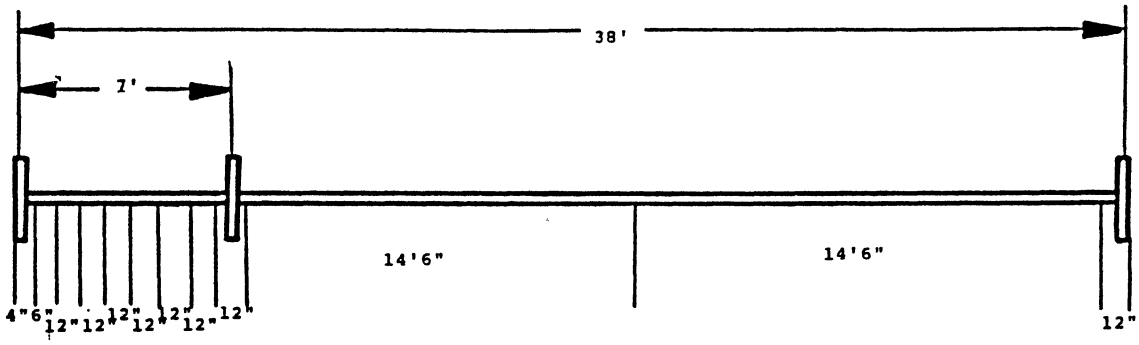

(a) 3/4" Test Section

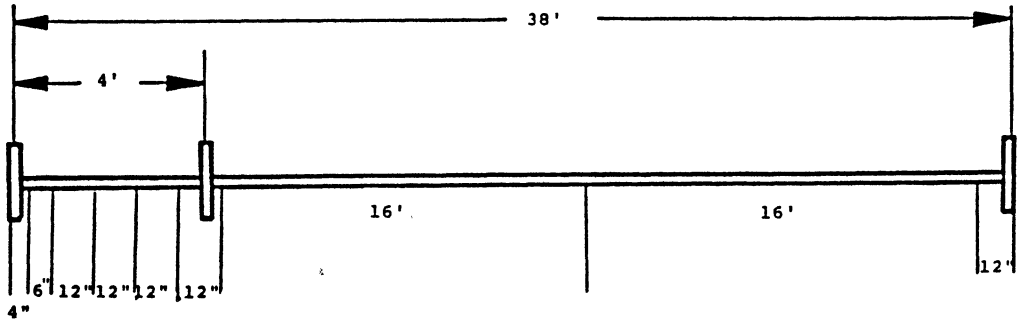

(b) 3/8" Test Section

Figure 3.3 Pressure Tap Locations

thickness to diameter ratio of 1.57. For the 3/4" pipe, 3/32" holes were drilled giving the ratio of 1.64. The inside surface of the tube was cleaned and deburred so that no ragged edges remained from the drilling operation. The edges of pressure tap holes were square and smooth so as to minimize the disturbance of flow. For the measurements of pressure drop, one multi-column water manometer and one U-tube mercury manometer were installed. Since the multi-column manometer can yield several simultaneous readings of pressure drop with good resolution, it was used for the measurements in the entrance region. The two pressure taps located at the far downstream of the tube were used to measure the pressure drop in the fully developed region. The long interval between these taps was expected to produce the relatively large pressure drop. So the mercury manometer was used for this measurement. The resolution of the manometers is 0.1 inches of the solutions used. The temperatures along the test section were measured with copper-constantan thermocouples of gage #30 manufactured by Omega Engineering, Inc.. The layout of thermocouples is shown in Figure 3.4. To obtain clean and fine beads, the ends of thermocouple wires were welded together using a nitrogen-arc welder. The length of each thermocouple wire was 12" plus 1.5 times the outside diameter of the tube. This length was long enough to eliminate thermocouple error due to lead wire heat conduction in the temperature gradient field [28]. Each thermocouple was wrapped around the tube about one and one half turns. All of the thermocouples were calibrated individually with the use of the data logger and the platinium resistance thermometer in the Temperature Calibration Room at Oklahoma State University. The maximum uncertainty of a temperature reading was estimated to be ±0.2 F due to

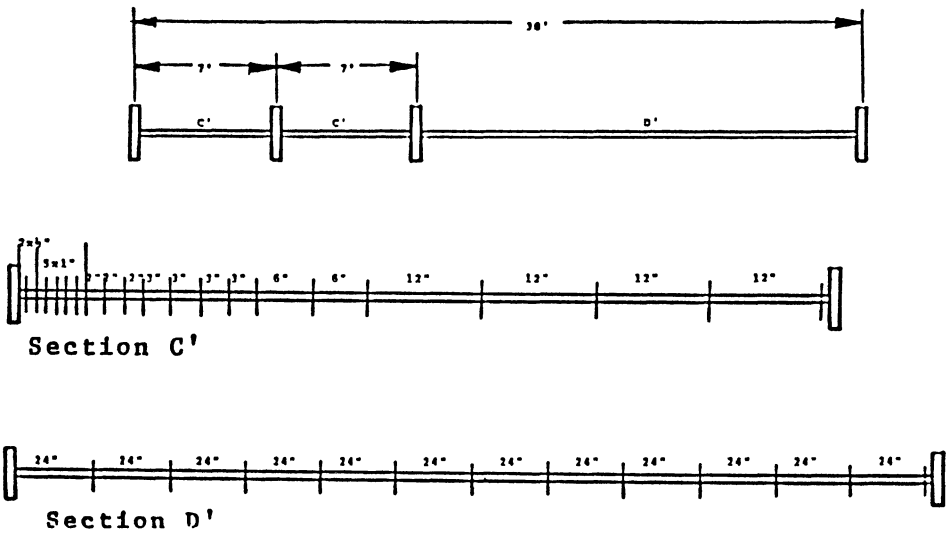

(a) 3/4" Test Section

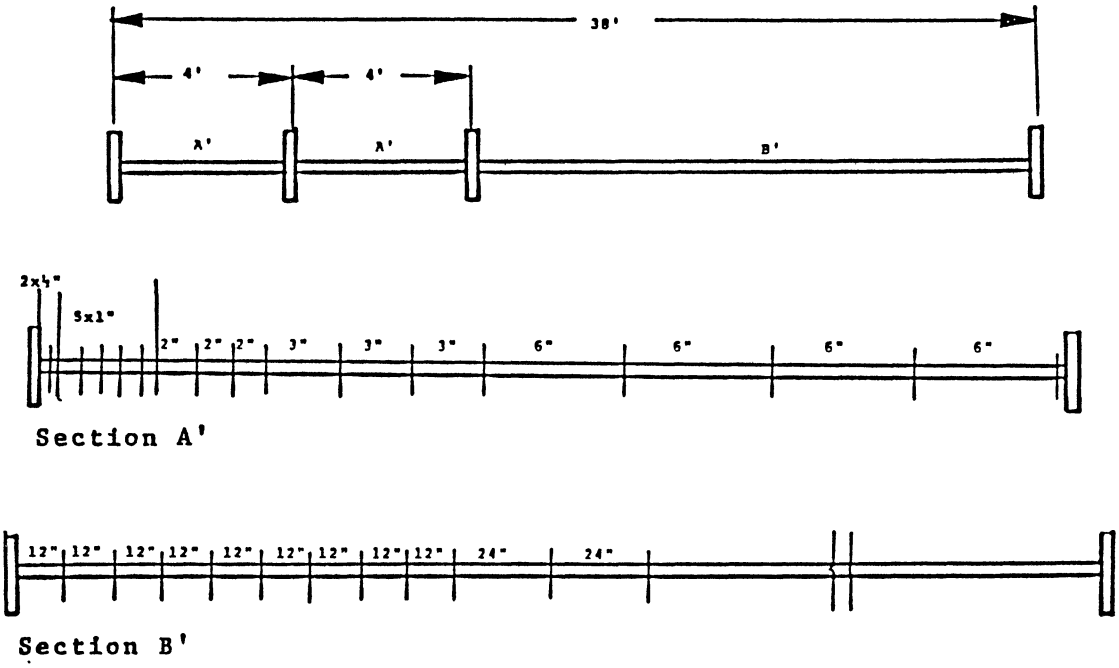

(b) 3/8" Test Section

Figure 3.4 Thermocouple Locations

the temperature fluctuation in the water bath. The calibrated thermocouples were connected to a forty channel data logger (Model 9302) manufactured by Monitor Labs, whose resolution is 0.1 F. The leading wire of thermocouples to the data logger was a copper-constantan duplex grade thermocouple wire of gage #20 manufactured by Omega Engineering, Inc.. To eliminate the effect of electrical current flowing through the test section on the thermocouple readings, copper-oxide cement was used as the adhesive. This procedure was verified through several calibration runs with tap water.

A calming chamber was installed upstream of each test section. It consists of three perforated screens in a plexiglass tube of 6" diameter. This calming section had dual purposes. First, it serves to straighten a flow that is likely to be distorted by rough connections. As the fluid passes the screens in the enlarged chamber, the flowfield settles down and adjusts itself. In this way, the conditions of incoming fluid are relatively well-defined. Secondly, the calming section serves to remove air bubbles in the fluid. Since the density of air is lighter than the fluid, the undesired air bubbles are collected in the upper part of the calming section and released through an air vent.

To obtain the bulk temperature at the end of the test section, a temperature well was installed just downstream of each test section. This consists of five baffles, which were considered to produce well-mixing of the fluid [28]. This ensured that a bulk mean temperature, rather than a local one, was measured. The layout of temperature well is shown in Figure 3.5. Since the inlet temperature of the fluid was uniform across the test section, it was measured by means of a

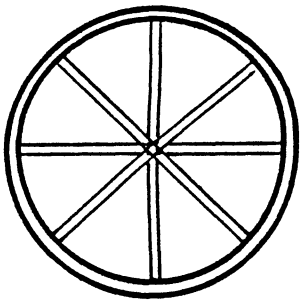

(a) Front View

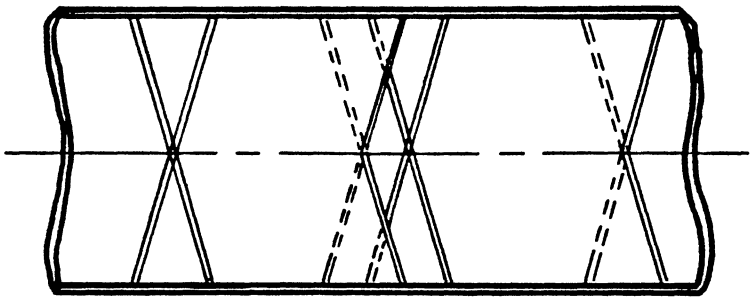

(b) Side View

Figure 3.5 Schematic of Temperature Well

thermocouple probe inserted in the calming section.

A one inch turbine meter manufactured by Halliburton, Inc. was installed upstream of the calming section for measurement of the flow rate. This meter produces a voltage spike which can be read with a frequency counter manufactured by Hewlett Packard and converted to a flow rate. As compared with the conventional method of directly weighing the solution volume collected over a certain time period, this technique can show any fluctuation in flow rate as well as yield an accurate value of average flow rate. For more details, see reference [73].

The experimental facilities also include one mixing tank of 600 gallons and two storage tanks of 600 and 3600 gallons. All of the test solutions were prepared in the mixing tank. The 600 gallon storage tank was used to store the test solutions. The 3600 gallon tank was used to store tap water which was needed to clean the built-up polymer on the inner surface of the test section after each experiment.

The test fluid was driven by the pneumatic control system whose layout is illustrated in Figure 3.6. The blowdown operation mode minimized polymer degradation due to the rupture of molecular bonds. The system largely consists of two pressure gages, one pressure regulator and one vernier flow control valve. The pressure in the air supply line was read by one pressure gage and the pressure in the tank by the other one. The tank pressure was controlled by the pressure regulator. The desired flow rate was obtained by the vernier flow control valve. While the supplied pressure was approximately 80 psi, the experiments were conducted by maintaining the pressure in the tank ranging from 30 to 40 psi. The flow rates obtained by this system, even

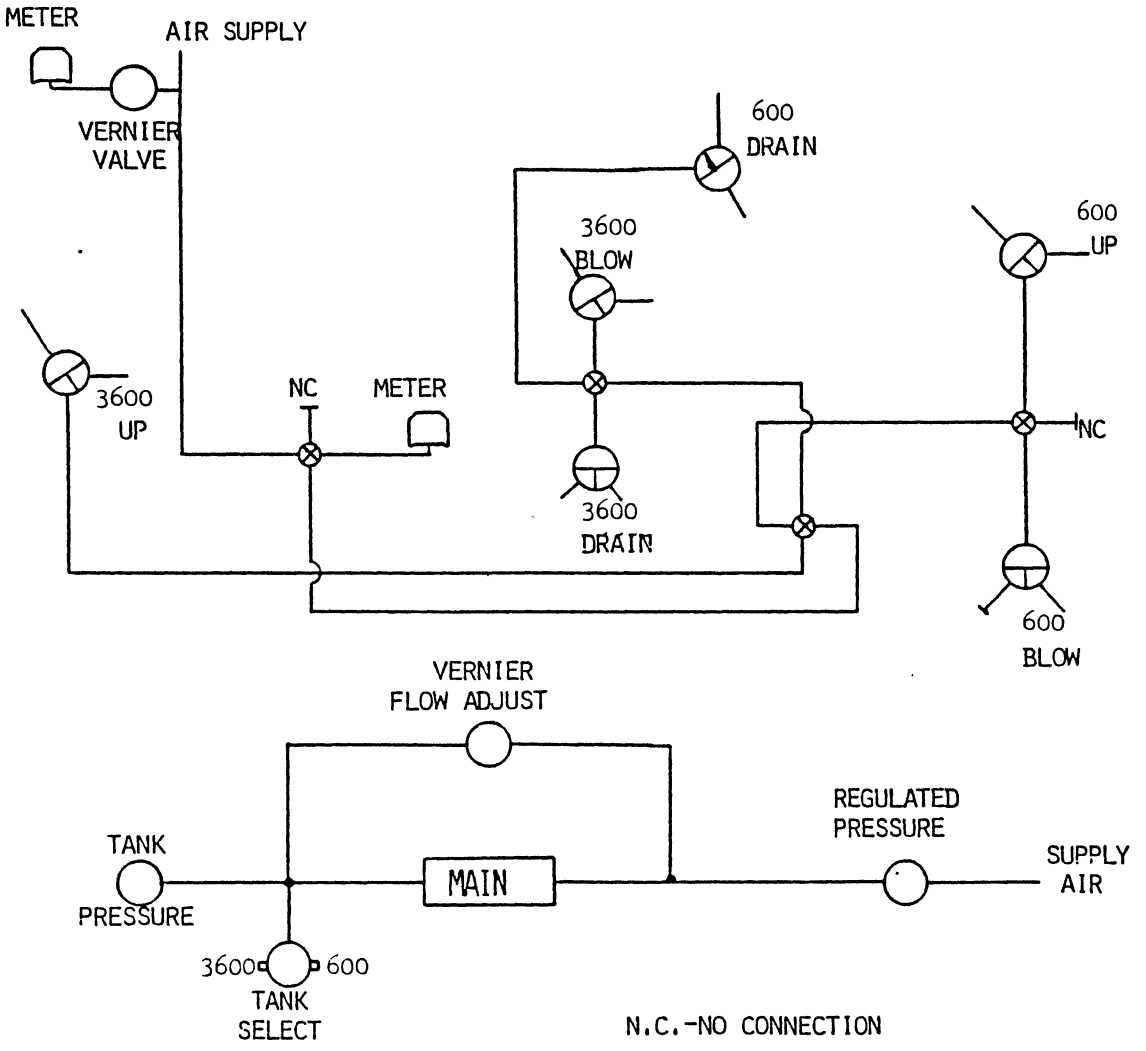

Figure 3.6 Layout of the Pneumatic Control System

though severely diminished due to considerable friction drag in the test section of small diameter and long length, have been proven to cover Reynolds number based on the apparent viscosity up to 1.2×10^5.

The viscosity data of polymer solution to be used in these experiments were measured as a function of shear rate. Solution samples were taken from the downstream head tank during each run or immediately after each run. Two Couette viscometers (Brookfield Synchro-Electric Model LVT with UL adaptor and a Fann Model VG) and a capillary tube viscometer (0.9398 mm I.D. and l/d = 325) were used to obtain shear rate dependence of viscosity. The Brookfield viscometer could cover shear rates from 0.36 sec^{-1} to 68.8 sec^{-1}; the Fann viscometer from 170 sec^{-1} to 3254 sec^{-1}. The capillary tube viscometer built for this project has been proven to cover shear rates from 10^3 sec^{-1} to 2×10^4 sec^{-1}. With these viscometers available, it was possible to measure viscosities at wide ranges of shear rates, which are required to obtain reliable estimation of the fluid time scale, and consequently the Weissenberg number. The calibration runs with Newtonian fluids for the viscometers employed showed that these viscometers would result in a maximum error of 3 ~ 5% as compared with the well-established data [28, 44]. It was estimated that the viscosity data for polymer solutions could be measured within the maximum uncertainty of 10%.

3.3 Experimental Procedure

3.3.1 Test Fluid Preparation

The polymer solutions employed in the current study were aqueous solutions of polyacrylamides (Separan AP-273 and Separan AP-30) from the Dow Chemical Company and Polyox (WSR-301) from the Union Carbide

Corporation. Polyacrylamide has the following molecular structure:

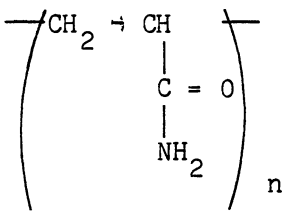

The average molecular weight was estimated as 4 millions and 6 millions for Separan AP-30 and Separan AP-273, respectively. The molecular structure of polyox is $\{ O - CH_2CH_2 \}_n$. The average molecular weight was estimated as 4 millions. All of these polymers are water-soluble and highly viscoelastic. For more details, refer to the commercial literatures [74, 75]. The basic solvent was Stillwater, Oklahoma tap water. Table V presents a summary of the test fluids used in this study.

The prescribed quantity of polymer required for the desired concentration was weighed on a balance scale. Approximately 500 gallons of water was collected in the catch tank. The water was agitated with a wooden paddle, and the polymer was added into the turbulent wake by gently sifting through a triple-screen flow sifter. The sifting effectively prevented the polymer from clumping, which would produce gelatinuous globes. After mixing, the solutions were allowed to stand over approximately one day for complete dissolution. Before the solutions were dumped into the storage tank, these solutions were thoroughly stirred for the breakdown of the possible stratification.

3.3.2 Test Procedure

The test section was cleaned by circulating tap water at high flow

TABLE V

TEST FLUIDS

Operation Mode	Pipe Diameter	Polymer Type	Polymer Concentration (PPM)
Once-through	3/4", 3/8"	Separan AP-273 WSR-301	10, 50, 100, 300, 500, 1000
Recirculation	3/4"	Separan AP-273	1500
Once-through (Dilution)	3/4"	Separan AP-30	3000

rate with the welder on. The cleanness of the test section was checked regularly with the measurements of pressure drop for tap water.

The test fluid was driven from the storage tank to the test section for the measurements of pressure drop and heat transfer coefficient. For accurate measurements, the air bubbles entrapped in the flow system and in the tubings between the pressure tap and the manometer should be eliminated by opening all air release valves. By adjusting the pressure regulator and the vernier flow control valve, the desired flow rate was obtained. In this stage, the welder was started to maintain the constant heat flux boundary condition. During operation of the welder, one should be extremely careful to avoid an incidental contact with the electricity of high current. When the system became steady, the data collection for friction factors and heat transfer coefficients was carried out simultaneously. This included the measurements of pressure drop, inlet and outlet fluid bulk temperatures, outside wall temperature, potential drop across the heated tube, and flow rate. Fluid samples were taken from the catch tank for the viscosity measurements. The test fluid leaving the test section was either emptied into the building drainage for the once-through flow mode or collected in the catch tank for the recirculation flow mode. For the latter case, the flow system was regularly cleaned out using tap water to avoid the built-up polymer on the tube wall. The data collection was carried out at several different flow rates.

3.3.3 Calibration Runs

Test runs with a Newtonian fluid (tap water) were performed to check the reliability of the experimental facilities and the overall

experimental procedures. The turbine meter, which was installed upstream of the calming section for the measurement of flow rate, was calibrated for tap water, polyox solution of 500 ppm, and Separan AP-273 solutions of 100, 200, 500, and 1000 ppm. The calibration results presented in Figure 3.7 suggested a linear relationship between the flow rate and the turbine meter frequency. All of the calibration data were correlated using the first order least squares equation [76, 77] as follows:

$$\dot{Q} = -0.00746 + 0.06748F \tag{3.5}$$

Where $\dot{Q}$ is the flow rate in gpm and F is the frequency in Hz. Equation (3.5) correlated the measured flow rates within ±5% of the reading as long as $F \geq 50$ Hz. Figure 3.7 indicates that there was slight effect of polymer on the turbine meter. For polymer concentrations greater than 500 ppm, it is recommended to use the correction factor of 0.95 for the better estimation of flow rate.

The measurements of friction factors and heat transfer coefficients for tap water were taken to check the reliability of the experimental apparatus. The ratio of $T_w(°F)/T_b(°F)$ was maintained less than or close to 1.1 for both water and polymer solutions so as to minimize the feasible effect of natural convection on heat transfer due to the large bulk-to-wall temperature difference. For friction factors for Newtonian fluids, Kays [78] suggested the following equations:

$$f = 0.079\ Re^{-0.25} \qquad 5 \times 10^3 \leq Re \leq 3 \times 10^4 \tag{3.6}$$

$$f = 0.046\ Re^{-0.2} \qquad 3 \times 10^4 \leq Re \leq 10^6 \tag{3.7}$$

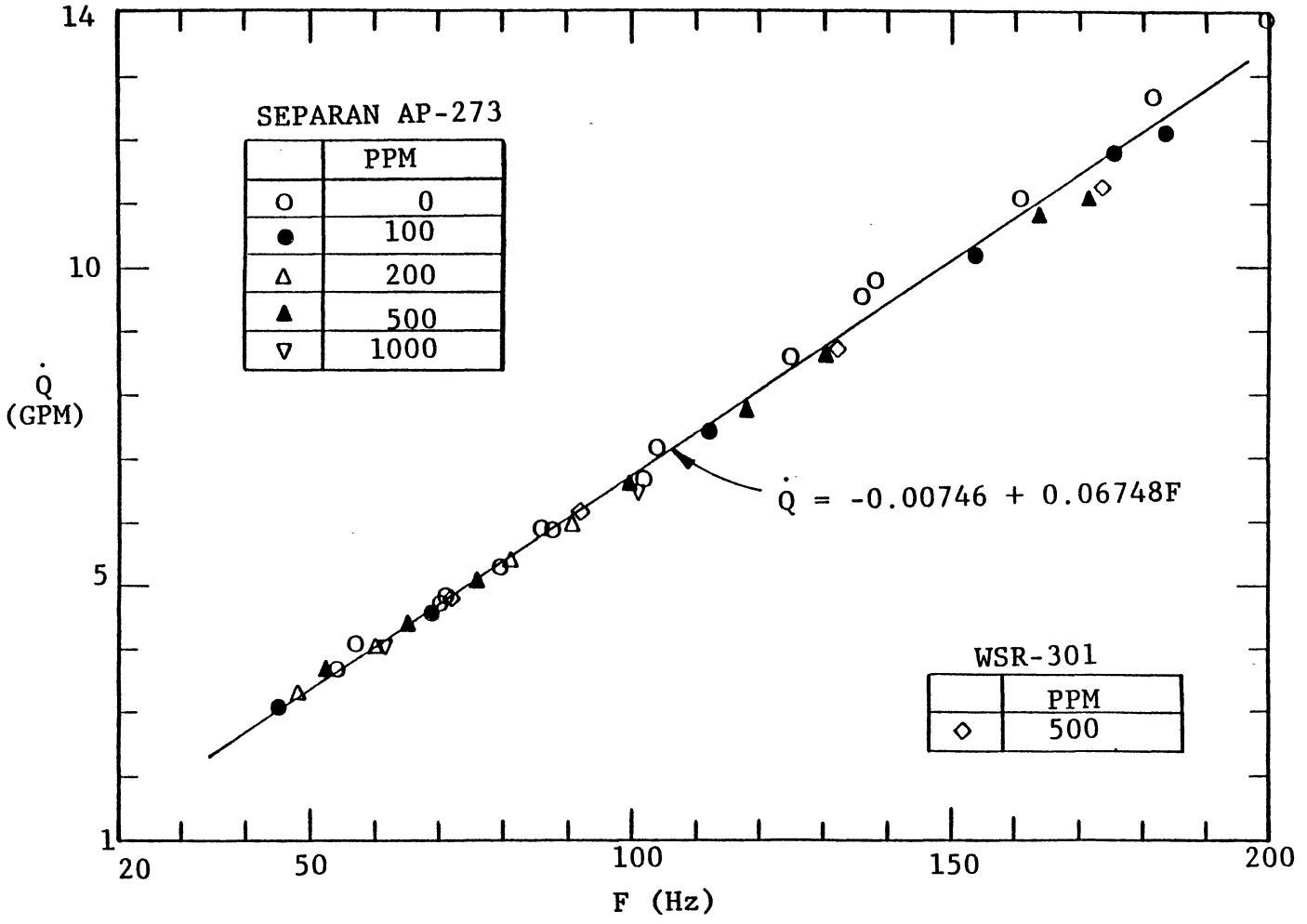

Figure 3.7 Calibration of Turbine Meter

Another empirical equation as given by McAdams [79] is:

$$f = 0.0014 + 0.125\ Re^{-0.32} \tag{3.8}$$

Figure 3.8(a) shows that the current experimental facilities can produce reliable friction factor data for the Newtonian fluid case. The experimental heat transfer results, interpreted as Nusselt number, are presented with the established correlations for Newtonian fluids in Figure 3.8(b). The correlations used for comparison are:

Allen and Eckert [80]: $$Nu = 0.0258\ Re^{0.8}\ Pr^{0.4} \tag{3.9}$$

Kays [78]: $$Nu = 0.0155\ Re^{0.83}\ Pr^{0.5} \tag{3.10}$$

Dittus and Boelter [81]: $$Nu = 0.023\ Re^{0.8}\ Pr^{0.4} \tag{3.11}$$

The results of the test runs with water are proven to be in good agreement with the well-established correlations for Newtonian fluids.

After several successful calibration runs for water, a series of experiments for polymer solutions were conducted in order to fulfill the objectives specified in Chapter I. The experimental data are presented with detailed discussion in Chapter IV.

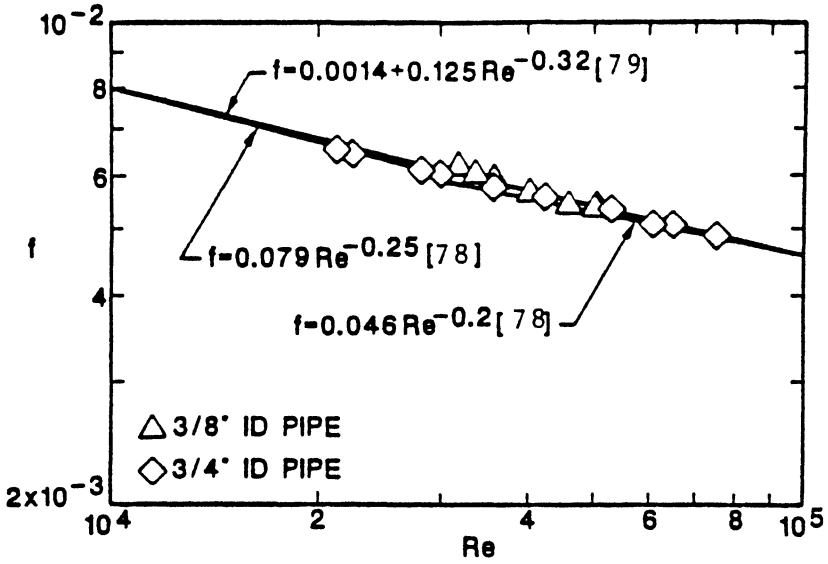

(a) FRICTION FACTOR

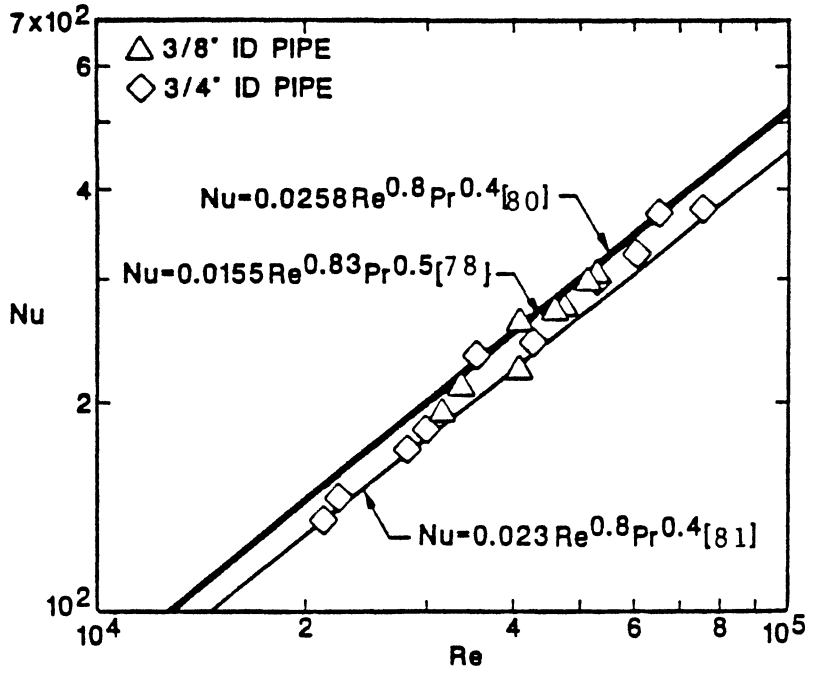

(b) NUSSELT NUMBER

Figure 3.8 Calibration Data for a Newtonian Fluid (Tap Water)

CHAPTER IV

RESULTS AND DISCUSSION

Numerous experiments have been conducted to fulfill the objectives specified in Section 1.3. All of the experimental data are presented and discussed here. This chapter is subdivided into the following areas: 1) study of the Powell-Eyring model, 2) characteristics of viscoelastic fluids, 3) scaling method for pipe diameter and polymer concentration, 4) critical Weissenberg number for heat transfer, and 5) heat transfer correlation.

4.1 Study of the Powell-Eyring Model

It was mentioned in Section 1.2.4 that the successful correlation of polymer characteristics in terms of Weissenberg number depends on the accurate estimation of the fluid time scale. In this study, the Powell-Eyring model, which has been known to be superior to other models, was used to estimate the fluid time scale. The Powell-Eyring model has the following expression:

$$\eta_a = \eta_\infty + (\eta_0 - \eta_\infty) \frac{\sinh^{-1}(\lambda\dot{\gamma})}{\lambda\dot{\gamma}} \qquad (4.1)$$

Since this model includes the zero shear rate and the infinite shear rate viscosities as major parameters, it is very important to study the sensitivity of the model to variations in those two parameters. The

rheological data of Kwack [26], which had been presented in Figure 1.2, was used.

4.1.1 Sensitivity of the Fluid Time Scale to Variations in the Zero Shear Rate Viscosity

It has been well-known that the elasticity in a viscoelastic fluid is reflected by the pronounced increase of shear viscosity with the decrease of shear rate at the low range of shear rates as shown in Figure 1.2. The Powell-Eyring model used in this study includes the zero shear rate viscosity as a key parameter. However, the mechanical sensitivity of the viscometer available for the particular use does limit the lowest measurable shear rate to a certain range. Skelland [44] pointed out that the extrapolation of shear viscosity data for non-Newtonian fluids is not reliable at such a low shear rate. So it is valuable to study the sensitivity of the Powell-Eyring model to the variation in the zero shear rate viscosity in the estimation of the fluid time scale. This study used the apparent viscosity data of Kwack [26] for Separan AP-273. Figure 4.1 shows the dependency of the fluid time scale on the variations in the zero shear viscosity for the concentrations of 10, 300, and 1000 ppm. It can be noticed from this figure that the higher concentration solution demands the zero shear rate viscosity to be measured at much lower shear rate in order to maintain the same accuracy in the estimation of the fluid time scale. Furthermore, the change of the fluid time scale is drastic for small variation in the zero shear rate viscosity for the high concentration solution. Figure 4.1 suggests that the reliable estimation of the fluid

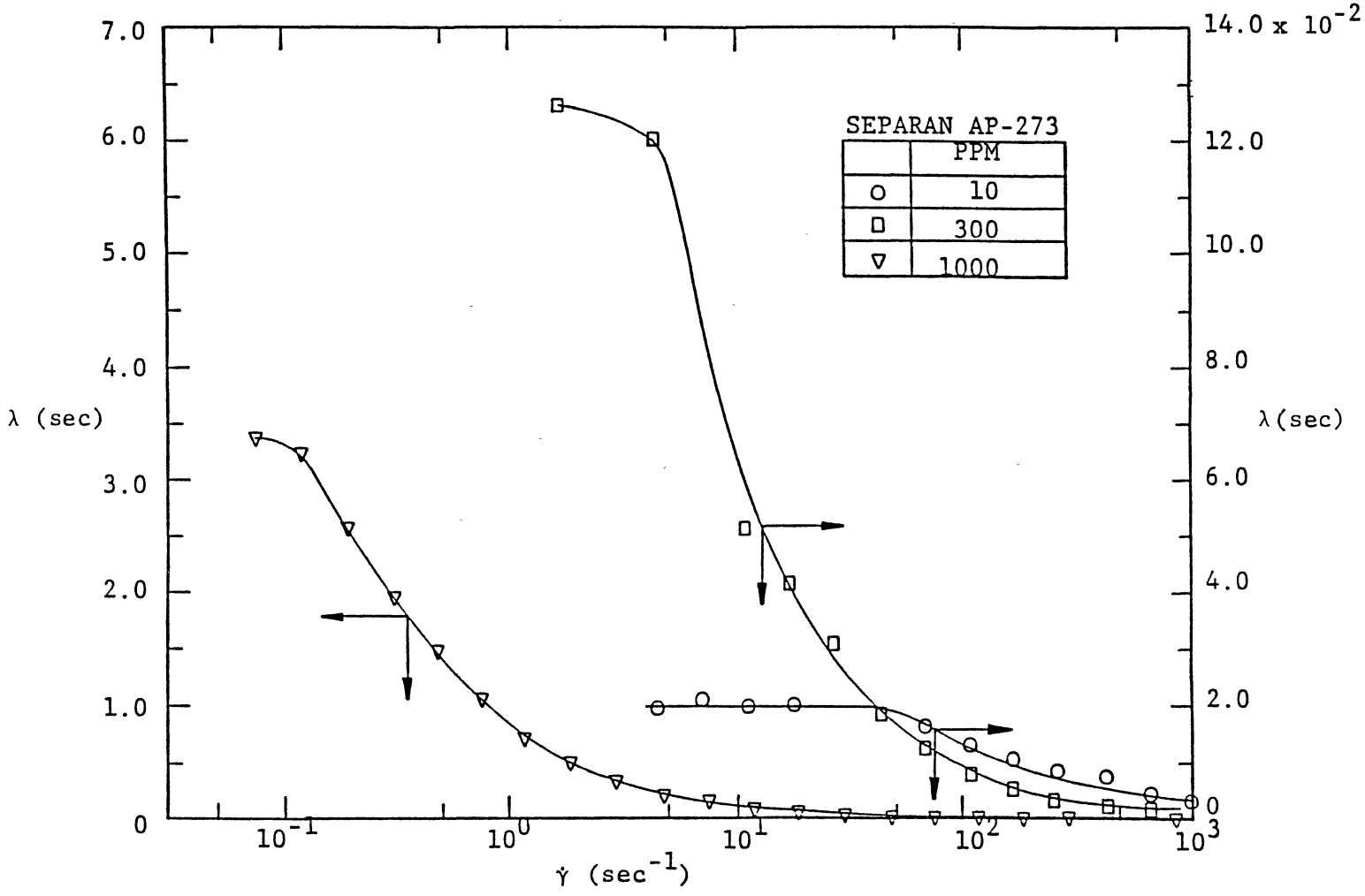

Figure 4.1 Sensitivity of the Fluid Time Scale to Variations in the Zero Shear Rate Viscosity Using Powell-Eyring Fluid Model

time scales for 10, 300 ppm and 1000 ppm demand the viscosity data to be measured at shear rates of order of 10 sec^{-1}, 1 sec^{-1} and $10^{-1}sec^{-1}$, respectively. This implies that with the increase of polymer concentration, the zero shear rate viscosity should be measured at much lower shear rates.

4.1.2 Sensitivity of the Fluid Time Scale to Variations in the Infinite Shear Rate Viscosity

The other parameter of the Powell-Eyring model is the infinite shear rate viscosity. Figure 1.2 indicates that as compared with the pronounced change in the zero shear rate viscosity, the infinite shear rate viscosity shows a modest increase with the increase of polymer concentration. Since it is not feasible to measure the viscosity at the infinite shear rate, the viscosity obtained at the possible highest shear rate should be used as the infinite shear rate viscosity. Consequently, it is essential to study the dependency of the fluid time scale on variations in the infinite shear rate viscosity. Figure 4.2 shows the sensitivity of the Powell-Eyring model to the variations in the infinite shear rate viscosity in the determination of the fluid time scale for the concentrations of 10, 300 and 1000 ppm. It can be noticed from this figure that the characteristic curves of the fluid time scale tend to flatten out at the high shear rate range, especially at the shear rates greater than $10^{3}sec^{-1}$. Kwack [26] suggested that the infinite shear rate viscosity should be evaluated at the shear rate greater than $10^{5}sec^{-1}$ for reliable estimation of the fluid time scale. However, the viscosity at such a high shear rate of $10^{5}sec^{-1}$ is

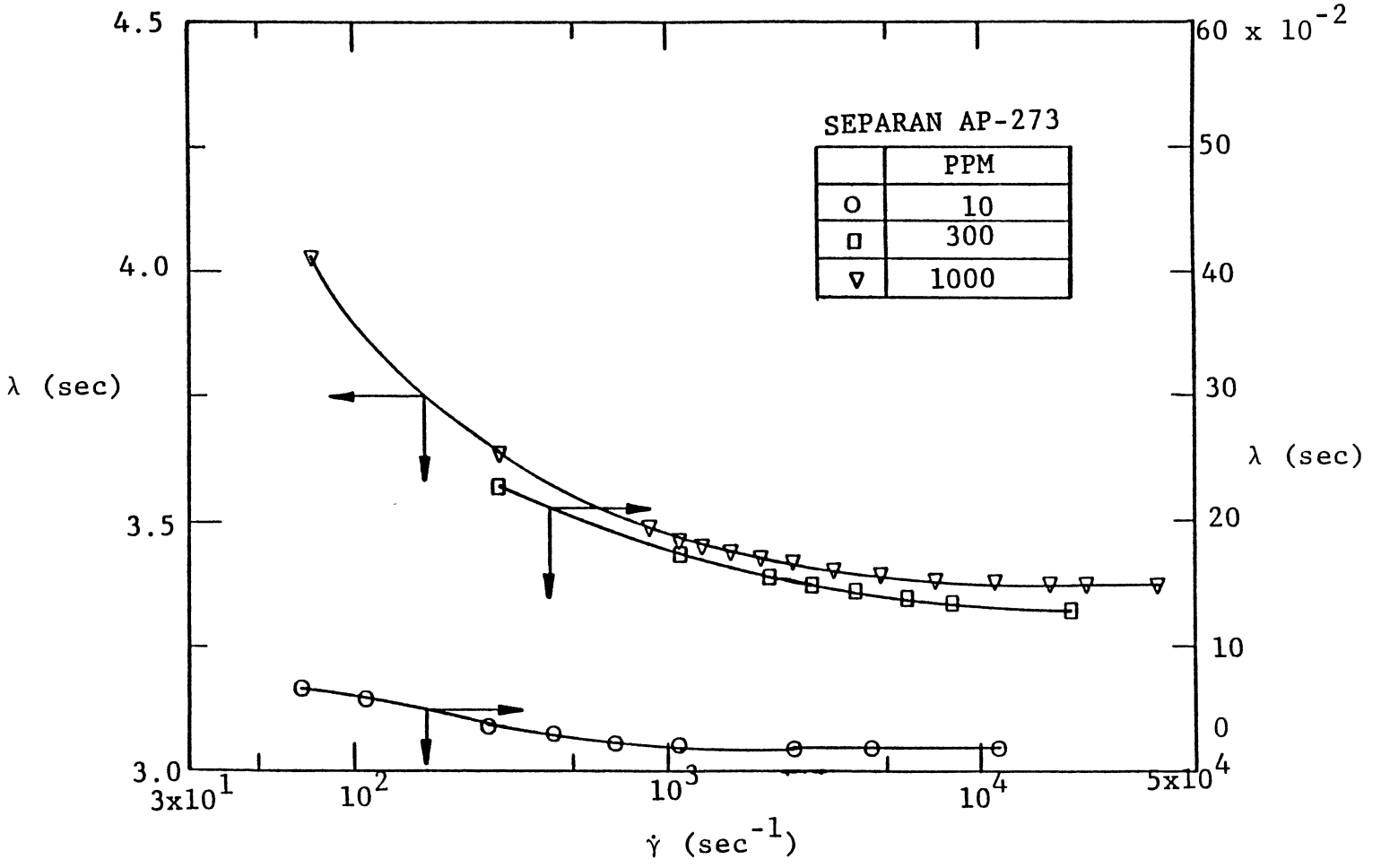

Figure 4.2 Sensitivity of the Fluid Time Scale To Variations in the Infinite Shear Rate Viscosity Using Powell-Eyring Fluid Model

obtainable not by a direct measurement, but by an extrapolation. Unfortunately, the uncertainty from the extrapolation of viscosity data at such high shear rates has not been fully known. The current study indicates that the uncertainty in the estimation of the fluid time scale, due to variations in the infinite shear rate viscosity, is negligible if the viscosity is measured at a shear rate greater than $10^4 sec^{-1}$. This shear rate can be readily obtained in most laboratories with the use of a capillary tube viscometer.

4.1.3 Performance of the Powell-Eyring Model

The fluid time scale was estimated by a linear regression method using all the viscosity data. So it is expected that the fluid model should be able to reproduce accurately all the viscosity data with the back-substitution of the fluid time scale into the expression with the measured values of the zero shear rate viscosity and the infinite shear rate viscosity. In this study, the performance of a model is defined as the capability of the model to generate the original viscosity data. Figure 4.3 shows the characteristic curves generated by the Powell-Eyring model and the Eyring model (see Table III) together with the original viscosity data (see Figure 1.2). Both models have been most commonly used in the previous works. It is clearly shown in Figure 4.3 that the performance of the Eyring model is extremely poor at the high shear rate regions. The Powell-Eyring is the improved version of the Eyring model with the addition of the infinite shear rate viscosity. As compared with the Eyring model, the Powell-Eyring model performs relatively well at both low and high shear rates. However, considerable gap still exists between the calculated data and the measured ones at

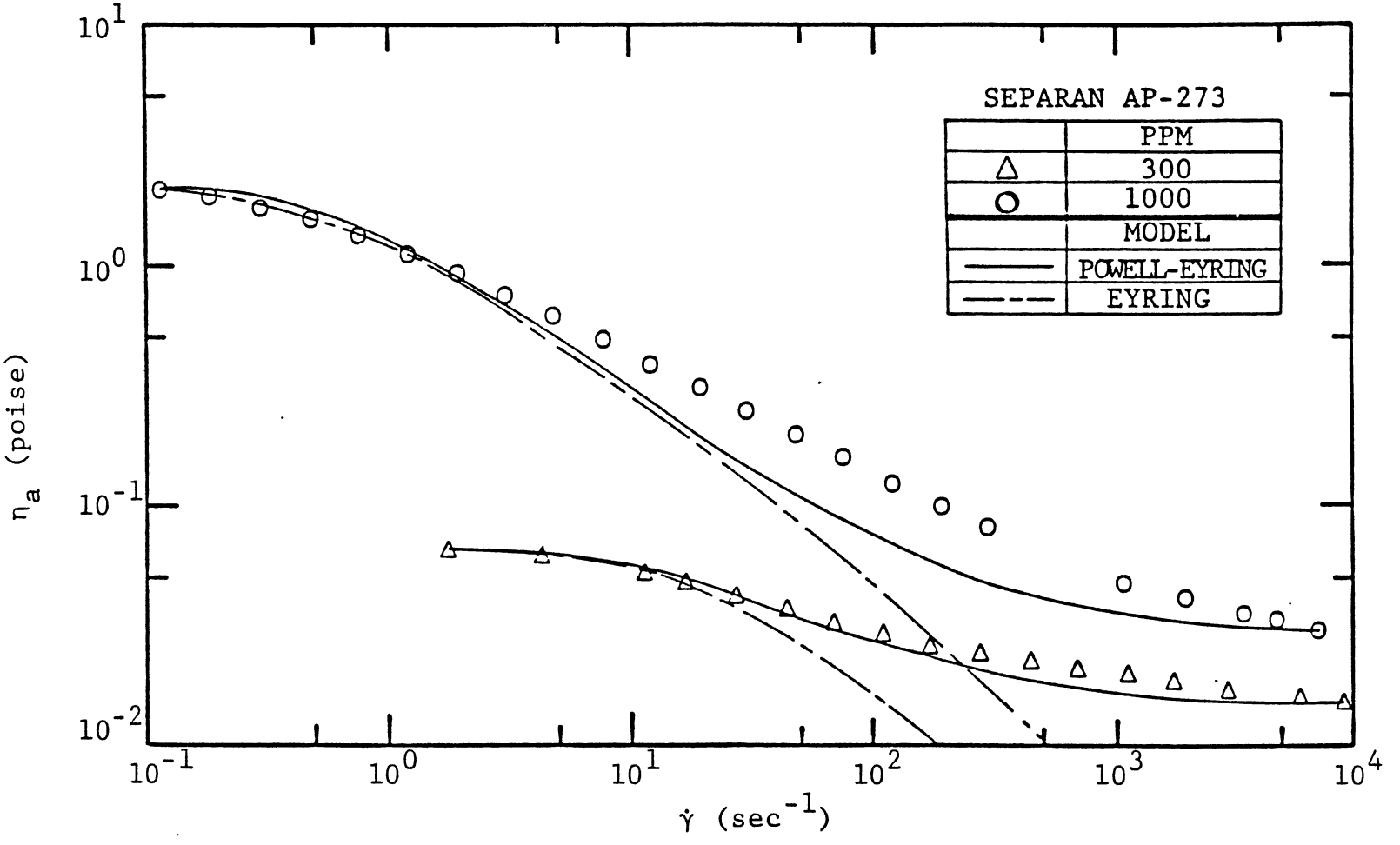

Figure 4.3 Performance of the Fluid Models as Compared With Measurements of Kwack [26]

the intermediate shear rates. This difference is more pronounced for the higher concentration. The case of 10 ppm is excluded from Figure 4.3, because there is virtually no difference between the predictions and the measurements. It can be noticed in Figure 4.3 that there are two regions showing gaps between the predictions and the measurements. The first region, where the predictions are greater than the measurements, is located at the low shear rate region. The second region, where the predictions are less than the measurements, is located at the relatively high shear rate region. It was found that in order to bring the predictions close to the measurements, a fluid time scale greater than the estimated value is needed at the first region, and smaller one at the second region. This implies that an arbitrary increase or decrease of the fluid time scale can not close the gap between the predictions and the measurements. It is not fully known that how much this gap can affect the estimation of the fluid time scale. However, since the elasticity of a fluid is mainly characterized by the zero shear rate viscosity, this effect should be of little significance. Even though there are a few fluid models available in the published literature [45] which are known to have slight edge in performance as compared with the Powell-Eyring model, the use of those models in this study was precluded because of their complexity and arbitrariness in the determination of the fluid time scale.

4.2 Characteristics of Viscoelastic Fluids

To interpret the characteristics of viscoelastic fluids, a set of friction factors and heat transfer coefficients have been measured in the test sections of different diameters for two different type polymer

solutions with various concentrations. These measurements were conducted simultaneously under the constant wall heat flux condition using the once-through mode in the hydrodynamically and thermally fully developed region. For study of the rheology, the apparent viscosity data for each solution were measured using two rotational viscometers and one capillary tube viscometer described in Section 3.2. Samples of polymer solutions were collected at the exit of the flow loop. In this study, particular attention was paid to the effects of polymer concentration, pipe diameter and polymer type on the momentum and heat transfer behaviors of the viscoelastic fluids. All of the experimental data are tabulated in Appendix B.

4.2.1 Polymer Concentration

A series of experiments were conducted in the 3/4" test section for aqueous Separan AP-273 solutions with the concentrations of 10, 50, 100, 300, 500, and 1000 ppm. The apparent viscosity data except for 10 ppm are presented in Figure 4.4 with the fluid time scales calculated using the Powell-Eyring model. This exception is due to the fact that the viscosity data for 10 ppm are lower than 10^{-2} poise (for the tabulated data, see Appendix B). It is shown in Figure 4.4 that the viscosity of a polymer solution has an asymptotic trend at the ranges of very low and high shear rates and strongly depends on the shear rate at the intermediated shear rate range. The effect of concentration on the viscosity is remarkable at the low shear rate range, which also implies the pronounced increase of elasticity in the solutions.

The Fanning friction factors are presented as a function of apparent Reynolds number in Figure 4.5. This figure shows that the

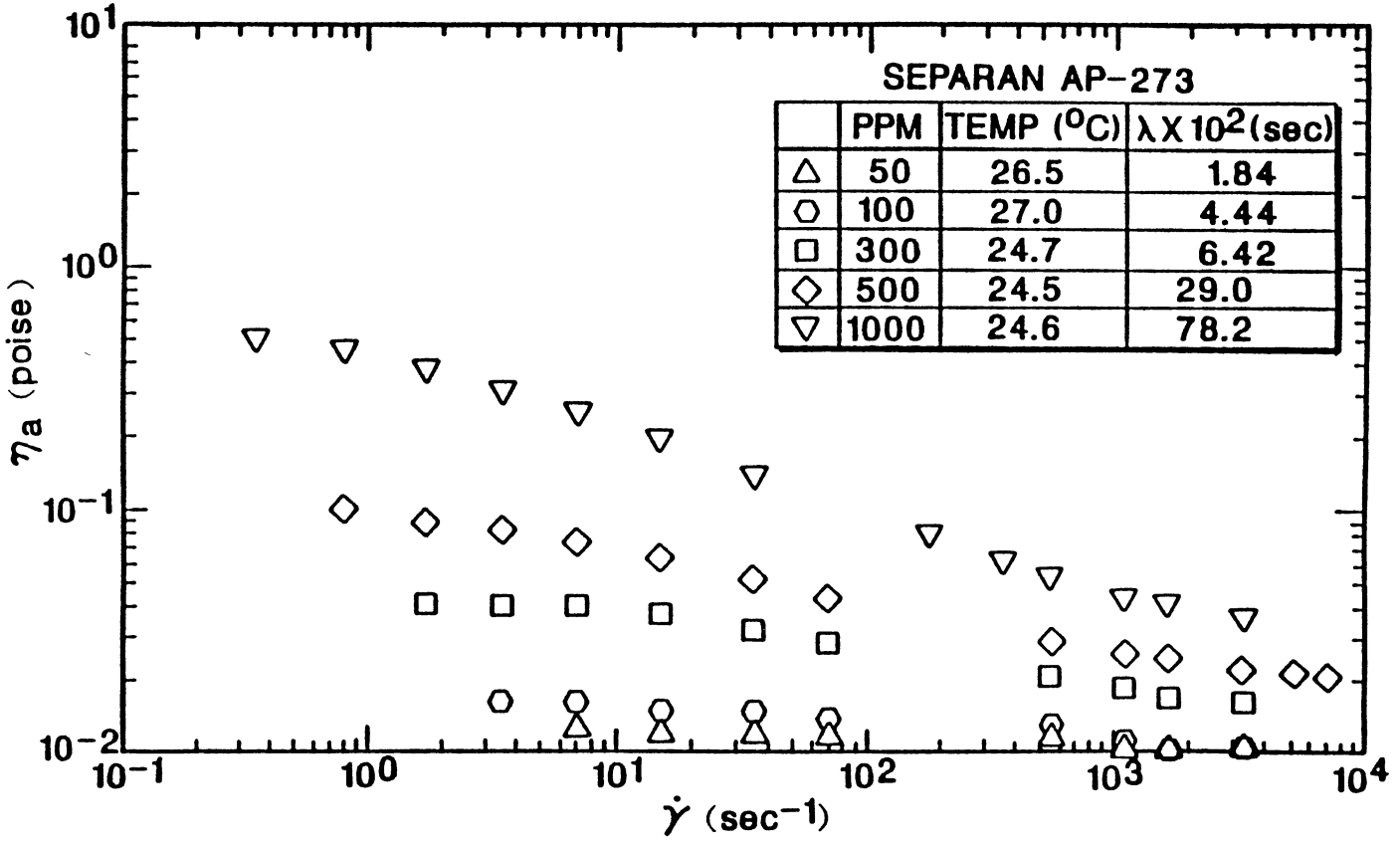

Figure 4.4 Apparent Viscosity Data of Separan AP-273 Solutions in the 3/4" Test Section

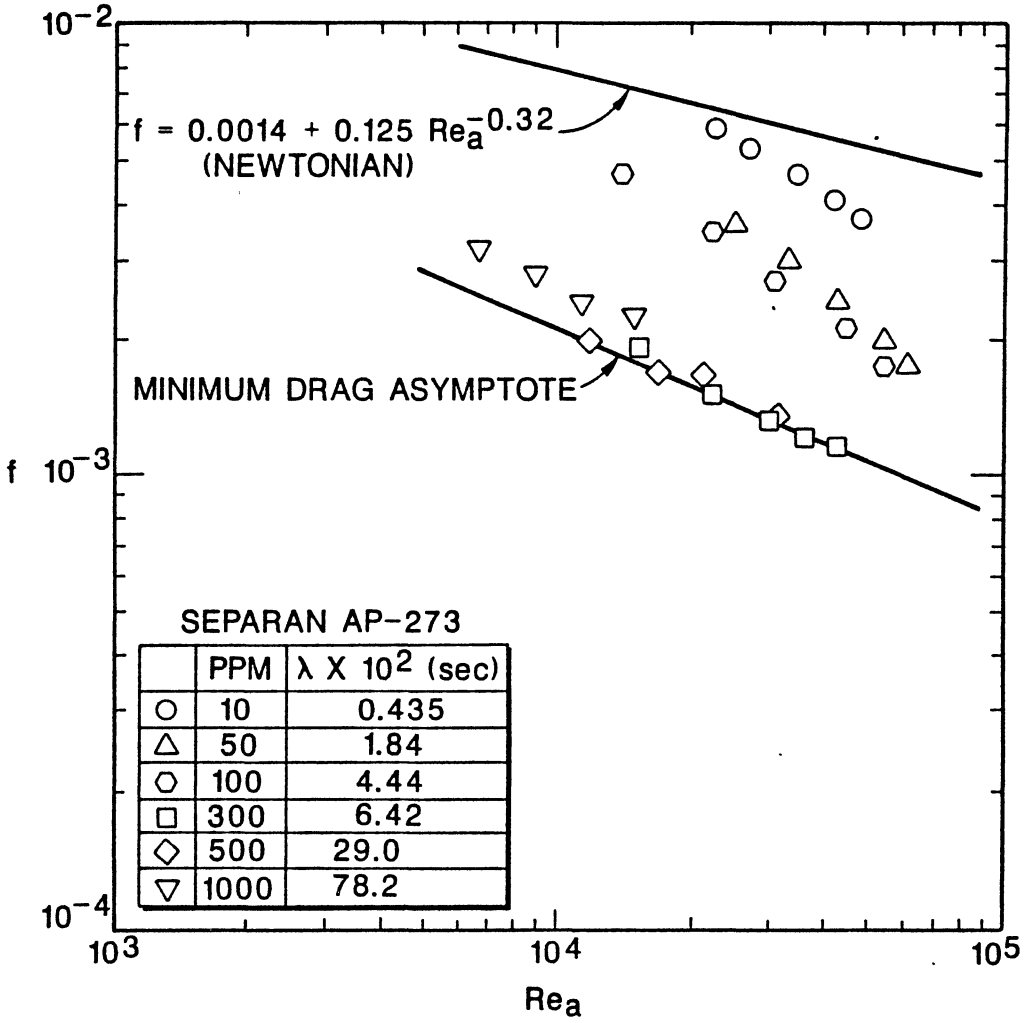

Figure 4.5 Friction Factors of Separan AP-273 Solutions in the 3/4" Test Section

friction factors measured in the 3/4" pipe flow decrease with the increasing polymer concentration up to 300-500 ppm of Separan AP-273 solution. Further increase of polymer concentration beyond 500 ppm results in the increase of friction factor. This can be explained by the following interpretation: the increase of shear friction due to the increase of viscosity surpasses the decrease of the friction drag due to the depression of turbulence eddy with the addition of polymer. Figure 4.5 also confirms the existence of a minimum asymptote for friction factor, which has been suggested by several investigators [2, 5, 11, 12, 26, 27, 82]. As compared with the well-established equation for Newtonian fluids [79], this minimum asymptote shows that there is a reduction in friction factor as much as 73% and 82% at Reynolds numbers of 10^4 and 10^5, respectively. The current minimum asymptote is approximately 5% lower than that of Kwack [26]. This difference is within the uncertainty of the current experimental facilities.

The heat transfer measurements were simultaneously conducted with the pressure drop measurements under the constant wall heat flux condition. The results are presented in Figure 4.6 in terms of Colburn j-factor ($St\ Pr_a^{2/3}$), which is a dimensionless group used to eliminate the effect of Prandtl number on the heat transfer phenomenon [2-10]. Figure 4.6 shows that the trend of heat transfer coefficients is similar to that of friction factors. A major difference between those two measurements is that the heat transfer reduction is more drastic. This figure also shows the existence of a minimum heat transfer asymptote, which is obtained at the concentrations of 500 to 1000 ppm in the present case. In contrast to the case for friction factors, there is no sign of an increase in the heat transfer coefficients due to an

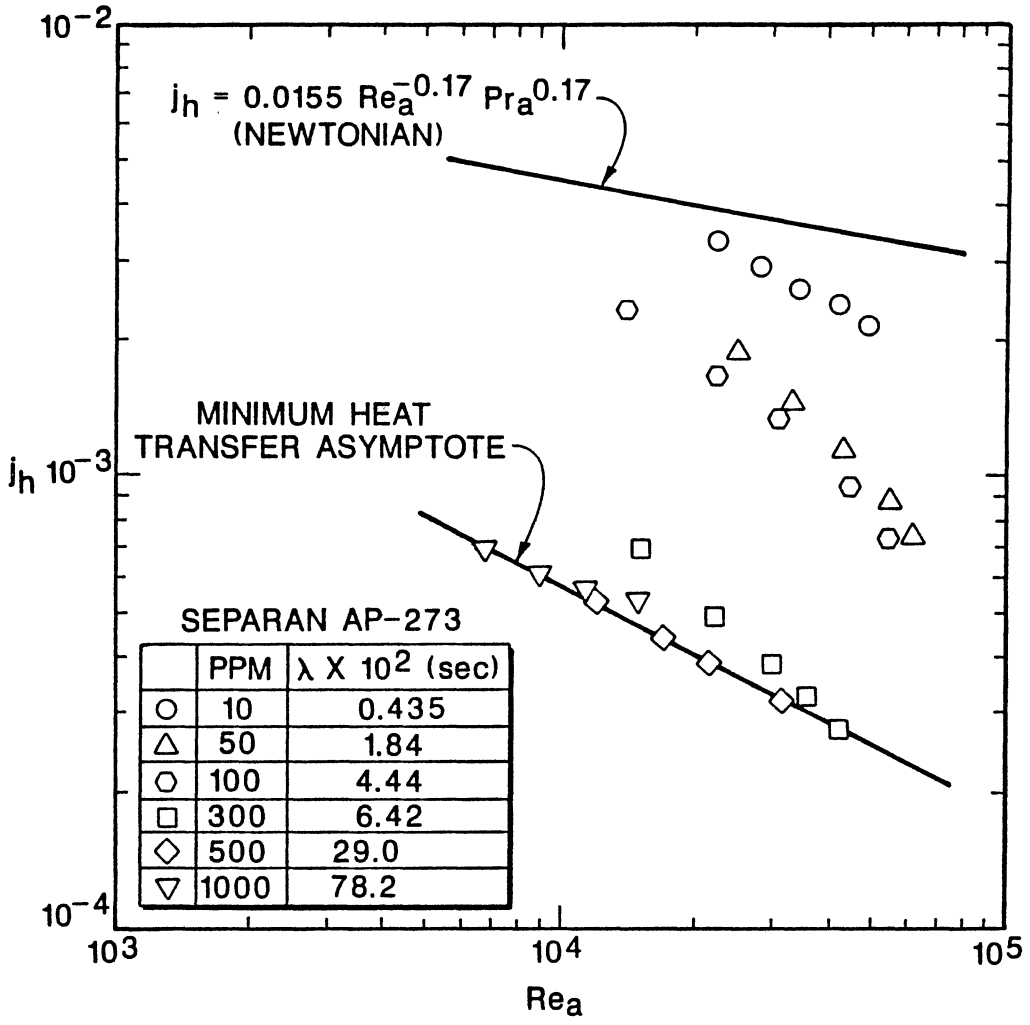

Figure 4.6 Colburn j-Factors of Separan AP-273 Solutions in the 3/4" Test Section

excessive addition of polymer beyond the concentration producing the minimum heat transfer asymptote. As compared with the well-established equation for Newtonian fluids [78], this minimum asymptote shows that there is a reduction in heat transfer coefficients as much as 87% and 94% at Reynolds number of 10^4 and 10^5, respectively. The current minimum asymptote for heat transfer is approximately 10% greater than that reported in the previous work [26]. This difference is also within the uncertainty of the current experimental facilities.

4.2.2 Pipe Diameter

To investigate the effect of pipe diameter on the behaviors of friction drag and heat transfer, a series of experiments were conducted in the 3/8" test section for aqueous Separan AP-273 solutions with the concentrations of 10, 50, 100, 300, 500 and 1000 ppm. Since the passage of the 1000 ppm solution through the long pipe (38 ft.) of small diameter (0.436 in.) caused so much shear friction due to high viscosity of the solution, turbulent flow could not be obtained for this solution. This solution was excluded from the measurements. The apparent viscosity data are presented in Figure 4.7 with the fluid time scales calculated using the Powell-Eyring model. The friction factors and heat transfer coefficients for both 3/4" and 3/8" test sections are shown in Figure 4.8 and 4.9, respectively. It is observed from these figures that the reduction in friction factors and heat transfer coefficients for the smaller pipe (3/8" test section) is more pronounced than that for the larger one (3/4" test section). This can be explained by the following interpretation: the polymer molecules are considered to influence the boundary layer close to the pipe wall. This influence

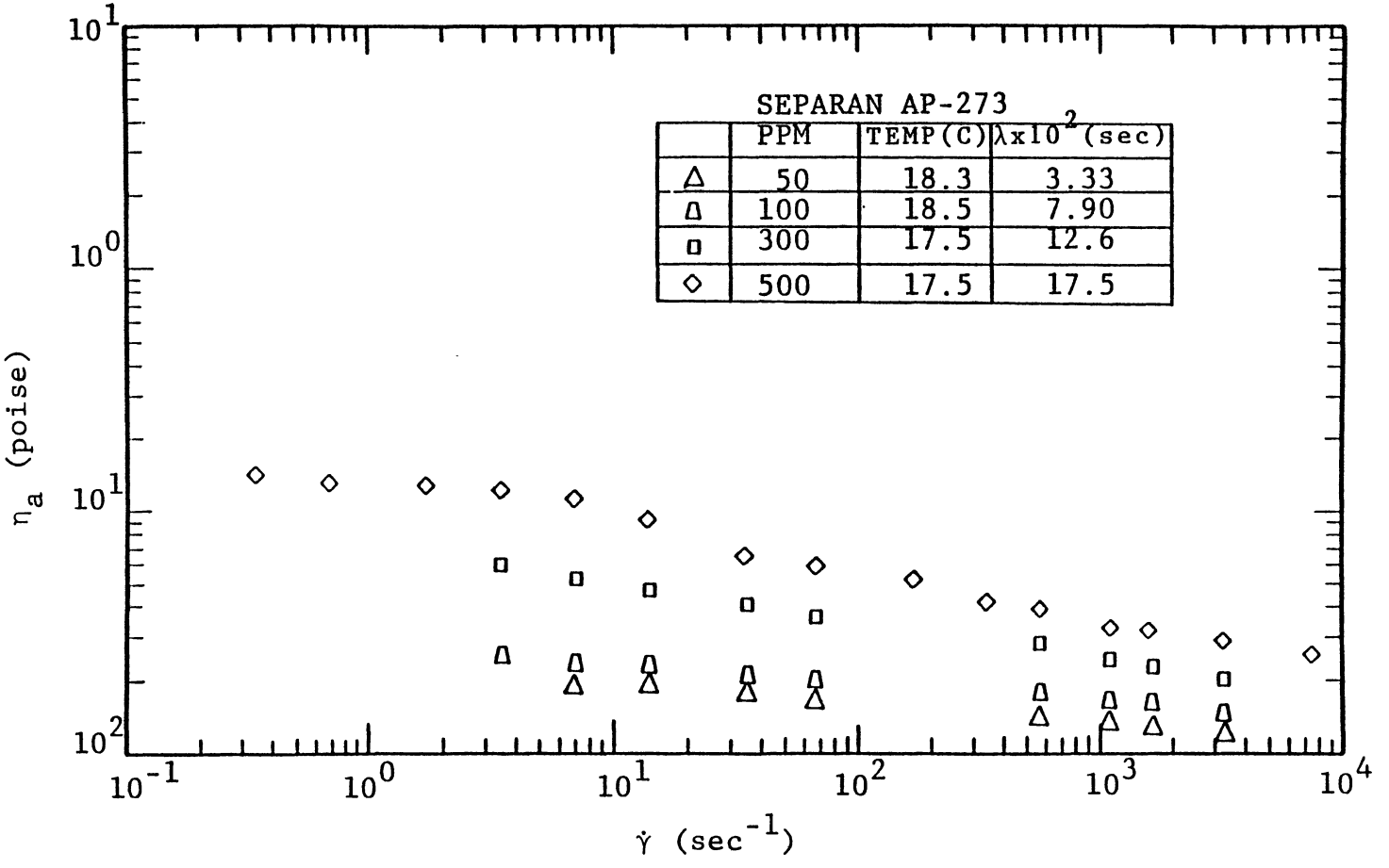

Figure 4.7 Apparent Viscosity Data of Separan AP-273 Solutions in the 3/8" Test Section

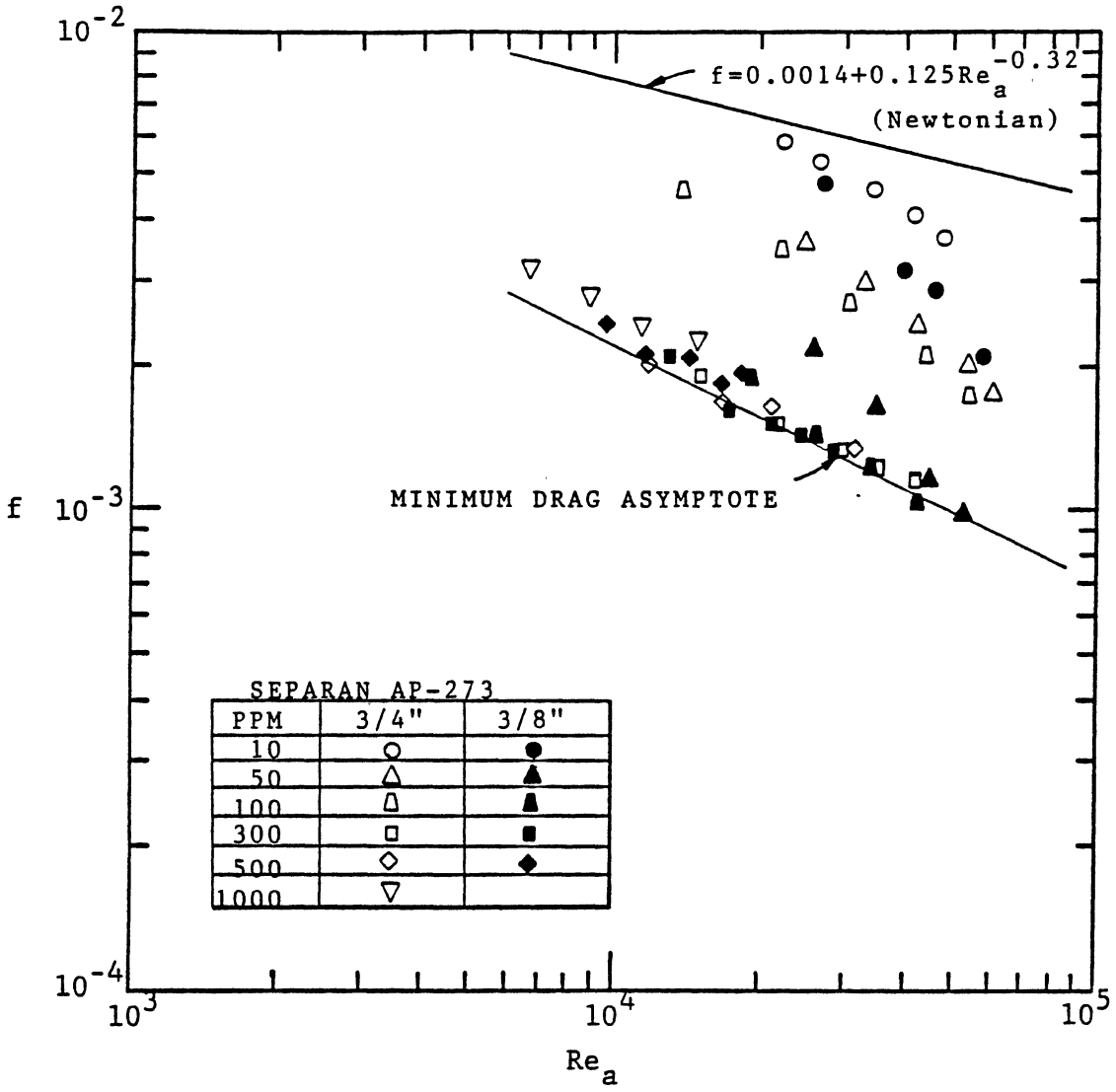

Figure 4.8 Diameter Effects on Friction Factors of Separan AP-273 Solutions

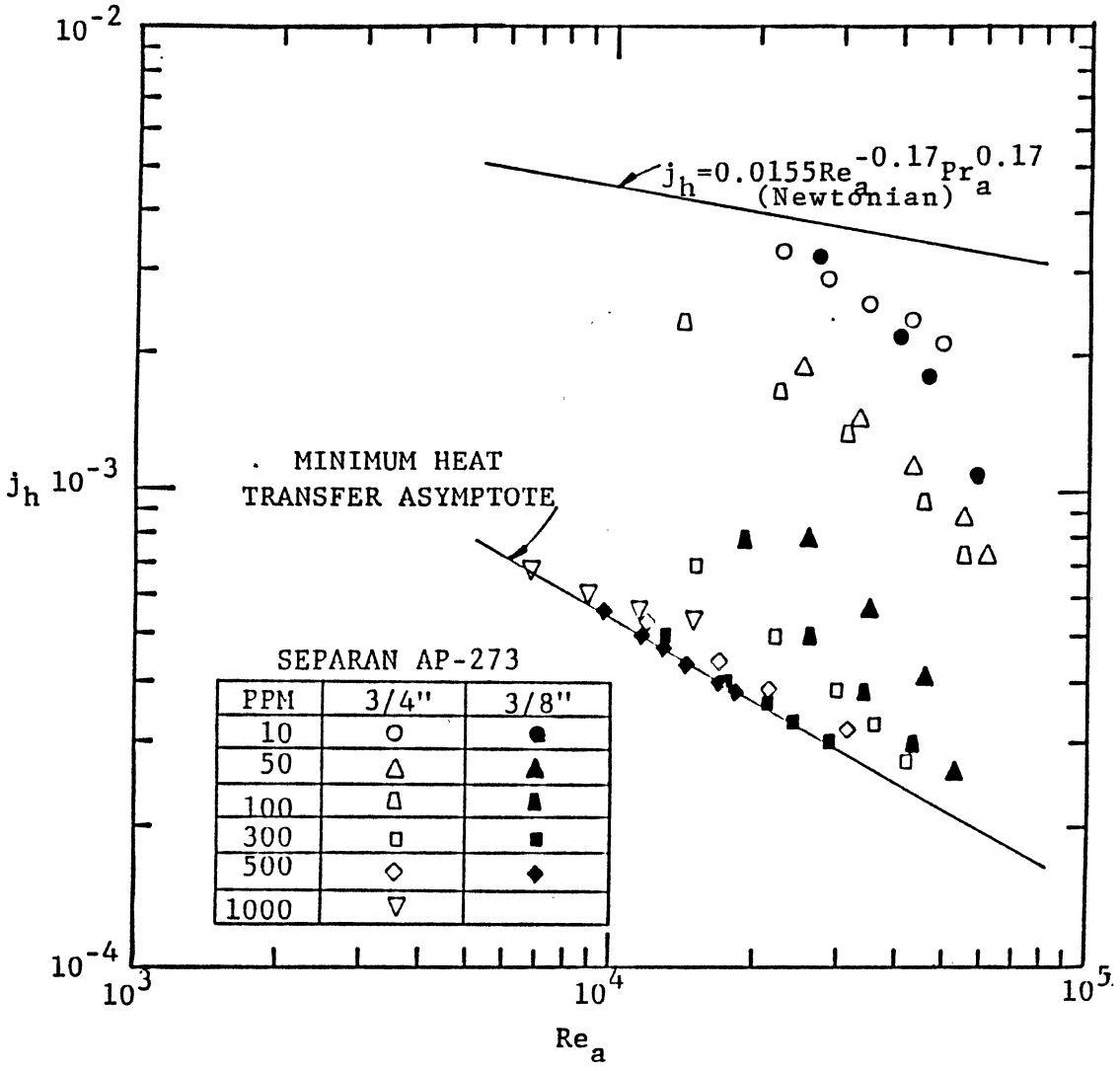

Figure 4.9 Diameter Effects on Colburn j-Factors of Separan AP-273 Solutions

should be seen in the smaller pipe before the larger one since the boundary layer would form a larger portion of the total flow in a small pipe. However, the minimum asymptotes for friction factors and heat transfer coefficients remain the same, independent of pipe diameter. This study suggests that a scaling law for pipe diameter is needed in order that the results obtained for one pipe diameter can be used to predict the characteristics for different pipe diameters. A scaling law associated with the diameter effect is presented in Section 4.3.

4.2.3 Polymer Effectiveness

It is expected that different types of polymers may yield different characteristics in the behaviors of friction drag and heat transfer. To study the effectiveness of polymers, a set of friction factors and heat transfer coefficients for aqueous WSR-301 solutions were measured in both 3/4" and 3/8" tubes using concentrations of 50, 100, 300, 500, and 1000 ppm. Since the solution of 10 ppm was so much degraded during mixing and circulation, this solution was excluded from the measurements. The apparent viscosity data tabulated in Table B.3 (see Appendix B) indicate that the WSR-301 solution is weakly shear dependent. However, the addition of WSR-301 does not yield the pronounced increase in viscosity, especially at low shear rates where Separan AP-273 did, as shown in Figure 4.4. Since the viscosity change at the low shear rates is directly related with the elasticity of a solution, it is expected that the WSR-301 solution is much less effective in reducing friction drag and heat transfer than the Separan AP-273 solution. The measurements of friction factors and heat transfer coefficients presented in figures 4.10 and 4.11 confirm the above

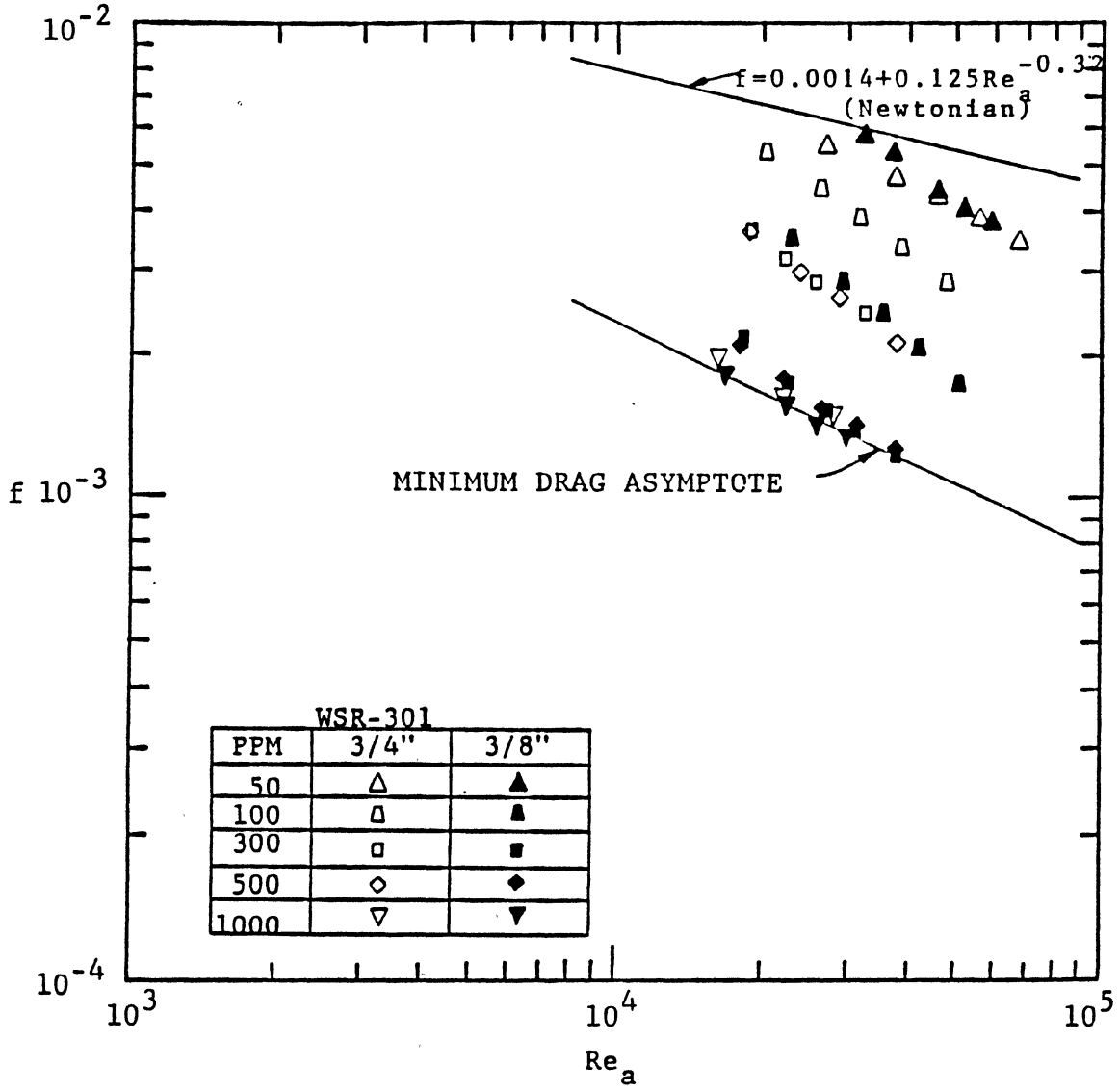

Figure 4.10 Friction Factors of WSR-301 Solutions in the 3/4" and 3/8" Tubes

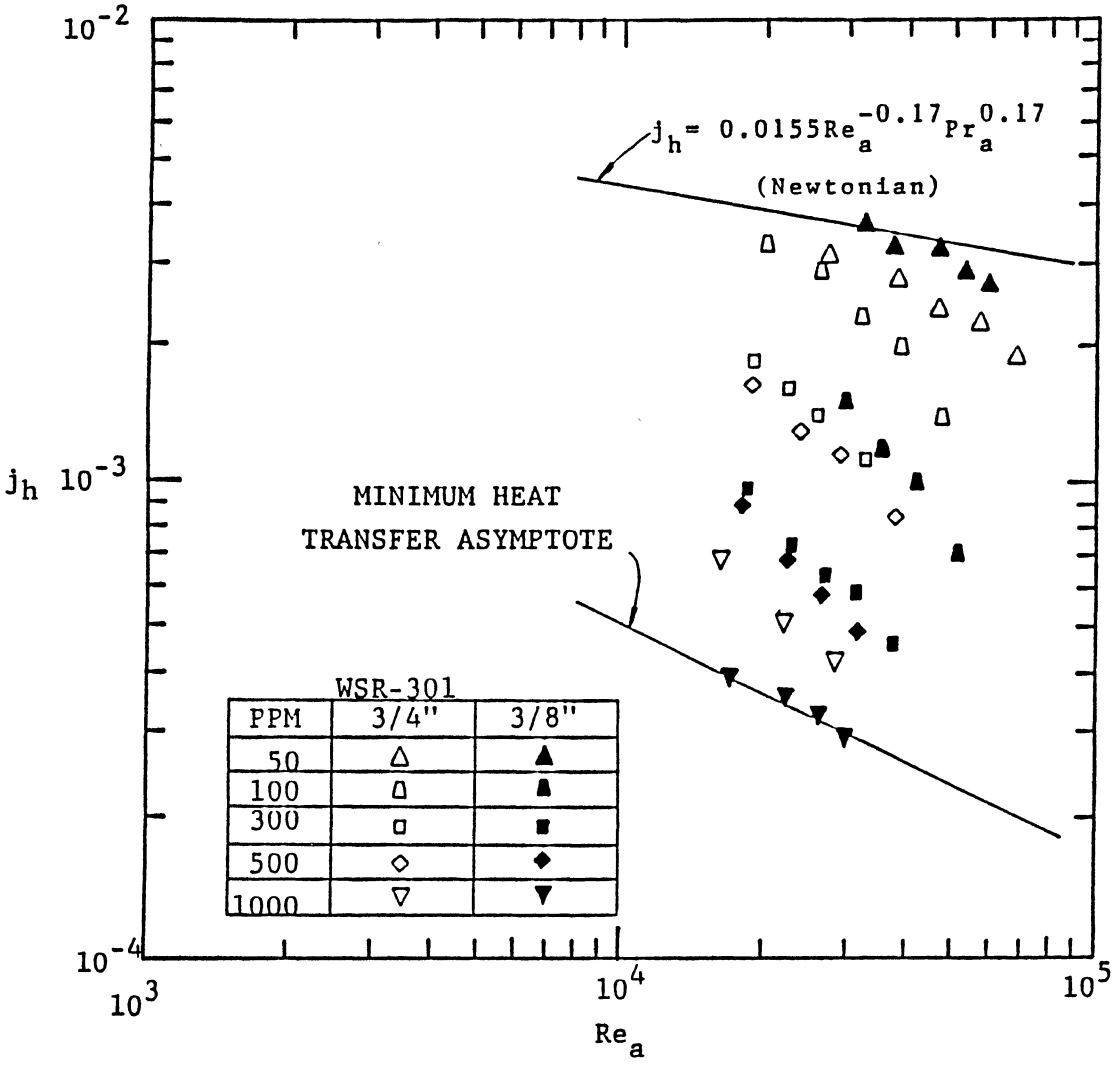

Figure 4.11 Colburn j-Factors of WSR-301 Solutions in the 3/4" and 3/8" Tubes

inference. It should be also remarked that the average molecular weight of Separan AP-273 (M = 6 millions) is much greater than that of WSR-301 (M = 4 millions). The current study suggests that the effectiveness of a polymer may be estimated on the basis of either the viscosity increase of a solution at the low shear rates or the average molecular weight of a polymer. Based on all of the experimental data collected, it is quite valuable to investigate the maximum reduction asymptotes for friction factor and heat transfer coefficient. These conditions will be used to determine the adjustable constants in the proposed equation for heat eddy diffusivity in Section 5.3 as well as to estimate the maximum benefits obtainable with the addition of polymer. Figure 4.12 shows that the current maximum reduction asymptotes are in agreement with those of Kwack [26] within the uncertainty range of the experimental apparatus of Kwack and this study. This confirms that the maximum reduction asymptotes are consistent, independent of the experimental conditions employed and the types of polymer used. The experimental data for WSR-301 solutions along with those for Separan AP-273 solutions will be used to establish the general predictability of the proposed equation for heat eddy diffusivity in Section 5.3.

4.3 Scaling Method for Pipe Diameter and Polymer Concentration

It has been known that the characteristics of polymer solutions can be affected by several factors such as pipe diameter, polymer concentration, solvent chemistry, polymer degradation and temperature dependent fluid properties. The current experimental study attempted to minimize the last three effects on the polymer solutions by using the

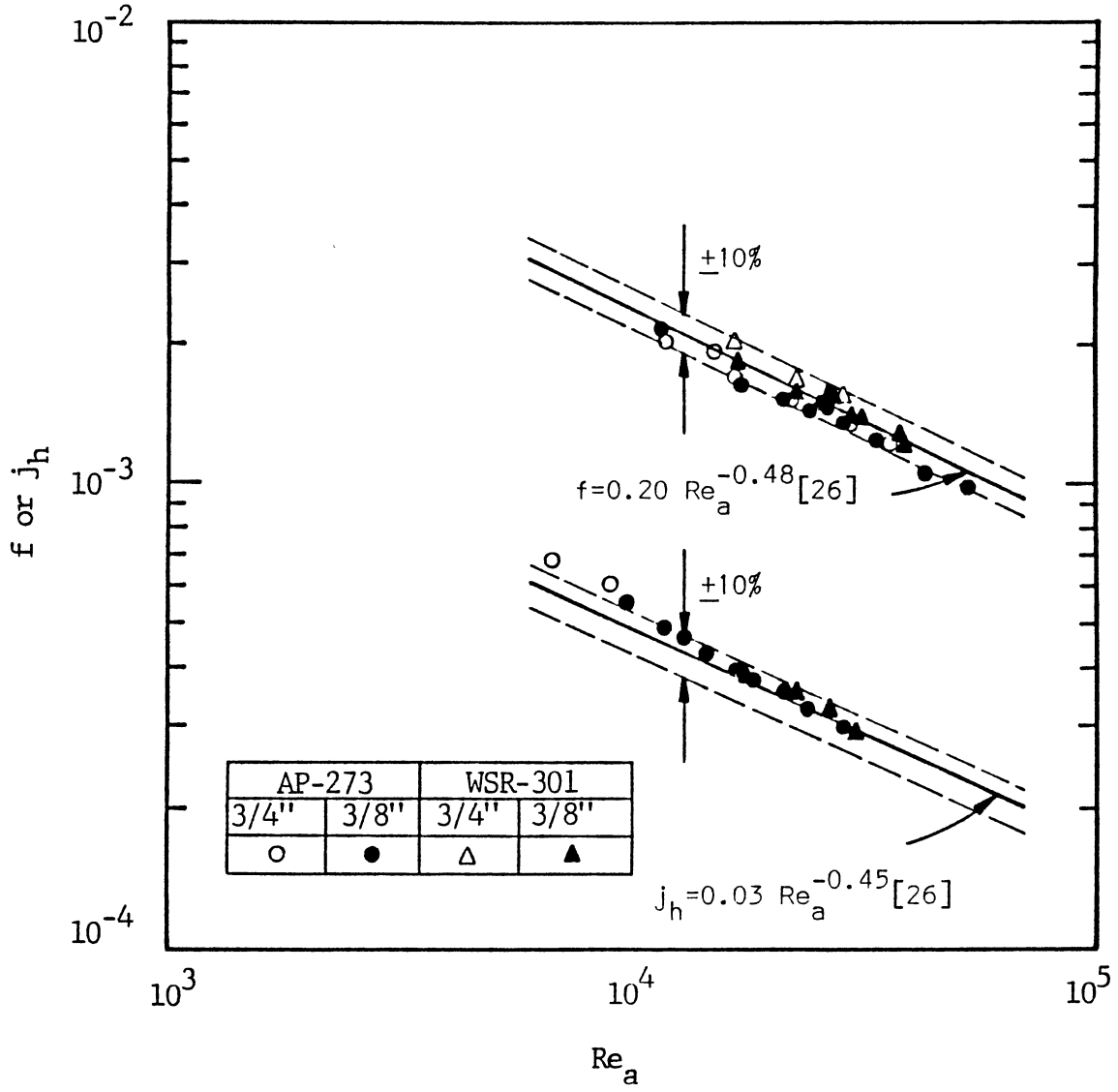

Figure 4.12 Comparison of the Maximum Reduction Asymptotes of This Study With the Correlations of Kwack [26]

same kind of tap water and the once-through operation mode and maintaining a small wall-to-bulk temperature difference. Therefore, the experimental results presented in Section 4.2 can be characterized by the pipe diameter and the polymer concentration. A few attempts [40-42, 56, 58] have been made to correlate the friction factor data obtained for different pipe diameters and polymer concentrations by a single expression. However, the scaling law for heat transfer coefficients is not available as yet. In this study, the scaling scheme proposed by Astarita et al. [42] for the friction factor data is applied to the current experimental data for the verification of its general applicability and is extended to the case of heat transfer coefficients.

To account for the effects of pipe diameter on drag reduction, Astarita et al. [42] used the characteristic frequency proposed by Seyer and Metzner [57] and it has the following expression:

$$\Omega = \frac{U}{D} Re_a^{0.75} \tag{4.2}$$

The above parameter was obtained from a phenomenological analysis of the mechanism of drag reduction: the drag reduction is observed only at the wall shear stress exceeding the critical value of shear stress. Further attempt was made to correlate the friction factor data for different concentrations. From the dimensional analysis, it was concluded that the friction factor should be a function of Reynolds number and Deborah number (or called Weissenberg number). They assumed that the value of drag reduction ratio ($DR = f_p/f_s$) was uniquely determined by the Deborah number of flow:

$$DR = DR(\Omega\lambda) \tag{4.3}$$

where λ is the fluid time scale. Since the value of λ was not unequivocally defined in terms of measurable rheological properties for dilute solutions, the following alternative method was proposed. Let $\Omega_{0.5}$ be the frequency corresponding to the drag reduction of 0.5:

$$0.5 = DR(\Omega_{0.5}\lambda) = DR(K) \tag{4.4}$$

where $K = \Omega_{0.5}\lambda$ is a constant which, if Equation (4.4) is valid, does not depend on the particular solution considered. Equation (4.4) can be written in the equivalent form:

$$DR = DR\left(\frac{\Omega K}{\Omega_{0.5}}\right) = DR'\left(\frac{\Omega}{\Omega_{0.5}}\right) \tag{4.5}$$

The above equation was proposed to correlate the friction factor data for different pipe diameters and different concentrations. The basic assumption of this scaling law was that the properties of dilute polymer solutions, which are most common in the practical engineering systems, are not far different from those of Newtonian fluids. Since the solutions of Separan AP-273 showed highly non-Newtonian trend (strongly shear dependent viscosity), these solutions were excluded from this study.

For the additional verification of the scaling method proposed by Astarita et al. [42], this method was applied to the current experimental data for WSR-301 solutions. The current study did not include the case of 50 ppm since the 50 ppm solution was affected by severe

degradation. Figure 4.13 shows the drag reduction ratio in terms of the characteristic frequency. The diameter effect seems to have been adequately taken into account. Figure 4.14 indicates that all the friction factor data can be correlated by a single curve, independent of pipe diameter and polymer concentration. It should be noted that in this study, the drag reduction ratio of 0.3 was used instead of 0.5 employed by Astarita et al. [42]. Since the reduction ratio of 0.3 could not be obtained for the case of 1000 ppm, this solution was excluded from the scaling for polymer concentration. This suggests that any constant value of drag reduction ratio can be used in correlating the friction factor data. The current result confirms the general applicability of the scaling method proposed by Astarita et al. [42].

Since the onset of transition for both momentum transfer and heat transfer was observed to occur simultaneously at Re' ≈ 5500 [5,53], it is expected that the critical values of shear stress are same for both cases. This indicates that the scale-up method for the friction factor can be also applied to the heat transfer. It is suggested that the characteristic frequency for heat transfer can be evaluated by Equation (4.2). It is also assumed that the value of heat transfer reduction ratio ($HR = j_{h,p}/j_{h,s}$) can be determined by the following expression:

$$HR = HR' \left(\frac{\Omega}{\Omega_c}\right) \tag{4.6}$$

where Ω_c is the characteristic frequency evaluated at certain constant value of HR. Just as the case of friction factor, the heat transfer reduction ratio of 0.3 was used. For the same reason for friction factor, the case of 1000 ppm was excluded. Figures 4.15 and 4.16

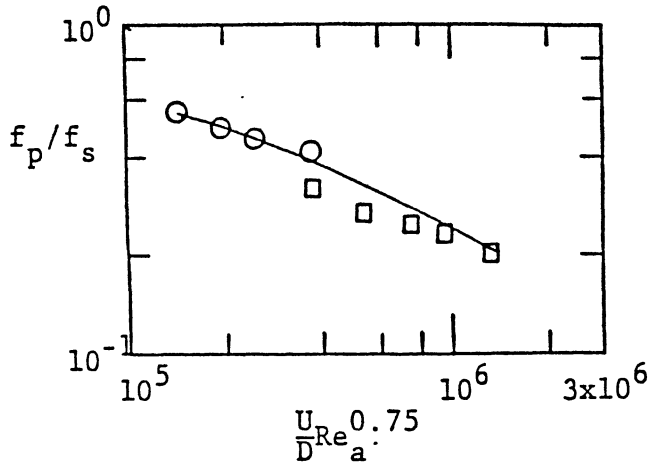

(b) 300 ppm

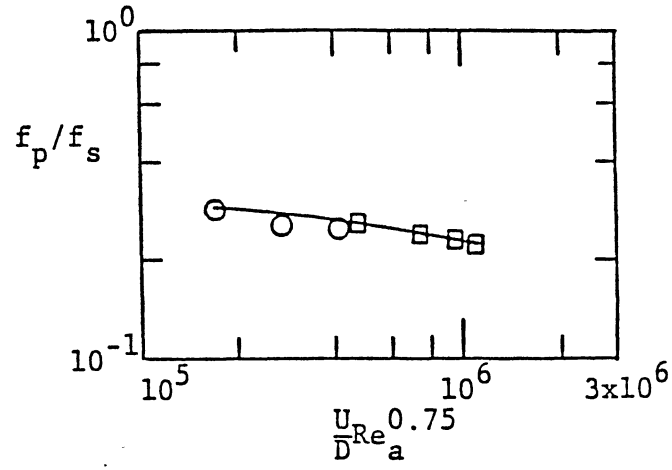

(d) 1000 ppm

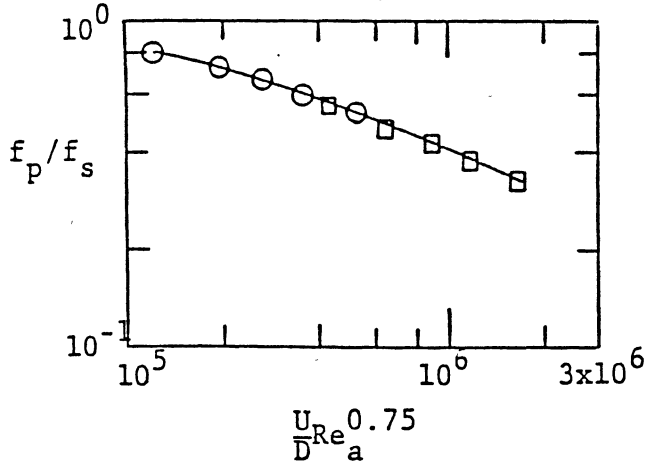

(a) 100 ppm

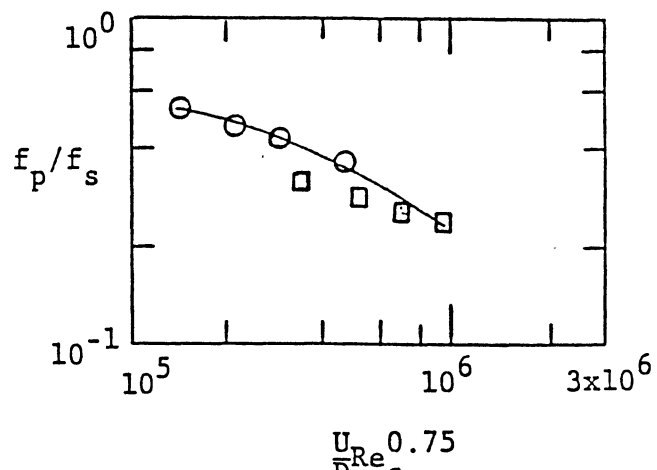

(c) 500 ppm

Figure 4.13 Drag Reduction Ratio Vs. Characteristic Frequency for WSR-301 (O: 3/4" Test Section and □: 3/8" Test Section)

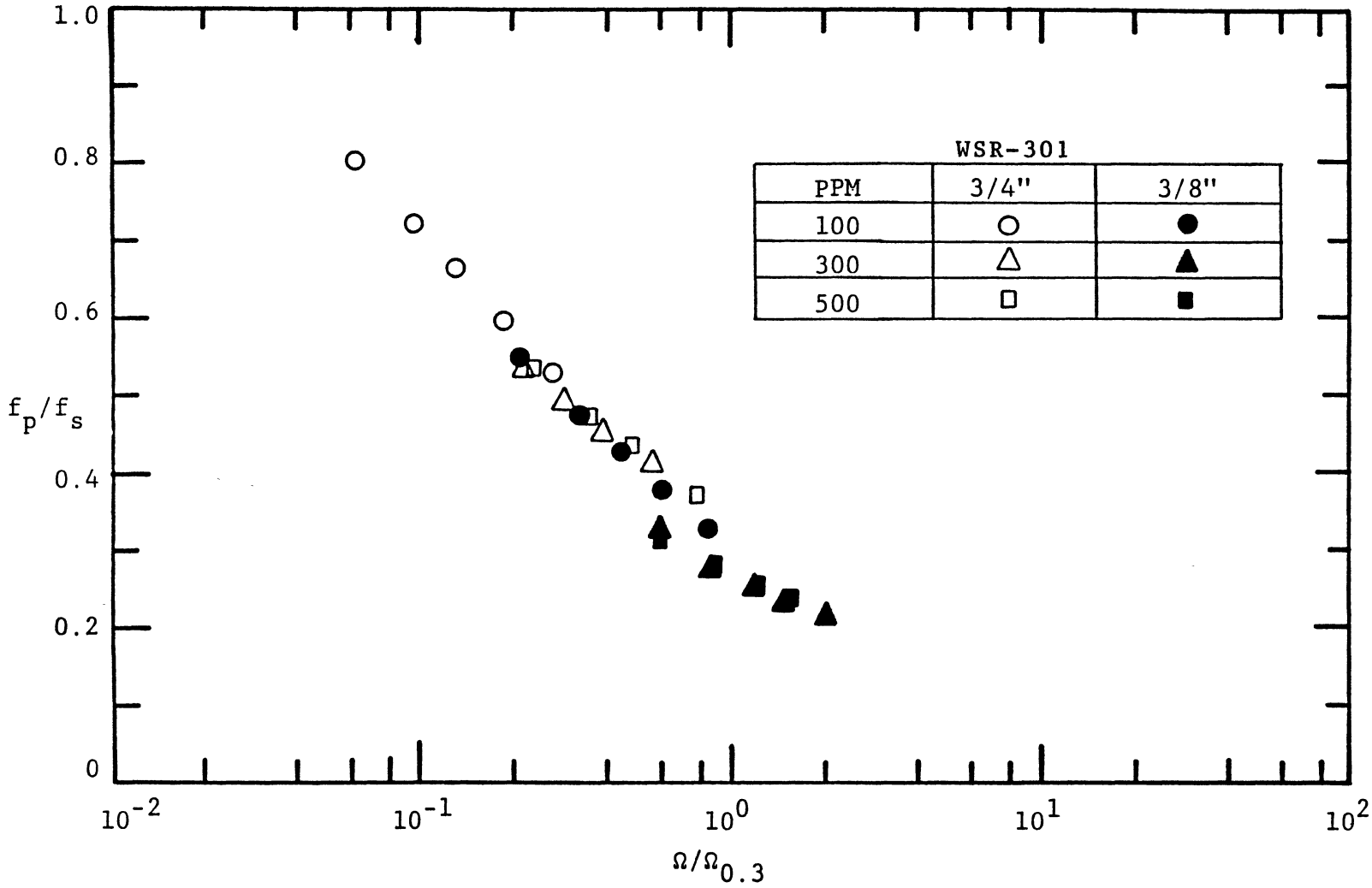

Figure 4.14 Scaling of Friction Factors With the Use of Equation (4.5)

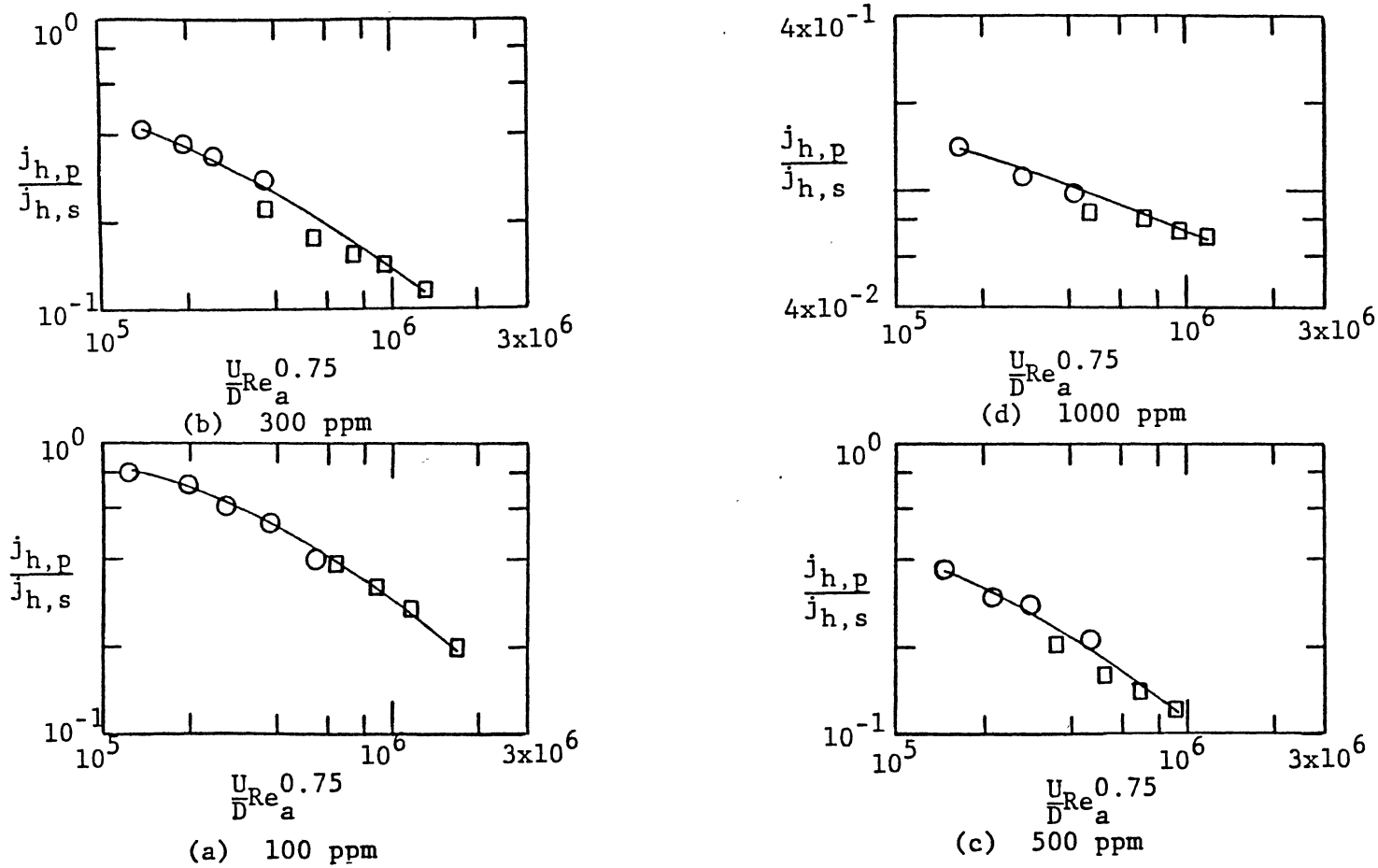

Figure 4.15 Heat Transfer Reduction Ratio Vs. Characteristic Frequency for WSR-301
(O: 3/4" Test Section and □: 3/8" Test Section)

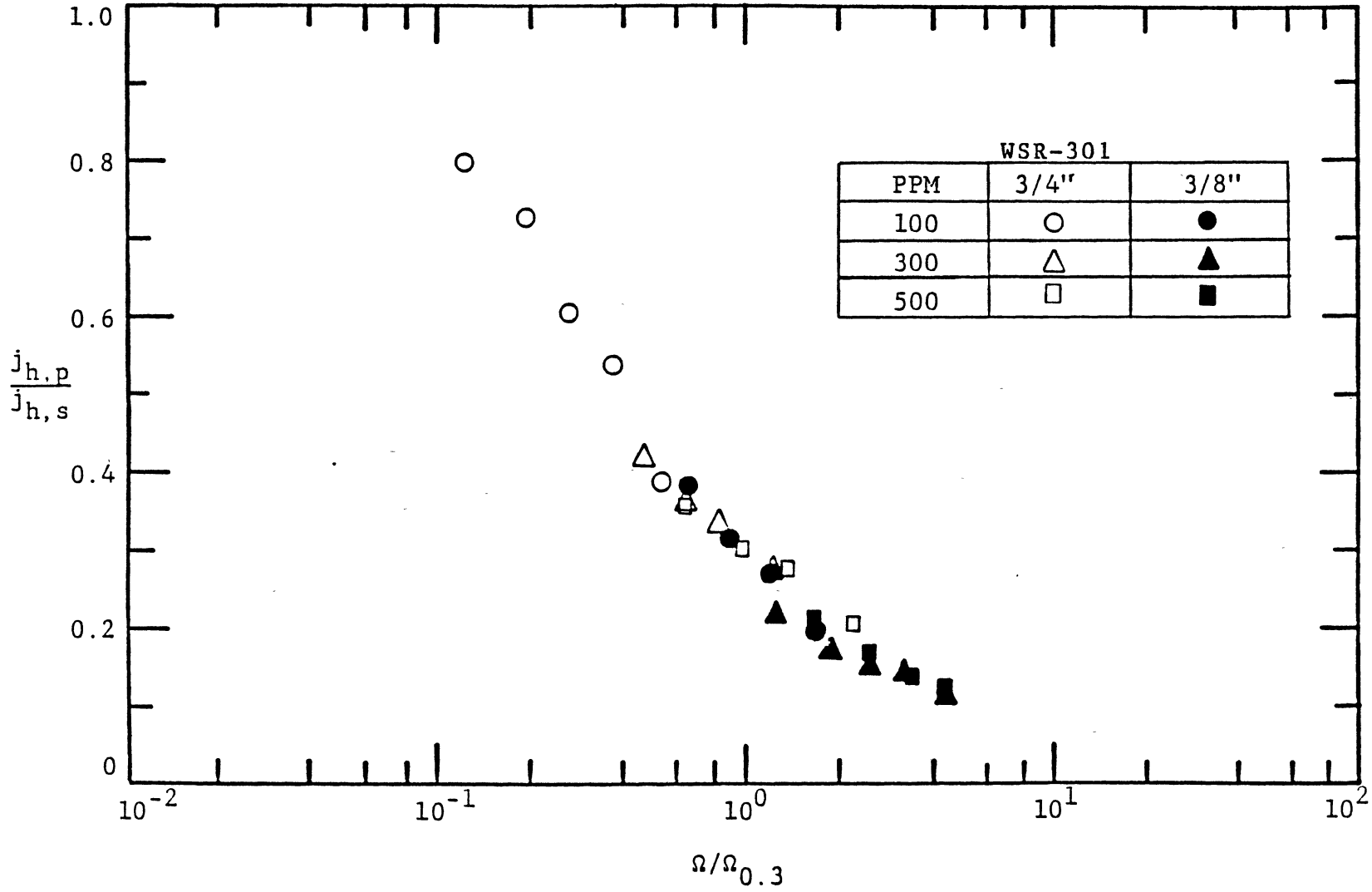

Figure 4.16 Scaling for Heat Transfer Coefficients with the Use of Equation (4.6)

illustrate that the scale-up method proposed for the heat transfer can correlate all the experimental data fairly well by a single curve.

4.4 Critical Weissenberg Number for Heat Transfer

The friction factor decreases with increase in concentration up to a certain value beyond which more addition of polymer does not have further effect on drag reduction and the friction factor has reached its minimum asymptotic value. The same behavior is found for heat transfer, except that much higher polymer concentrations are required for heat transfer. Since the polymer concentration is directly related to the elasticity of the fluid, this behavior suggests that there may be critical Weissenberg numbers for friction and heat transfer. Several previous works [6, 26, 30, 43] conducted at University of Illinois at Chicago Circle using aqueous polyacrylamide solutions have reported the critical Weissenberg numbers, which were estimated to be Ws_{cf} = 5~10 for friction and Ws_{ch} = 200~250 for heat transfer over the Reynolds number range of 20,000 to 30,000. These works also suggested that the critical Weissenberg numbers are independent of pipe diameter, solute and solvent chemistry, and weakly dependent on Reynolds number. These critical Weissenberg numbers indicate the optimum concentration compromising the performance and the economics of polymer addition. Particularly, since the critical Weissenberg number for heat transfer is one of the key parameters in the proposed equation for heat eddy diffusivity (see Section 5.3), it is very important to make an accurate evaluation of this value. The current study is planned to confirm the previous results and verify the general applicability of them to other polymer

solutions. There are two methods commonly used to do this work. One is to degrade a highly concentrated solution using the recirculation mode, and the other is to dilute the solution by adding solvent. Both methods were employed here.

The first experiment was conducted to check the results of previous works. An aqueous Separan AP-273 solution was recirculated 47 times through the 3/4" test section while the Reynolds number (the flow rate) was maintained close to 7000. During recirculation runs, the viscosity and heat transfer coefficient data were measured periodically to check whether there was enough degradation of the solution. Figure 4.17 shows that there is a pronounced decrease in the viscosity of polymer solution at the low shear rates, but a modest one at the high shear rates during recirculation runs. These viscosity data were used in estimating the values of fluid time scale with the Powell-Eyring model, and the results are presented in Figure 4.17. The measurements of heat transfer coefficients are shown in terms of recirculation runs in Figure 4.18. This figure indicates that the heat transfer coefficients begin to increase after approximately 10 runs due to mechanical degradation and solution aging. This increase becomes more remarkable with the increase in the number of recirculation runs. The data of heat transfer coefficients are replotted as a function of Weissenberg number in Figure 4.19. From this figure, the critical Weissenberg number for heat transfer is estimated to be 150-200. This value is somewhat lower than that of Kwack [26], who suggested 200-250 over Reynolds number range of 20,000 to 30,000. If the influence of Reynolds number on the critical Weissenberg number is accounted for, this difference may be within the acceptable range.

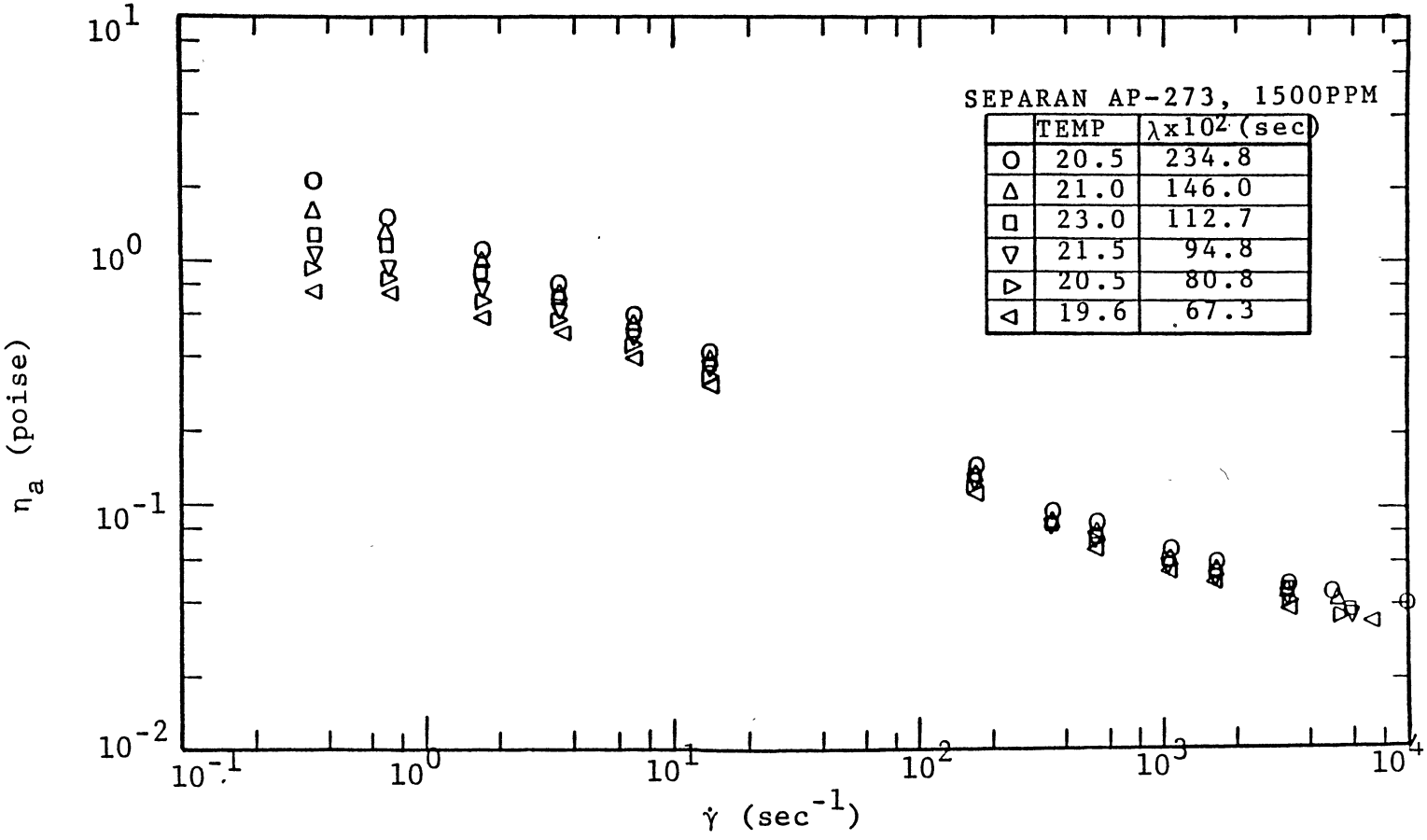

Figure 4.17 Degradation Effect on Apparent Viscosity of 1500 ppm Separan AP-273 Solution in the 3/4" Tube

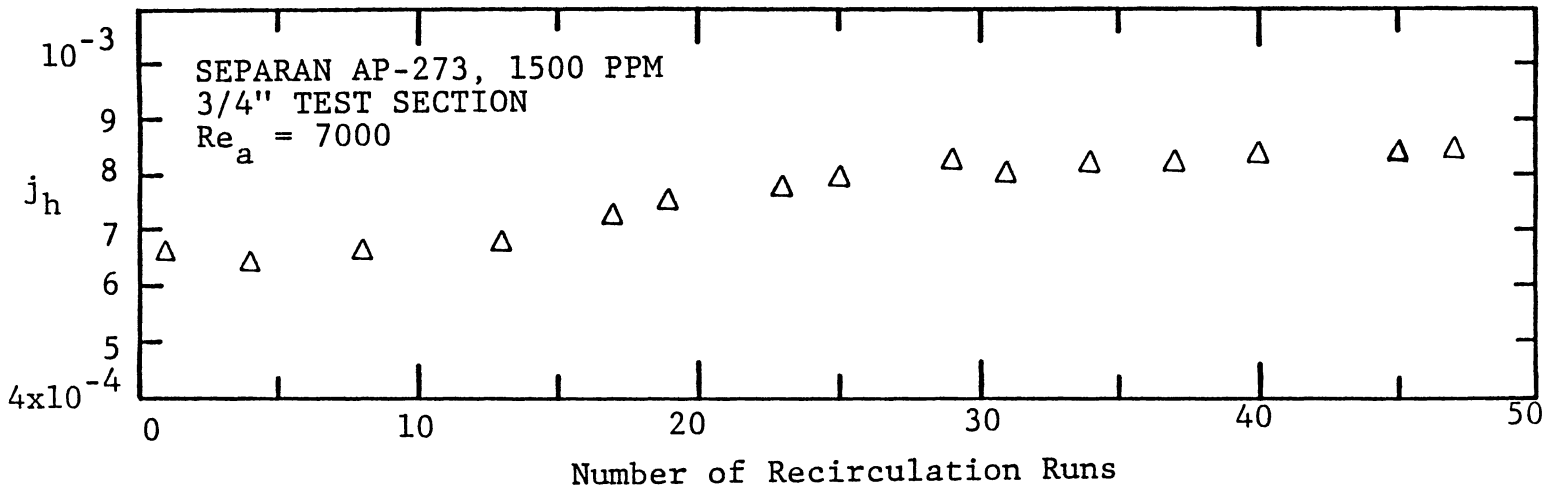

Figure 4.18 Degradation Effect on Colburn j-Factors in Terms of Recirculation Runs

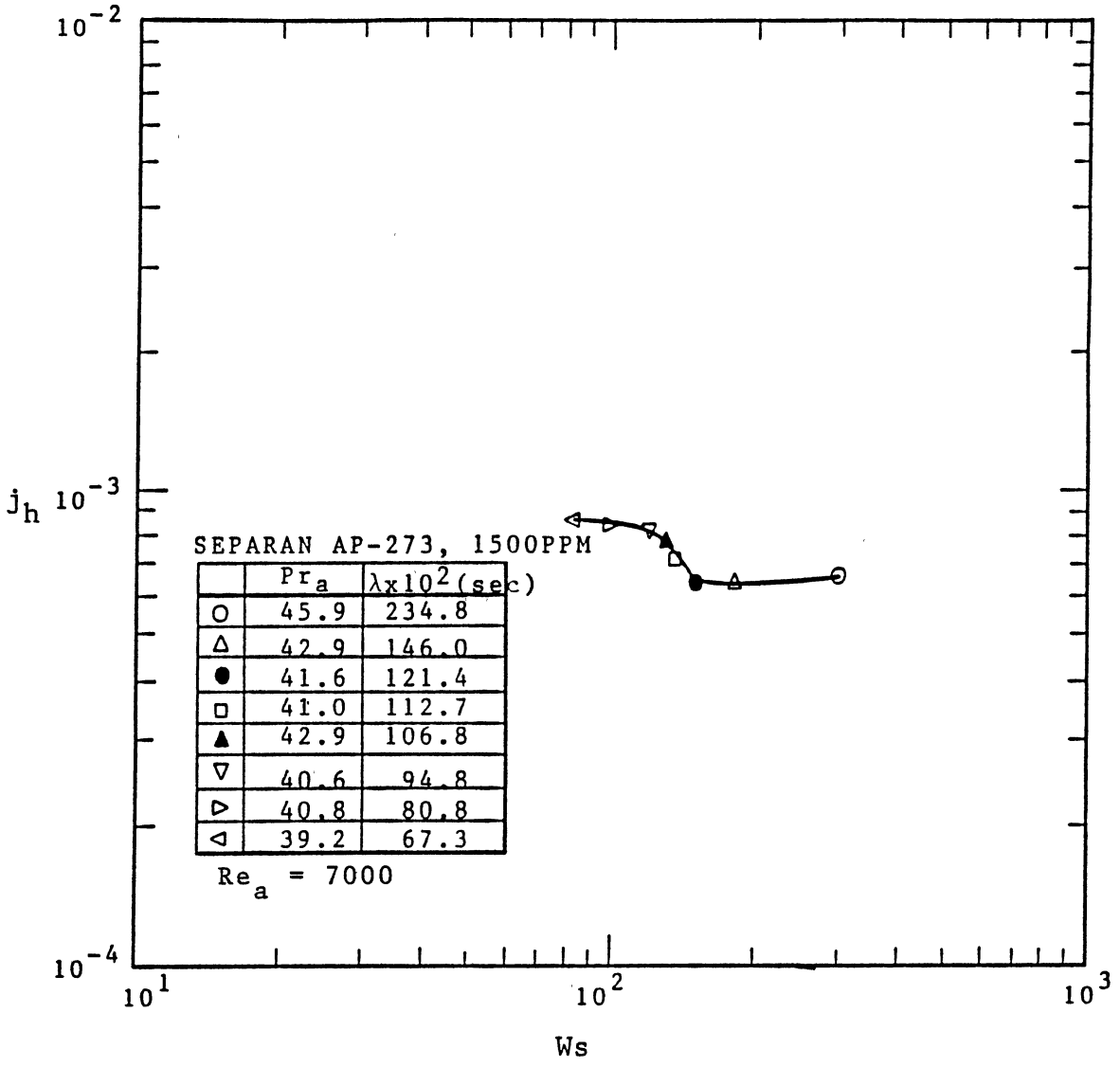

	Pr_a	$\lambda x10^2$(sec)
○	45.9	234.8
△	42.9	146.0
●	41.6	121.4
□	41.0	112.7
▲	42.9	106.8
▽	40.6	94.8
▷	40.8	80.8
◁	39.2	67.3

Figure 4.19 Degradation Effect on Relations of Colburn j-Factors and Weissenberg Number

To confirm the result obtained for a Separan AP-273 solution and investigate its general applicability to other type of polymer, an additional experiment was planned. Since the first experiment using the recirculation method for degradation seemed to fail in producing wide range of Weissenberg numbers, the second experiment employed the dilution method. For this purpose, an aqueous Separan AP-30 solution of 3000 ppm, which is known to be a very effective drag reducer, was prepared for dilution. For each concentration, the heat transfer data were taken at various flow rates together with the apparent viscosities at wide range of shear rates. For dilution, the proper amount of tap water was added to obtain the desired concentration. This process of dilution continued until the heat transfer data showed considerable deviation from the minimum heat transfer asymptote. The apparent viscosity data and the fluid time scales are presented in Figure 4.20. This figure shows that the viscosity data for Separan AP-30 solution follow the similar trend to that for Separan AP-273. This solution is also strongly shear dependent. The heat transfer coefficients at Reynolds number of 10,000 are presented in terms of Weissenberg number in Figure 4.21. From this figure, the critical Weissenberg number is estimated to be 200-250. This result is consistent with those of the previous works conducted for Separan AP-273 solutions [6, 26, 30]. The current study indicates that the critical Weissenberg number for heat transfer is independent of the polymer type and weakly dependent on the Reynolds number.

4.5 Heat Transfer Correlation

Several attempts have been made to develop reliable heat transfer

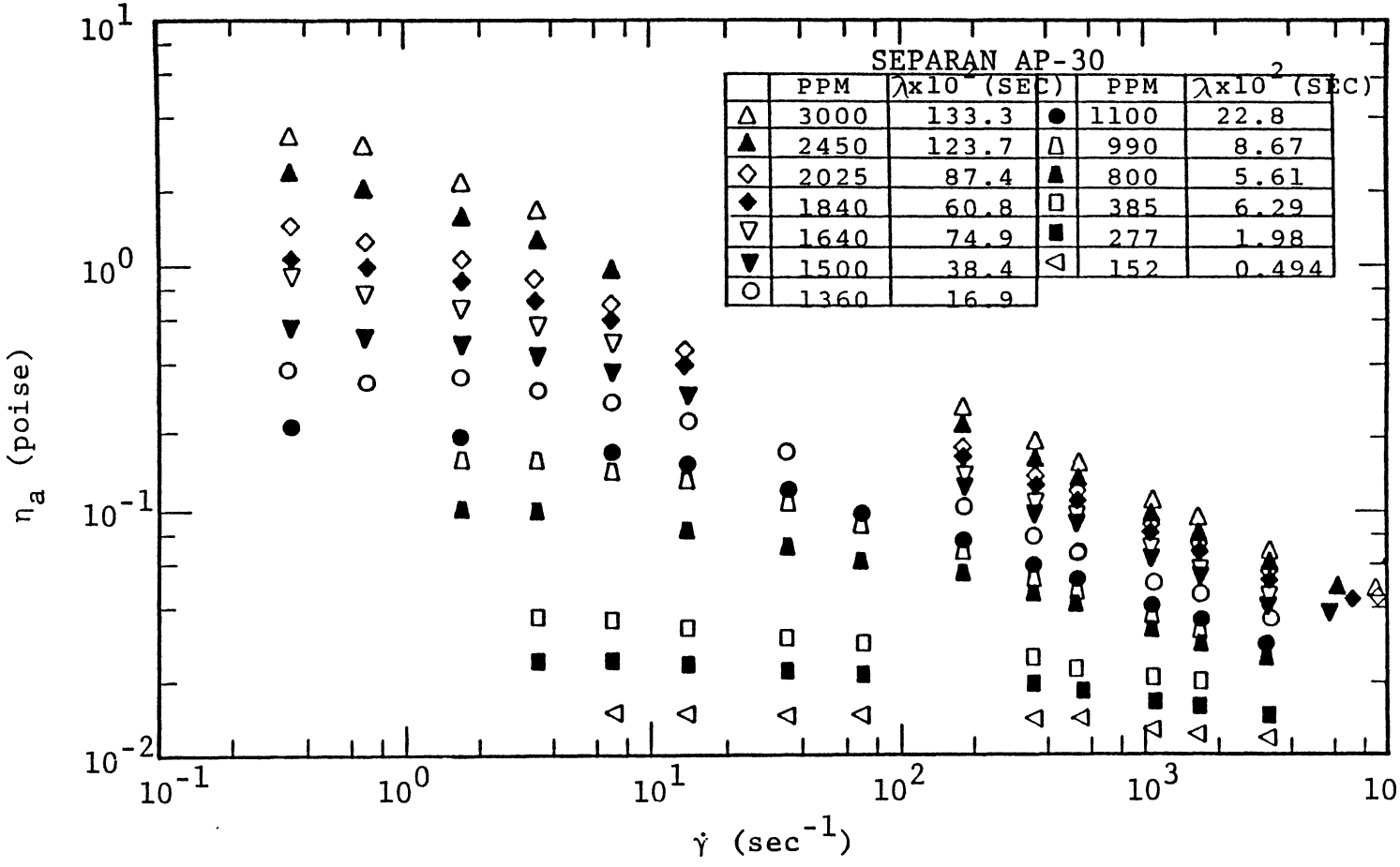

Figure 4.20 Viscosity Data of Separan AP-30 Solutions in the 3/4" Test Section

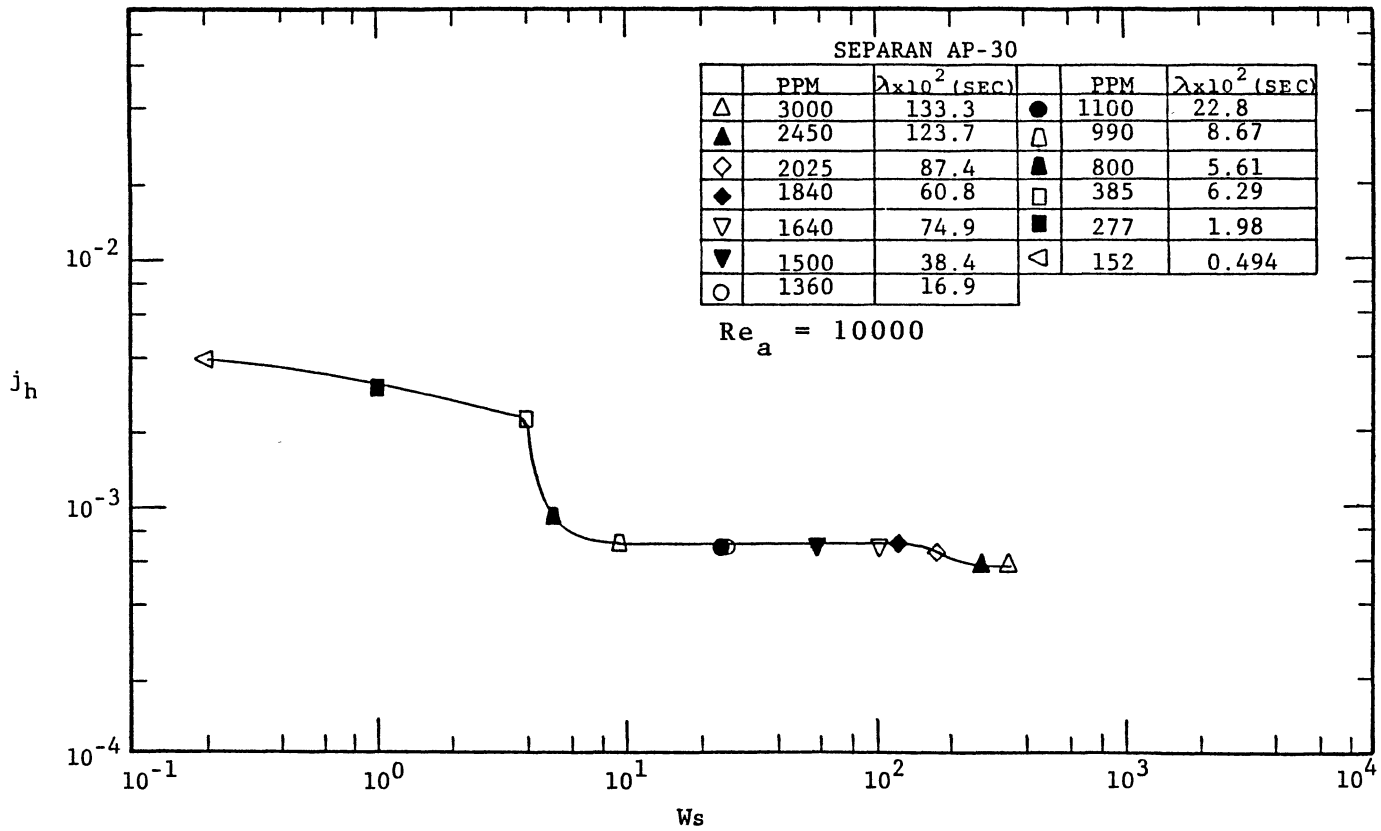

Figure 4.21 Colburn j-Factors in Terms of Weissenberg Numbers for Separan AP-30 Solutions in the 3/4" Test Section

correlations for drag-reducing turbulent pipe flows. Not available is a single correlation which can accurately predict the heat transfer coefficients for various polymer solutions with wide range of concentrations in the thermally fully developed region. The inadequacy of existing heat transfer correlations was mainly due to the fact that these correlations were developed and established using inaccurate experimental data. Based on the extensive and reliable experimental data of this study, an attempt was made to develop a heat transfer correlation.

Kale [35] extended to viscoelastic fluids the Reichardt's expression for heat transfer in Newtonian turbulent flows. The heat transfer correlation suggested for viscoelastic flows was:

$$St = \frac{f/2}{1.2 + (Pr-1)(f/2)^{1/2}\{9.2\ Pr^{-0.258} + 1.2\ De\ Pr^{-0.236}\}} \qquad (4.7)$$

where De (Deborah number) was defined as $\lambda U\tau^2/\nu$. Kale verified the predictability of Equation (4.7) with several experimental data [13, 27, 49, 51], which were obtained under inadequate experimental conditions as discussed in Chapters I and II. The recent study of Kwack [26] suggested that the use of Equation (4.7) resulted in considerably high heat transfer coefficients as compared with his experimental data, especially for highly concentrated solutions. Kale employed the equation of Seyer and Metzner [57] in estimating the fluid time scale (λ). This equation demands the measurements of normal stress, which is not an easily obtainable rheological property, especially for low concentration solutions. To remedy the inadequacy of the Kale's heat transfer correlation, in this study the following modifications have

been made: 1) the numerator (f/2) in Equation (4.7) was multiplied by the correction factor, $(1-FR)^{0.6}$. This is analogous to the modification made by Pruitt et al. [37] for viscoelastic fluids (see Equation (2.25)); and 2) the Deborah number (De) in Equation (4.7) was replaced by a function of Weissenberg number (Ws^a), in which the fluid time scale is estimated from viscosity data using the Powell-Eyring fluid model (see Equation (4.1)). For the maximum heat transfer reduction case, Kale suggested De to be 20, and the current study showed Ws to be 200. From this, the adjustable constant a was evaluated to be 0.565. The final proposed expression for heat transfer correlation is

$$St = \frac{f/2\ (1 - FR)^{0.6}}{1.2 + (Pr_a - 1)\sqrt{(f/2)}\ \{9.2\ Pr_a^{-0.258} + 1.2\ Ws^{0.565}\ Pr_a^{-0.236}\}} \qquad (4.8)$$

The verification of Equation (4.8) was conducted with the experimental data of Kwack [26] and this study. Figure 4.22 shows that the proposed heat transfer correlation can predict the heat transfer coefficients within the maximum deviation of 30%.

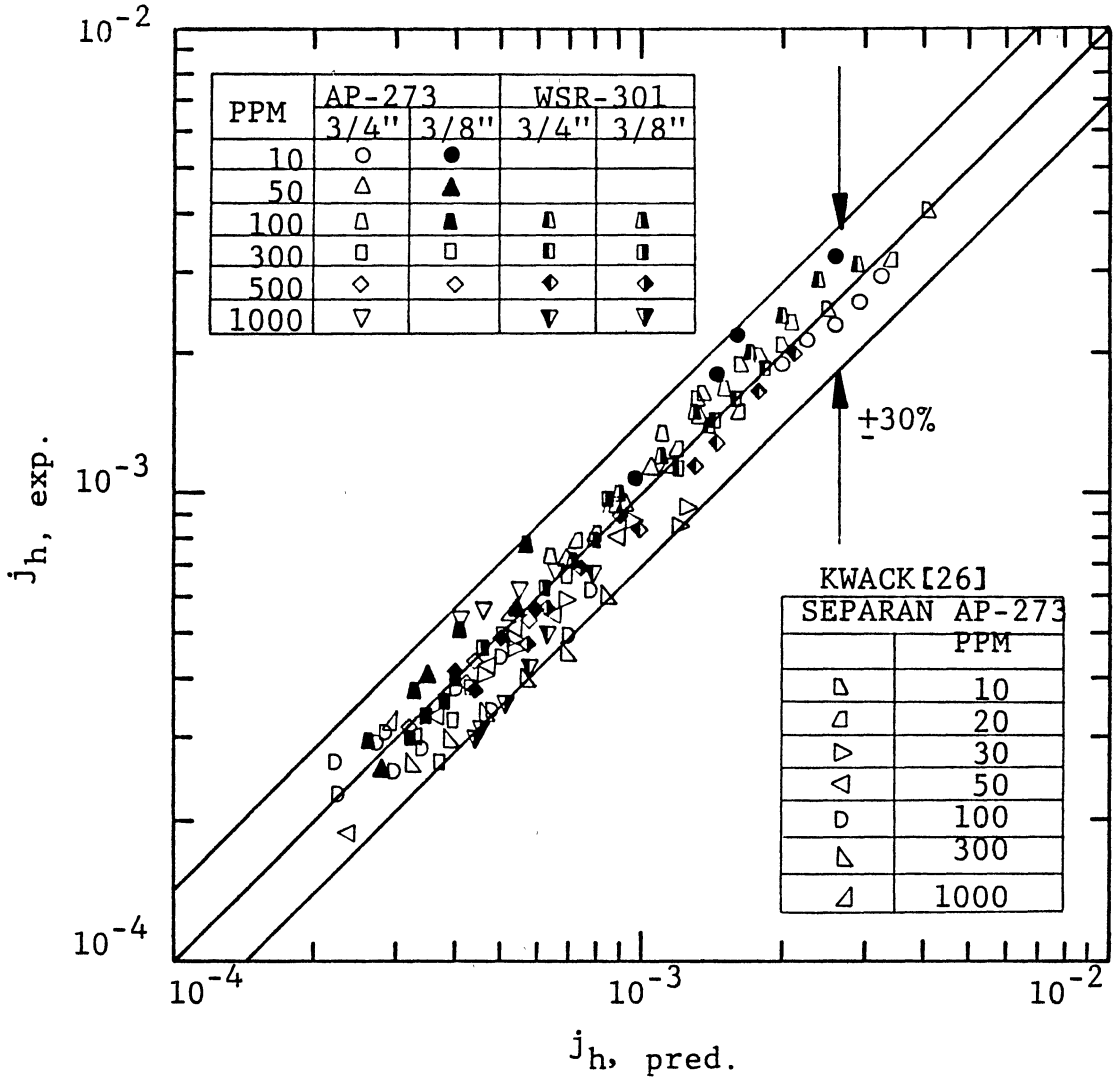

Figure 4.22 Comparison of the Predicted Colburn j-Factors Using the Proposed Correlation for Heat Transfer With the Experimental Data

CHAPTER V

ANALYTICAL STUDY

Numerous attempts have been made to predict the heat transfer characteristics of viscoelastic fluids in turbulent pipe flows by solving the time-mean energy equation with an expression for eddy diffusivity of heat, ε_h. However, most analytical studies used either an inadequate expression for eddy diffusivity of heat which was based on unreliable experimental data as discussed in Section 1.2, or a direct analogy between eddy diffusivities of heat and momentum. For the latter case, several studies [4, 23, 26] have shown that the turbulent Prandtl numbers of the concentrated viscoelastic fluids are not unity, especially near the wall, where it is important to have accurate values of heat eddy diffusivity for reliable heat transfer calculation.

Since the characteristics of viscoelastic turbulent flows can be affected by several factors such as pipe diameter, purity of the water, aging, type and concentration of the polymer, as well as method of formulating the solution, predictions based solely on first principles are not likely to exist in the near future. The objective of this study is to develop a general semi-empirical equation for eddy diffusivity of heat in terms of pertinent dimensionless parameters for viscoelastic fluids, which can be determined directly from experimental measurements of pressure drop and rheological properties. The developed expression is validated with the experimental data of Kwack [26] and the current

study. This chapter comprises of mathematical background, eddy diffusivity for momentum, and eddy diffusivity for heat.

5.1 Mathematical Background

The basic field equations of a fluid based on the axioms and the theories of continuum mechanics, i.e. the conservation equations for mass, linear momentum and energy, can be used for both Newtonian and non-Newtonian fluids. The time-averaged field equations for turbulent flows can be written as

mass:

$$\frac{\partial u_i}{\partial x_i} = 0 \tag{5.1}$$

momentum:

$$u_j \frac{\partial u_i}{\partial x_j} = \nu \frac{\partial^2 u_i}{\partial x_j^2} - \frac{1}{\rho} \frac{\partial P}{\partial x_i} - \frac{\partial(\overline{u_i' u_j'})}{\partial x_j} \tag{5.2}$$

energy:

$$u_j \frac{\partial T}{\partial x_j} = \alpha \frac{\partial^2 T}{\partial x_j^2} - \frac{\partial(\overline{T' u_j'})}{\partial x_j} \tag{5.3}$$

For the fully developed axisymmetric flow in a circular tube, Equation (5.2) becomes

$$\frac{1}{r} \frac{\partial}{\partial r}[r(\nu + \varepsilon_m) \frac{du}{dr}] = \frac{1}{\rho} \frac{\partial P}{\partial x} \tag{5.4}$$

where $\overline{u'v'} = - \varepsilon_m \frac{\partial u}{\partial r}$ (5.5)

For the thermally fully developed turbulent tube flow, Equation (5.3) becomes

$$\frac{1}{r}\frac{\partial}{\partial r}\left[r(\alpha + \varepsilon_h)\frac{\partial T}{\partial r}\right] = u\frac{\partial T}{\partial x} \tag{5.6}$$

where

$$\overline{v'T'} = -\varepsilon_h \frac{\partial T}{\partial r} \tag{5.7}$$

Equations (5.4) and (5.6) should be non-dimensionalized before integrations for general application of the results. The process employed in the current study was based on the work of Ghajar [83]. First of all, non-dimensionalize the variables such that

$$\bar{u} = \frac{u}{U} \quad , \quad \bar{P} = \frac{P}{\rho U^2} \quad , \quad \bar{x} = \frac{x}{r_0} \quad , \quad \bar{r} = \frac{r}{r_0} \tag{5.8}$$

Equation (5.4) with the use of Equation (5.8) can be written as

$$\frac{1}{\bar{r}}\frac{\partial}{\partial \bar{r}}\left[\bar{r}\,(1 + \varepsilon_m/\nu)\frac{d\bar{u}}{d\bar{r}}\right] = RF \tag{5.9}$$

where

$$R = \frac{r_0 U}{\nu} \quad , \quad F = \frac{d\bar{P}}{d\bar{x}} \tag{5.10}$$

Equation (5.9) may be integrated twice with the aid of boundary conditions

$$\frac{d\bar{u}}{d\bar{r}} = 0 \qquad \text{at } \bar{r} = 0$$

and (5.11)

$$\bar{u} = 0 \qquad \text{at } \bar{r} = 1$$

This integration results in the non-dimensionalized form of the mean velocity profile:

$$1 = RF \int_0^1 \int_1^{\bar{r}} \left[\frac{r}{1 + \varepsilon_m(r)/\nu}\,dr\right] \bar{r}\,d\bar{r} \tag{5.12}$$

The eddy diffusivity expression in Equation (5.12) must be chosen so

that this equation is satisfied. Consequently, the eddy diffusivity for momentum must be determined such that the product of RF determined from Equation (5.12) agrees with the experimental data. Details concerning the eddy diffusivity for momentum are discussed in Section 5.2.

For the thermally fully developed flow under the constant wall heat flux condition, the following relationship holds

$$\frac{dT}{dx} = \frac{dT_b}{dx} = \frac{2\dot{q}''}{r_0 U \rho C} \tag{5.13}$$

Equation (5.6) may be integrated twice with the use of Equation (5.13) and the boundary conditions

$$T = T_w \qquad \text{at } r = r_0$$

and (5.14)

$$\frac{\partial T}{\partial r} = 0 \qquad \text{at } r = 0$$

The final dimensionless expression for heat transfer coefficient can be derived as:

$$St = \frac{\int_0^1 \bar{u}\,\bar{r}\,d\bar{r}}{Re \int_0^1 \bar{u}\,\bar{r} \left\{ \int_0^{\bar{r}} \left[\frac{\int_{\bar{r}_1}^1 \bar{u}\,\bar{r}_2 d\bar{r}_2}{\frac{1}{\varepsilon_h(\bar{r}_1)/\nu + \frac{1}{Pr}}} \right] d\bar{r}_1 \right\} d\bar{r}} \tag{5.15}$$

Details of the mathematical derivations may be found in Ghajar [83]. With the velocity profile obtained from Equation (5.12), the heat transfer coefficient can be calculated with the use of Equation (5.15) only if an eddy diffusivity for heat is available. The eddy diffusivity for heat is discussed in Section 5.3.

5.2 Eddy Diffusivity for Momentum

An accurate prediction of velocity profile is essential not only to investigate the mechanism of momentum transfer but also to predict the phenomenon of heat transfer. In this study, the momentum eddy diffusivity model proposed by Cess [64] was used to solve Equation (5.12). The Cess model is a combination of the van Driest's sublayer equation [63] and the Reichardt's middle law equation [84]. To account for the viscous effect on turbulent eddies due to the proximity of the wall, van Driest [63] included the damping factor $[1-\exp(-y^+/A^+)]$ of Stokes [85] in the Prandtl mixing length. The van Driest's model was expressed as

$$\frac{\varepsilon_m}{\nu} = \frac{1}{2}\left\{1 + 4K^2 (y^+)^2[1 - \exp(-y^+/A^+)]^2\right\}^{1/2} - \frac{1}{2} \tag{5.16}$$

where

$$y^+ = \frac{yu_\tau}{\nu} \tag{5.17}$$

This expression yields the continuous velocity and shear distribution near a smooth wall. From the experimental data available, Reichardt [84] found that the eddy diffusivity for momentum could be well-correlated by the following polynomial:

$$\frac{\varepsilon_m}{\nu} = \frac{Kr_0^+}{6}[1 - (\bar{r})^2][1 + 2(\bar{r})]^2 \tag{5.18}$$

where

$$r_0^+ = \frac{r_0 u_\tau}{\nu} \tag{5.19}$$

This expression eliminates the inherent failing of the mixing length theory in which the eddy diffusivity does go to zero at the tube axis.

Cess [64] observed that Equation (5.16) given by van Driest [63]

for the flow close to the wall reduces to the Prandtl's expression

$$\frac{\varepsilon_m}{\nu} = 0.4y^+ \tag{5.20}$$

for large value of y^+. It was also observed that the Reichardt's middle law [84] given by Equation (5.18) reduces to the Prandtl's expression for $\bar{r}$ close to unity for K = 0.4. In other words, for a region sufficiently far from the wall such that the fluid viscosity does not affect the mechanism of turbulence, but yet close enough to the wall such that the Prandtl's mixing length theory still holds, Equations (5.16) and (5.18) give effectively the same result. Consequently, the van Driest's expression and the Reichardt's equation may be combined to give

$$\frac{\varepsilon_m}{\nu} = \frac{1}{2}\left\{1 + \frac{K^2 r_0^{+2}}{9}[1 - (\bar{r})^2]^2[1 + 2(\bar{r})^2]^2[1 - \exp(\frac{\bar{r}-1}{A^+/r_0^+})]^2\right\}^{1/2} - \frac{1}{2} \tag{5.21}$$

This equation yields a continuous expression for momentum eddy diffusivity throughout the entire flowfield. Furthermore, Equation (5.21) satisfies the Elrod's condition [86] that the turbulent eddy diminishes with a power of y^+ not less than four near the wall as well as applies in the central region of the tube where the mixing length theory fails. In Equation (5.21), K and A^+ are free constants. K is called the von Karman constant and 1/K is proportional to the slope of the log portion of the universal law of the wall. A^+ is a constant that characterizes the thickness of the sublayer.

When the Cess model is applied to viscoelastic flows, it is very important that the determined values of parameters, K and A^+, are compatible with the experimental observations. It has been established

by several studies [1, 2, 48] that the addition of polymer shifts the velocity for solvent upward with no virtual change of the slope in the log portion of the universal law. The slope is known to be 0.4. The parameter A^+ should be determined such that it can properly account for the variations of the laminar layer thickness with the addition of polymer. In the current study, the parameter A^+ was determined using the iterative computational scheme proposed by Tiederman and Reischman [65] for calculation of velocity profile in viscoelastic turbulent flows. The procedure requires only pressure drop and flow rate information. The predictions based on this scheme have been compared with several experimental velocity profiles for channel flows [65] and limited pipe flows [83]. In all cases the predictions showed excellent agreement with experimentally measured profiles in turbulent viscoelastic flows. In order to further verify the computational scheme, this technique was used to predict the velocity profiles and the momentum eddy diffusivities in both Newtonian and viscoelastic pipe flows. As for comparison data, the measurements of Mizushina and Usui [4] were adopted. They used a laser-Doppler anemometer technique, which can produce accurate measurements of the flowfield with the least amount of disturbance to the flow. As shown in Figure 5.1, the predictions show excellent agreement with experimentally measured velocity profiles in both Newtonian and drag-reducing flows. Figure 5.2 illustrates that the Cess model can be used successfully in predicting the eddy diffusivities of momentum for the maximum drag reduction case as well as the Newtonian case.

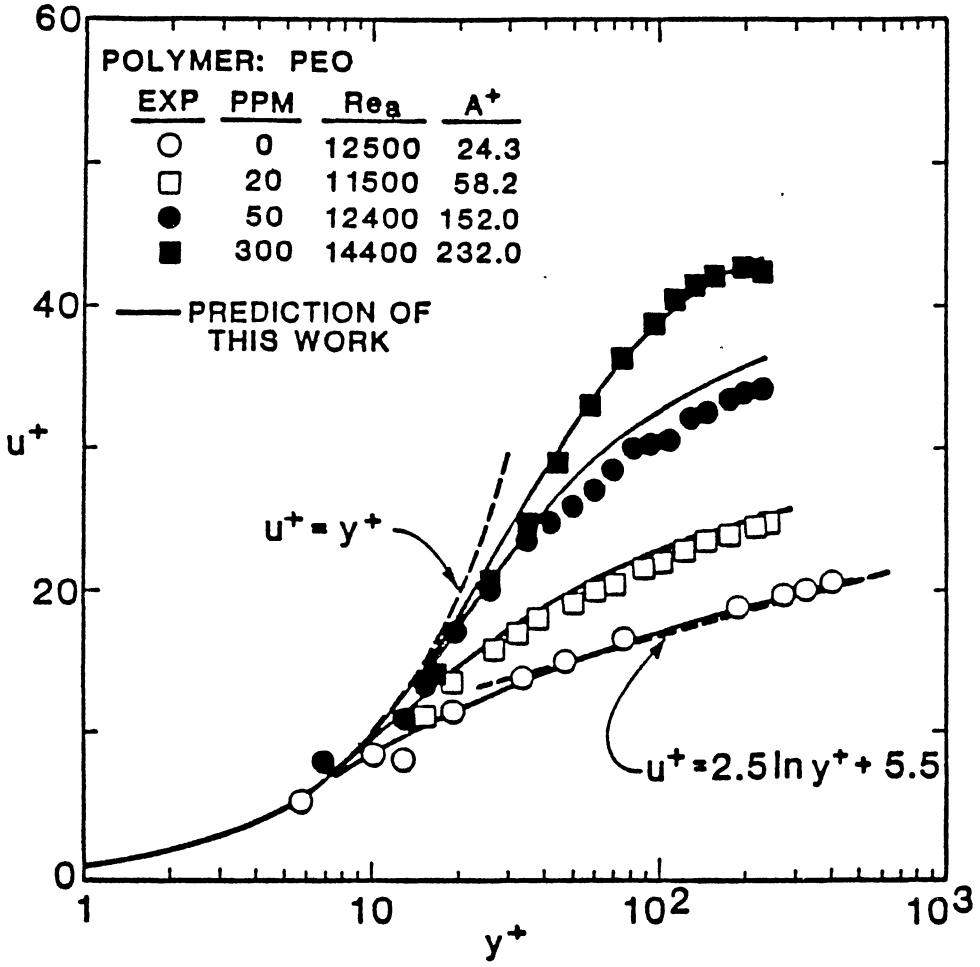

Figure 5.1 Time-Mean Velocity Profile for Newtonian and Viscoelastic Flows: Predicted and Experimental [4]

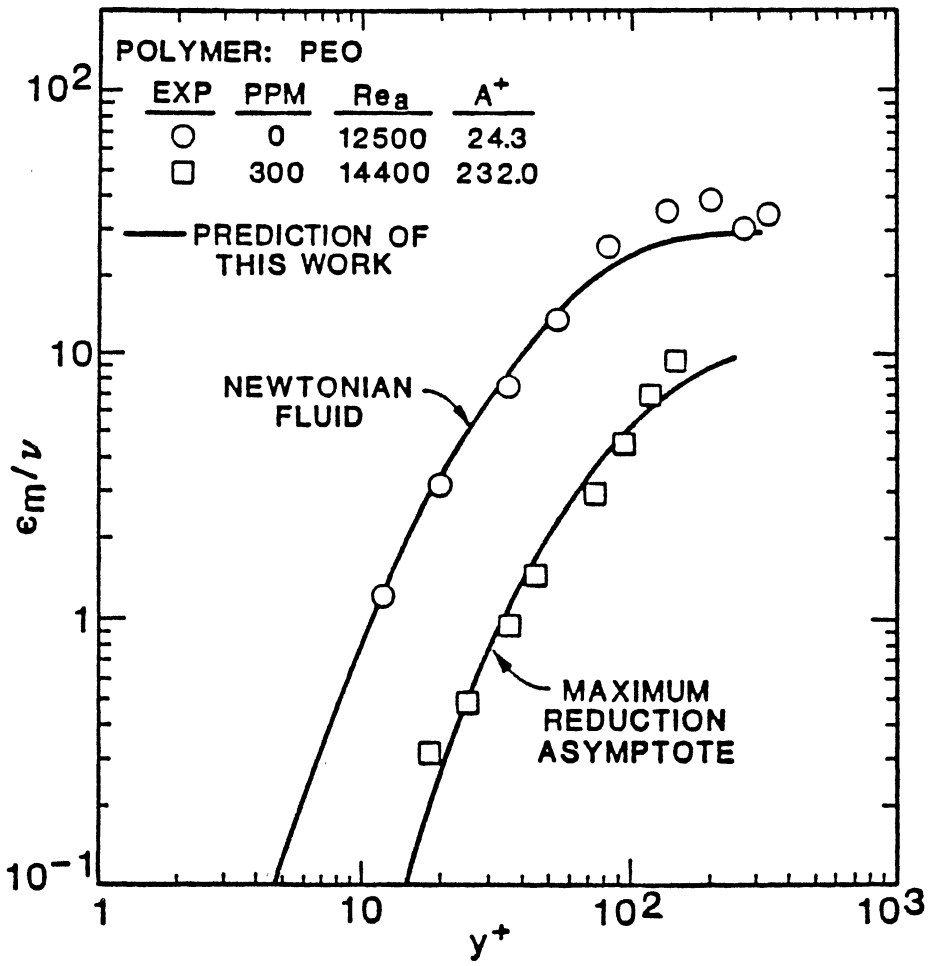

Figure 5.2 Momentum Eddy Diffusivities for Newtonian and Viscoelastic Flows: Predicted and Experimental [4]

5.3 Eddy Diffusivity for Heat

With the known velocity profile, the heat transfer coefficient can be determined by solving Equation (5.15) with the use of an eddy diffusivity expression for heat which takes into account particular characteristics of viscoelastic fluids. As pointed out earlier, most previous studies have used a direct analogy between momentum and heat transfer for viscoelastic pipe flows. This could introduce considerable error in heat transfer predictions as shown in Figure 5.3, especially at high concentrations. This discrepancy is due to the fact that these analytical studies did not account for the effect of elasticity on the friction and heat transfer in viscoelastic fluids. For the better predictions, the previous work of the author [23] used three different expressions for eddy diffusivity of heat, depending on the Prandtl number of the polymer solutions. However, the subsequent study established that the effect of elasticity on heat transfer in viscoelastic flows can not be well-characterized in terms of Prandtl number. To remedy the inadequacy of the existing analytical studies for viscoelastic turbulent pipe flows, the current study is to develop a semi-empirical equation for eddy diffusivity of heat in terms of pertinent dimensionless parameters for viscoelastic fluids, which can be determined directly from experimental measurements of pressure drop and rheological properties.

The fluid time scale (λ) is the most useful and readily measurable material property that can be used to measure the elasticity of a fluid. It can be accurately determined from the rheological properties of the fluid with the use of an appropriate constitutive equation. Several studies have used the fluid time scale to interpret the

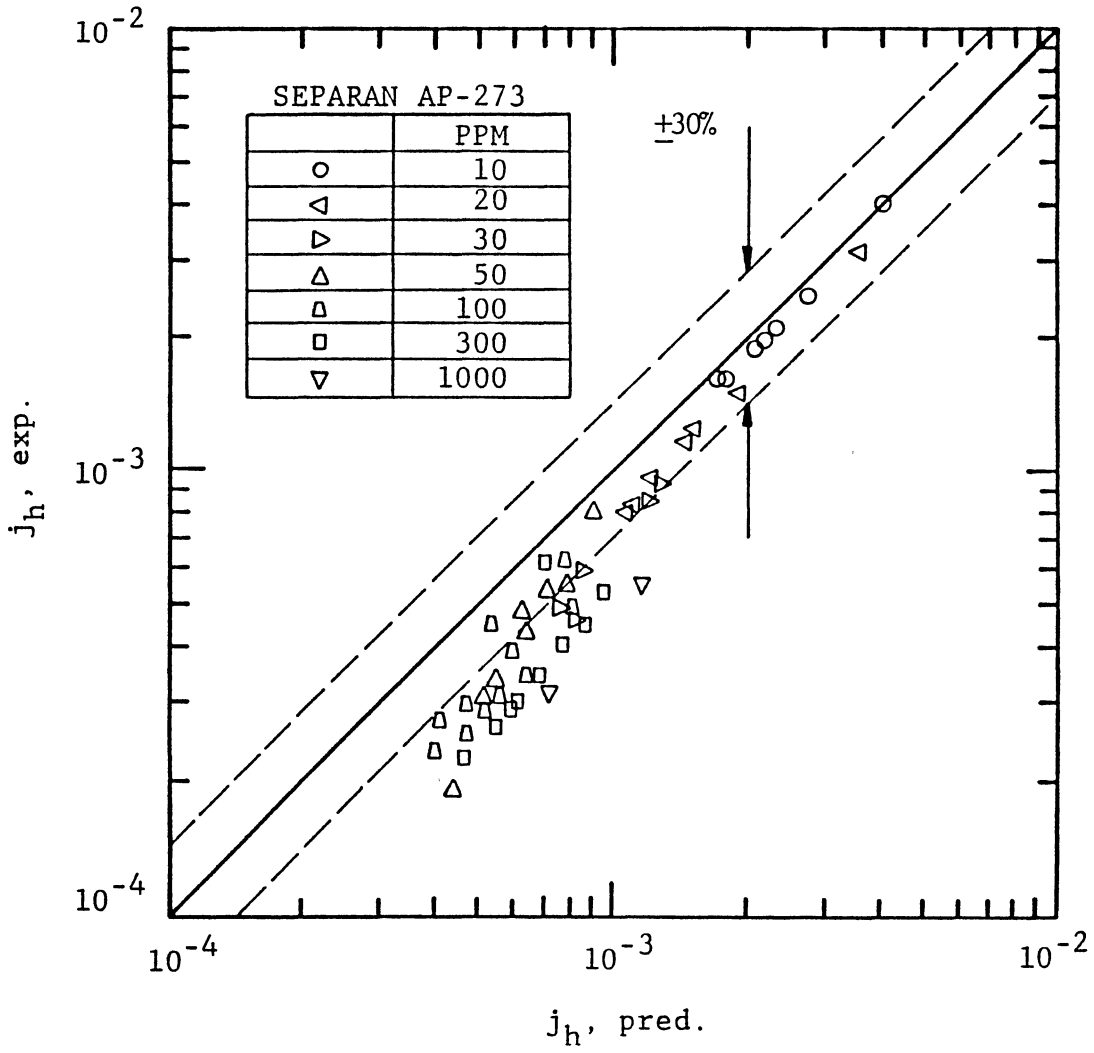

Figure 5.3 Comparison of the Predicted Colburn j-Factors Using a Direct Analogy Between Heat and Momentum Transfer With Measurements [26]

influence of the elasticity of the solution on the friction and/or heat transfer behavior of viscoelastic turbulent flows. Corman [38] included the fluid time scale in the expression for the dimensionless thickness of the laminar layer to account for the thickening of this layer due to the addition of polymer. Poreh and Paz [13] explained the drag reduction phenomenon as the upward shift of velocity profile in the log portion of the universal law. The velocity shift was expressed in terms of the fluid time scale. Mizushina and Usui [4] suggested that the drag reduction phenomenon is due to the increased effect of damping near the wall region. They modified the van Driest's damping factor model for momentum with the use of the fluid time scale. Darby and Chang [58] developed a generalized correlation for friction loss in drag reducing polymer solutions, which includes a fluid time scale. Kale [35] used the fluid time scale to correlate heat transfer coefficient with friction factor for viscoelastic turbulent pipe flows. Recently, Kwack [26] suggested that for the fully developed turbulent pipe flows, the friction factor and heat transfer coefficient can be expressed as a function of Reynolds number and Weissenberg number (the ratio of the fluid time scale to the flow time scale). The above studies indicate that the fluid time scale is one of the key properties for proper representation of the elasticity in viscoelastic turbulent pipe flows. Since the friction and heat transfer behaviors of viscoelastic turbulent pipe flows are affected by not only the fluid conditions but also the flow conditions, such as the pipe diameter and the flow rate, the fluid time scale should be combined with the flow time scale (D/U) to form a complete dimensionless parameter. In this study, the Weissenberg number (Ws) was used as one of the key dimensionless parameters in the eddy

diffusivity expression for heat.

Another important parameter in viscoelastic fluids is the friction drag reduction ratio (FR), which can be determined from the experimental measurements of pressure drop. Since the energy equation is directly related to the equation of motion, in heat transfer calculations involving viscoelastic fluids, the friction drag reduction ratio plays a very important role. Pruitt et al. [37] used the friction drag reduction ratio in correlating friction factor with heat transfer coefficient in viscoelastic turbulent pipe flows. Mizushina and Usui [4] showed that Colburn's analogy in general does not hold for viscoelastic fluids except in the high Reynolds number range of low concentrations. They suggested that the correction factor for the deviation from Colburn's analogy depends only on the Reynolds number and the friction drag reduction ratio. Hughmark [14, 87] in the development of the expression for friction factor and heat transfer coefficient using the three region resistance model, related the wall region frequency to the ratio of friction factor for the polymer solution to that for the solvent. The above studies indicate that the friction drag reduction ratio is another important dimensionless parameter relating friction and heat transfer behavior in viscoelastic turbulent pipe flows.

Based on the above observations, a new semi-empirical equation for eddy diffusivity of heat was formulated in terms of Weissenberg number and friction drag reduction ratio. The basic assumptions made in the formulation of the equation were: a) the ratio of eddy diffusivity for heat to that for momentum is constant across the test section; b) the eddy diffusivity of heat decreases exponentially with the increase of Weissenberg number up to the critical value of Weissenberg number for

heat transfer (Ws_{ch}), which corresponds to the minimum heat transfer asymptote. This is analogous to the observations made by Kwack [26] for the behavior of heat transfer coefficient with respect to Weissenberg number; and c) the influence of friction drag reduction ratio on the eddy diffusivity of heat is of the form (1-FR), which is consistent with the correlation of Pruitt et al. [37]. Based on these assumptions, the following expression for eddy diffusivity of heat is proposed:

$$\varepsilon_h/\varepsilon_m = a(1 - FR)^b \, e^{[1-Ws/Ws_{ch}]^c} \qquad (5.22)$$

The proposed equation is in qualitative agreement with the experimental observations, and is presented in a generalized form which is applicable to non-Newtonian viscoelastic as well as Newtonian fluids. For Newtonian fluids (FR = 0 and Ws = 0) the ratio of eddy diffusivities is equal to a constant which is in agreement with Equation (5.22). For viscoelastic fluids the degree of reduction in heat transfer is even more drastic than that in friction. This behavior is accounted for through the use of the two dimensionless parameters FR and Ws. Particularly, even after the friction factor of a solution reaches the maximum drag reduction asymptote, there is still a decrease in the heat transfer coefficient up to the critical Weissenberg number for heat transfer. This behavior is accounted for by the second term in Equation (5.22). Even though the reduction in heat transfer is limited by the minimum heat transfer asymptote, further polymer addition results in an increased Weissenberg number beyond the critical value. The proposed equation can not explain this phenomenon. For the case of $Ws \geq Ws_{ch}$, the term (Ws/Ws_{ch}) in Equation (5.22) is set to unity.

The three constants in the proposed equation should be determined such that the equation is applicable to non-Newtonian viscoelastic as well as Newtonian fluids. The constant **a** has a fixed value which is determined from the Newtonian fluid behavior. It is known that for Newtonian fluids, FR and Ws are equal to zero and $\varepsilon_h/\varepsilon_m$ is close to unity. The substitution of FR = 0, Ws = 0 and $\varepsilon_h/\varepsilon_m = 1$ into Equation (5.22) determines the constant **a** to be 0.37. The constants **b** and **c** will be evaluated with the experimental data of Kwack [26] for Separan AP-273. Kwack's data are considered reliable and well-documented. His experiments reported enough information to start the calculations. For the minimum heat transfer asymptote ($Ws \geq Ws_{ch}$), the proposed equation becomes a function of FR only. Kwack [26] showed that for this case the ratio of eddy diffusivities, $\varepsilon_h/\varepsilon_m$, has the limiting values of 0.134 for Re = 20,000 and 0.124 for Re = 30,000. The calculations of FR with the use of the minimum drag asymptotic correlation ($f = 0.20\ Re_a^{-0.48}$) of Kwack [26] and the well-established Newtonian correlation ($f = 0.0014 + 0.125\ Re_a^{-0.32}$) of McAdams [79] for friction factor show that the friction drag reduction ratios are 0.74 for Re_a = 20,000 and 0.76 for Re_a = 30,000. The substitution of $\varepsilon_h/\varepsilon_m$ and FR values into Equation (5.22) with **a** = 0.37 determines the constant **b** to be 0.75. Before the constant **c** can be determined, Ws_{ch} should be known. The critical Weissenberg number for heat transfer was evaluated between 200 and 250 by Ng and Hartnett [30] and confirmed by Kwack [26] using a polyacrylamide (Separan AP-273). A careful examination of their experimental results and our current results presented in Section 4.4 shows that Ws_{ch} is closer to 200, even though slightly dependent on Reynolds number. In this study, Ws_{ch} was taken to be 200. To determine

the constant c, the experimental data on the minimum drag asymptote (50 ppm) but not on the minimum heat transfer asymptote were used. The preferential choice of experimental data for the minimum drag asymptote was because this asymptotic condition was consistent with the results of this study (see Figure 4.12). Through a linear regression method, the constant **c** was evaluated to be 3. The substitution of the above determined values in Equation (5.22) results in

$$\varepsilon_h/\varepsilon_m = 0.37\ (1 - FR)^{0.75}\ e^{[1 - (Ws/200)]^3} \qquad (5.23)$$

where FR and Ws in Equation (5.23) can be determined from the measurements of pressure drop and apparent viscosity of the solution.

It should be remarked that the constant **a** was determined from the Newtonian fluid behavior, and the constants **b** and **c** from the minimum asymptotic conditions for heat transfer and friction, respectively. Since the conditions used for the determination of the constants should be consistent, independent of the experimental procedures, it is expected that Equation (5.23) can be used to predict the heat transfer behavior of all viscoelastic turbulent pipe flows without any adjustment of the constants.

The proposed equation is validated with heat transfer experimental results of Kwack [26], for aqueous solutions of polyacrylamide (Separan AP-273) for concentrations ranging from 10 to 1000 ppm in turbulent flows through pipes under the constant wall heat flux condition. Figure 5.4 shows that the predictions of heat transfer coefficients with the use of the proposed equation are in good agreement with the experimental results. Is should be noted that even though the form of the proposed

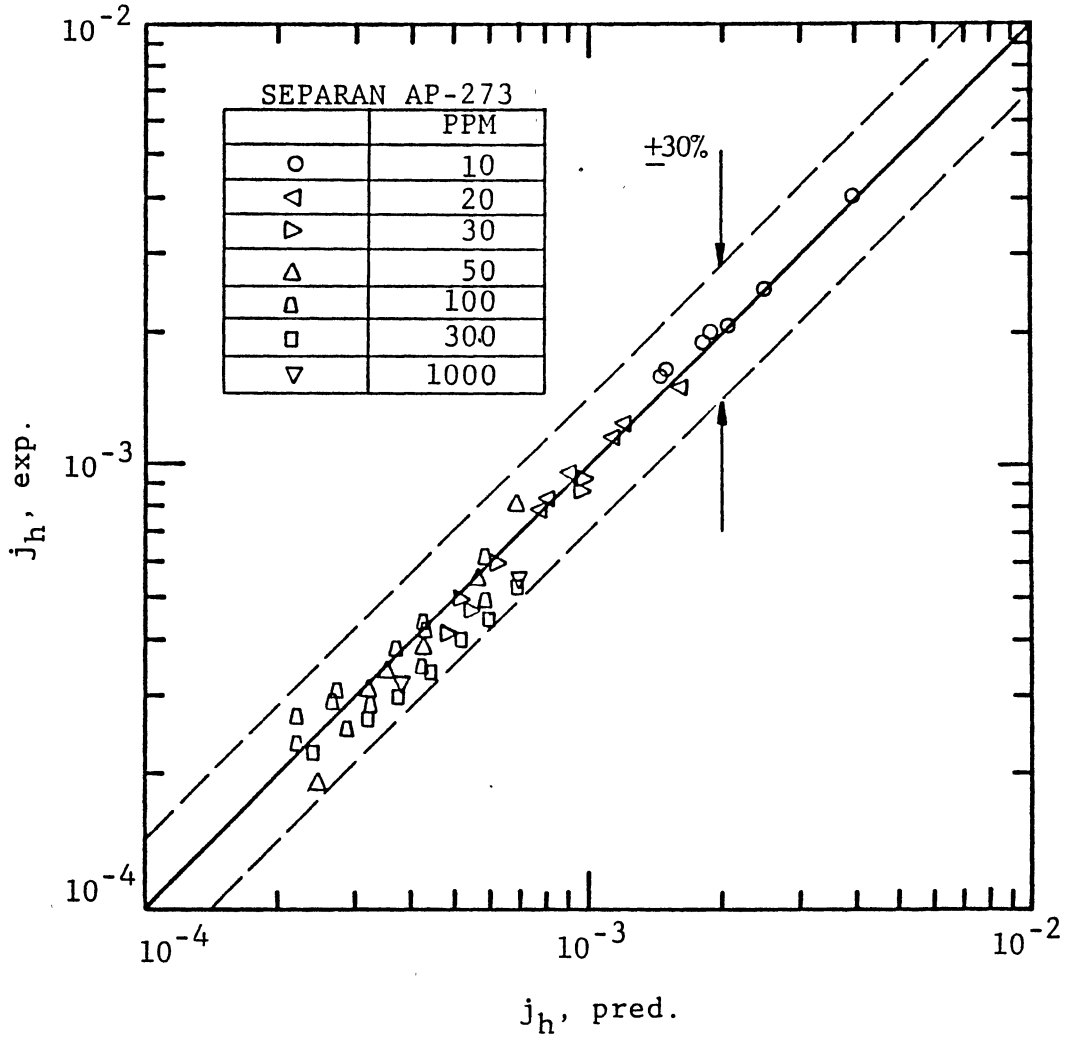

Figure 5.4 Comparison of the Predicted Colburn j-Factors Using the Proposed Heat Eddy Diffusivity Equation With Measurements [26]

equation and the two adjustable constants were established based on the experimental data of Kwack [26] for the minimum drag and heat transfer asymptotic conditions, the proposed equation was able to predict comparably the heat transfer coefficients for all polymer concentrations obtained from Kwack's experiments without any adjustment of the constants. The predictions for all concentrations result in a maximum of 30 percent deviation from the measurements. The results of this study indicate that the proposed equation for eddy diffusivity of heat is capable of predicting experimental heat transfer coefficients for Separan AP-273 in turbulent pipe flows with wide range of polymer concentrations provided that the experimental measurements of the pressure drop and the fluid time scale are available. It is also expected that the proposed equation is applicable to different types of polymers with wide ranges of concentrations. This is due to the fact that the fluid time scale and the flow time scale in the proposed equation can account for several important factors influencing the friction and heat transfer behavior of viscoelastic turbulent pipe flows, such as pipe diameter, solvent chemistry, degradation, as well as the type and the concentration of polymer. The general applicability of the proposed Equation (5.23) is further verified with extensive experimental data of this study, which were obtained for Separan AP-273 and WSR-301 solutions with the concentration range of 10 to 1000 ppm in the thermally fully developed region of two different pipe diameters. Figure 5.5 indicates that the proposed equation can predict all of the experimental data within the maximum deviation of 30%.

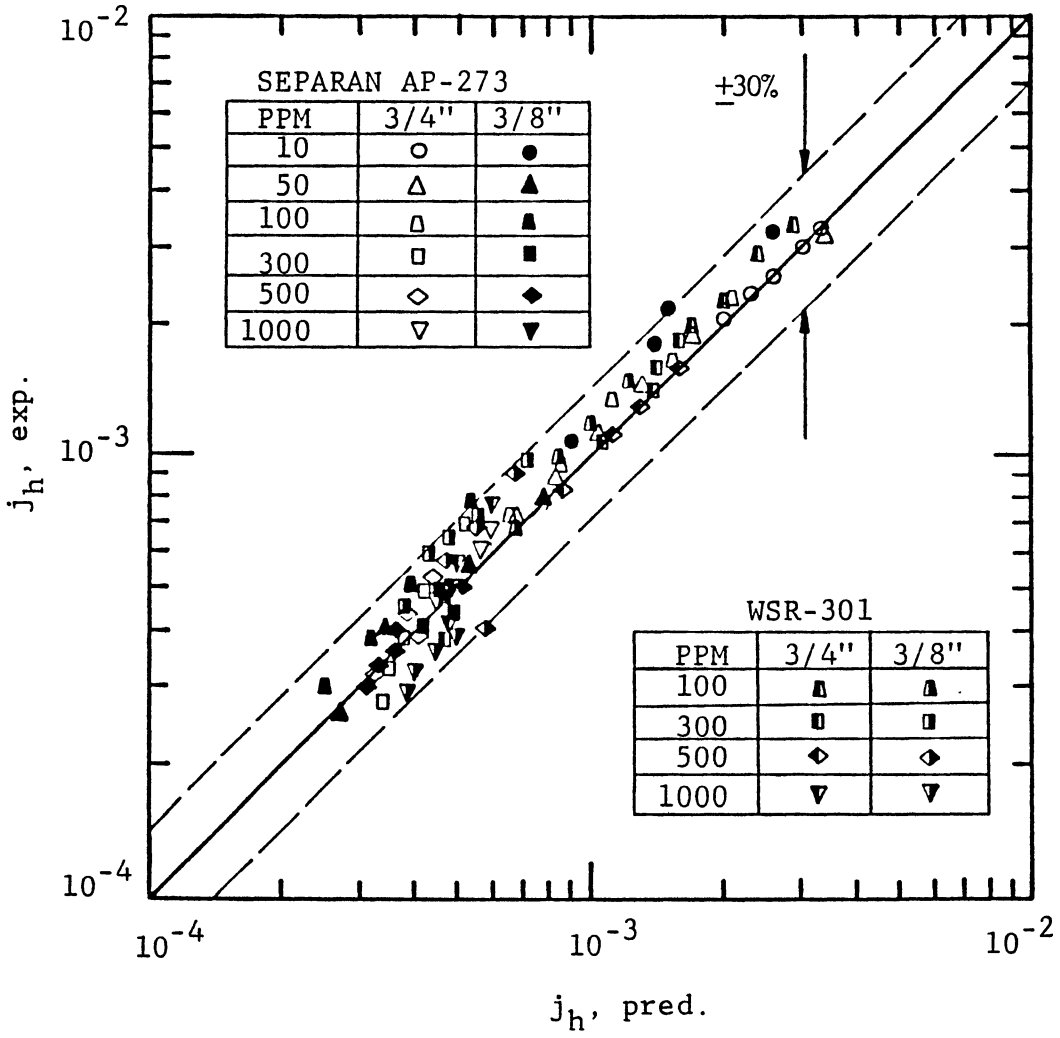

Figure 5.5 Comparison of the Predicted Colburn j-Factors Using the Proposed Heat Eddy Diffusivity Equation With the Current Experimental Data

CHAPTER VI

CONCLUSIONS AND RECOMMENDATIONS

To obtain the better understanding of the flow characteristics for viscoelastic turbulent pipe flows under the constant wall heat flux condition, a series of experimental and analytical studies have been conducted and their results were presented and discussed in detail in chapters IV and V. In this chapter, the accomplishments of the present study will be summarized and the recommendations for the future work will be specified.

6.1 Conclusions

The general conclusions drawn from this study may be summarized as:

1. The Powell-Eyring fluid model used to estimate the fluid time scale was investigated. It was found that this model is extremely sensitive to small variations in the zero shear rate viscosity, especially for the high concentration solutions. It was shown that the accurate estimation of fluid time scale for the high concentrations demands the zero shear rate viscosity data at shear rates of order of $10^{-1}sec^{-1}$. On the other hand, the Powell-Eyring model was found to be moderately sensitive to variations in the infinite shear rate viscosity. The current study indicates that the uncertainty in the estimation of the fluid time scale using the Powell-Eyring model, due to variations in the infinite shear rate viscosity, is negligible if the

viscosity is measured at a shear rate greater than $10^4 sec^{-1}$. As compared with other fluid models, the Powell-Eyring model is known to produce quite consistent results in the calculation of the fluid time scale at various polymer concentrations. However, this model still has room for improvement.

2. The characteristics of viscoelastic fluids were investigated using Separan AP-273 solutions and WSR-301 solutions with the concentrations of 10-1000 ppm. All the experimental data were presented in terms of pertinent dimensionless groups. The reductions in friction drag and heat transfer were more pronounced with the increase of polymer concentration and the decrease of pipe diameter. However, those reductions were limited to the maximum reduction asymptotes, which of the current study fairly well agreed with Kwack's results [26]. It was found that Separan AP-273 is a more effective drag reducer as compared with WSR-301. From this, it was postulated that the effectiveness of a polymer may be estimated on the basis of either the viscosity increase of a solution at the low shear rates, or the average molecular weight of a polymer.

3. The scaling scheme for pipe diameter and polymer concentration suggested by Astarita et al. [42] for friction factor was applied to the current experimental data for additional verification of its general applicability to other polymers and extended to the case of heat transfer. The current study suggested that this scheme may be generally applicable. The extension of this scheme to the case of heat transfer was found to yield fairly good results, except for the high concentration solutions. Since most of the practical engineering systems use dilute polymer solutions, this scheme is considered

valuable.

4. The critical Weissenberg number for heat transfer was studied using a Separan AP-273 solution of 1500 ppm and a Separan AP-30 solution of 3000 ppm. This study implied that the critical Weissenberg number for heat transfer is independent of polymer types, but weakly dependent on Reynolds number. The critical Weissenberg number for heat transfer was evaluated to be 200-250.

5. Based on the extensive and reliable experimental data of Kwack [26] and this study, an attempt was made to develop a heat transfer correlation in a closed form. The proposed expression is:

$$St = \frac{f/2\ (1 - FR)^{0.6}}{1.2 + (Pr_a - 1)\sqrt{(f/2)}\ \{9.2\ Pr_a^{-0.258} + 1.2\ Ws^{-0.565}\ Pr_a^{-0.236}\}} \qquad (4.8)$$

The predictability of equation (4.8) was validated with the various experimental data of Kwack [26] and this study. This correlation was proven to predict the experimental data fairly well.

6. A semi-empirical equation for heat eddy diffusivity was developed as a function of friction drag reduction ratio (FR) and Weissenberg number (Ws). The proposed equation is

$$\varepsilon_h/\varepsilon_m = 0.37\ (1 - FR)^{0.75}\ e^{[1-(Ws/200)]^3} \qquad (5.23)$$

The two main parameters in the expression can be directly determined from the measurements of pressure drop and rheological properties. The predictability of Equation (5.23) was validated with the experimental data of Kwack [26] and this study. This equation was proven to predict the experimental data within the maximum difference of 30%.

6.2 Recommendations

Based on the observations made during this study, the following recommendations are suggested:

1. The Powell-Eyring fluid model used in the estimation of the fluid time scale should be further studied with an aim to improve its performance.

2. The effects of variable properties on the characteristics of viscoelastic fluids need to receive further attention, since some rheological properties are significantly temperature dependent. This may aid in the development of the variable property prediction scheme in the future.

3. The current scaling scheme for pipe diameter and polymer concentration should be further validated with various experimental data. If feasible, it is valuable to relate this scheme to the rheological properties of fluid.

4. The characteristics of viscoelastic fluids in the hydrodynamically and thermally developing regions should be further investigated, since there are numerous instances using the fluids in these regions. An attempt should be made to develop a reliable prediction scheme for developing solutions.

5. The low Reynolds number phenomena in viscoelastic fluids should be further investigated, since in some cases the viscoelastic flows are laminar because of the large viscosities of polymer solutions.

REFERENCES

1. Dimant, Y., and Poreh, M., "Heat Transfer in Flows with Drag Reduction," Advances in Heat Transfer, Vol. 12, 1976, pp. 77-113.

2. Cho, Y. I., and Hartnett, J. P., "Non-Newtonian Fluids in Circular Pipe Flow," Advances in Heat Transfer, Vol. 15, 1982, pp. 59-141.

3. Yoo, S. S., and Hartnett, J. P., "Thermal Entrance Lengths for Non-Newtonian Fluids in Turbulent Pipe Flows," Letters in Heat and Mass Transfer, Vol. 2, 1975, pp. 189-198.

4. Mizushina, T., and Usui, H., "Reduction of Eddy Diffusion for Momentum and Heat in Viscoelastic Fluid Flow in a Circular Tube," The Physics of Fluids, Vol. 20, No. 10, Pt. 11, October 1977, pp. S100-S108.

5. Ng, K. S., Cho, Y. I., and Hartnett, J. P., "Heat Transfer Performance of Concentrated Polyethylene Oxide and Polyacrylamide Solutions," AIChE J., Vol. 26, 1980, pp. 250-256.

6. Kwack, E. Y., Cho, Y. I., and Hartnett, J. P., "Heat Transfer in Polyacrylamide Solutions in Turbulent Pipe Flow: The Once-Through Mode," AIChE J., Vol. 27, 1981, pp. 123-130.

7. Kwack, E. Y., and Hartnett, J. P., "Effect of Diameter on Critical Weissenberg Numbers for Polyacrylamide Solutions in Turbulent Pipe Flow," Int. J. Heat Mass Transfer, Vol. 25, No. 6, 1982, pp. 797-805.

8. Kwack, E. Y., Hartnett, J. P., and Cho, Y. I., "Chemical Effects in the Flow of Dilute Polymer Solutions," Letters in Heat and Mass Transfer, Vol. 7, 1980, pp. 1-6.

9. Kwack, E. Y., Cho, Y. I., and Hartnett, J. P., "Solvent Effects on Drag Reduction of Polyox Solutions in Square Duct and Capillary Tube Flows," J. Non-Newtonian Fluid Mech., Vol. 9, 1981, pp. 79-90.

10. Kwack, E. Y., and Hartnett, J. P., "Effect of Solvent Chemistry on Critical Weissenberg Numbers," Int. J. Heat Mass Transfer, Vol. 25, No. 9, 1982, pp. 1445-1450.

11. Monti, R., "Heat Transfer in Drag Reducing Solutions," Progress in Heat Transfer, Vol. 5, Oxford: Pergamon Press, 1972, pp. 239-261.

12. Howard, R. G., "Characterization of Heat and Momentum Transfer for Polyox WSR-301 and Polyhall M-295 Solutions," Naval Ship Research and Development Center, Report 7-551, October 1971.

13. Poreh, M., and Paz, U., "Turbulent Heat Transfer to Dilute Polymer Solutions," Int. J. Heat Mass Transfer, Vol. 11, 1968, pp. 805-818.

14. Hughmark, G. A., "Heat and Mass Transfer for Turbulent Pipe Flow," AIChE J., Vol. 17, No. 4, July 1971, pp. 902-909.

15. Smith, R., and Edwards, M. F., "Heat Transfer to Non-Newtonian and Drag-Reducing Fluids in Turbulent Pipe Flow," Int. J. Heat Mass Transfer, Vol. 24, No. 6, 1981, pp. 1059-1069.

16. Metzner, A. B., and Reed, J. C., "Flow of Non-Newtonian Fluids - Correlation of the Laminar, Transition, and Turbulent Flow Regions," AIChE J., 1955, pp. 434-440.

17. Edwards, M. F., and Smith, R., "The Turbulent Flow of Non-Newtonian Fluids in the Absence of Anomalous Wall Effects," J. Non-Newtonian Fluid Mech., Vol. 7, 1980, pp. 77-82.

18. Bird, R. B., "Experimental Tests of Generalized Newtonian Models Containing a Zero Shear Viscosity and a Characteristic Time," Canadian J. Chem. Eng., Vol. 43, 1965, pp. 161-168.

19. Elbirli, B., and Shaw, M. T., "Time Constant from Shear Viscosity Data," J. Rheology, Vol. 22, 1978, pp. 561-566.

20. Cramer, S. D., and Marchello, J. M., "Procedure for Fitting Non-Newtonian Viscosity Data," AIChE J., Vol. 14, No. 5, 1968, pp. 814-815.

21. Cho, Y. I., and Hartnett, J. P., "The Falling Ball Viscometer - a New Instrument for Viscoelastic Fluids," Letters in Heat and Mass Transfer, Vol. 6, 1979, pp. 335-342.

22. Cho, Y. I., Hartnett, J. P., and Kwack, E. Y., "A Study of Wall Effect for Viscoelastic Fluids in the Falling Ball Viscometer," Chem. Eng. Commun., Vol. 6, 1980, pp. 141-149.

23. Yoon, H. K., and Ghajar, A. J., "An Analysis of the Heat Transfer to Drag Reducing Turbulent Pipe Flows," ASME Journal of Heat Transfer, Vol. 106, No. 4, pp. 898-900, November 1984.

24. Cho, Y. I., and Hartnett, J. P., "Analogy for Viscoelastic Fluids -- Momentum, Heat, and Mass Transfer in Turbulent Pipe Flow," Letters in Heat and Mass Transfer, Vol. 7, 1980, pp. 339-346.

25. Ng., K. S., "An Experimental Study of Heat and Momentum Transfer in Pipe Flow of Viscoelastic Fluids," Ph.D. Thesis, U. of Illinois at Chicago Circle, 1982.

26. Kwack, E. Y., "Effect of Weissenberg Number on Turbulent Heat Transfer and Friction Factor of Viscoelastic Fluids," Ph.D. Thesis, University of Illinois at Chicago Circle, 1983.

27. Debrule, P. M., and Sabersky, R. H., "Heat Transfer and Friction Coefficients in Smooth and Rough Tubes with Dilute Polymer Solutions," Int. J. Heat Mass Transfer, Vol. 17, 1974, pp. 529-540.

28. Yoo, S. S., "Heat Transfer and Friction Factors for Non-Newtonian Fluids in Turbulent Pipe Flow," Ph.D. Thesis, U. of Illinois at Chicago Circle, 1974.

29. Tung, T. T, Ng, K. S., and Hartnett, J. P., "Pipe Friction Factors for Concentrated Aqueous Solutions of Polyacrylamide," Letters in Heat and Mass Transfer, Vol. 5, 1978, pp. 59-69.

30. Ng, K. S., and Hartnett, J. P., "Effects of Mechanical Degradation on Pressure Drop and Heat Transfer Performance of Polyacrylamide Solutions in Turbulent Pipe Flow," Studies in Heat Transfer, McGraw-Hill Book Co., 1979, pp. 297-307.

31. Cho, Y. I., Ng, K. S., and Hartnett, J. P., "Viscoelastic Fluids in Turbulent Pipe Flows -- A New Heat Transfer Correlation," Letters in Heat and Mass Transfer, Vol. 7, 1980, pp. 341-351.

32. Wells, C. S., "Turbulent Heat Transfer in Drag Reducing Fluids," AIChE J., Vol. 14, No. 3, May 1968, pp. 406-410.

33. Mizushina, T., Usui, H., and Yamamoto, T., "Turbulent Heat Transfer of Viscoelastic Fluids FLow in Pipe," Letters in Heat and Mass Transfer, Vol. 2, 1975, pp. 19-26.

34. Ghajar, A. J., and Tiederman, W. G., "Prediction of Heat Transfer Coefficients in Drag Reducing Turbulent Pipe Flows," AIChE J., Vol. 23, No. 1, January 1977, pp. 128-131.

35. Kale, D. D., "An Analysis of Heat Transfer to Turbulent Flow of Drag Reducing Fluids," Int. J. Heat Mass Transfer, Vol. 20, 1977, pp. 1077-1080.

36. Hanna, O. T., Sandall, O. C., and Maznet, P. R., "Heat and Mass Transfer in Turbulent Flow Under Conditions of Drag Reduction," AIChE J., Vol. 27, No. 4, July 1981, pp. 693-697.

37. Pruitt, G. T., Whitsitt, N. F., and Crawford, H. R., "Turbulent Heat Transfer to Viscoelastic Fluids," NASA Contract No. NAS 7-369, 1966.

38. Corman, J. C., "Experimental Study of Heat Transfer to Viscoelastic Fluids," Ind. Eng. Chem. Process Des. Develop., Vol. 9, 1970, pp. 254-259.

39. Hoyt, J. W., "The Effect of Additives on Fluid Friction," Transactions of the ASME, Vol. 94, June 1972, pp. 258-285.

40. Granville, P. S., "Scaling-up of Pipe Flow Frictional Data for Drag Reducing Polymer Solutions," Proceedings, 2nd International Conference on Drag Reduction, British Hydromechanics Research Association, Cambridge, UK, 1974, Paper B3.

41. Sellin, R. H. J. and Ollis, M., "Effect of Pipe Diameter on Polymer Drag Reduction," Ind. Eng. Chem. Prod. Res. Dev., Vol. 22, 1983, pp. 445-452.

42. Astarita, G., Greco, Jr., G., and Nicodemo, L., "A Phenomenological Interpretation and Correlation of Drag Reduction," AIChE J., Vol. 15, No. 4, 1969, pp. 564-567.

43. Kwack, E. Y., Cho, Y. I., and Hartnett, J. P., "Effect of Weissenberg Number on Turbulent Heat Transfer of Aqueous Polyacrylamide Solutions," presented at the 7th International Heat Transfer Conference, Munich, West Germany, 1982.

44. Skelland, A. H., Non-Newtonian Flow and Heat Transfer, Wiley, New York, 1967.

45. Cramer, S. D., and Marchello, J. M., "Numerical Evaluation of Models Describing Non-Newtonian Behavior," AIChE J., Vol. 14, No. 16, 1968, pp. 980-983.

46. Ree, F. H., Ree, T., and Eyring, H., "Relaxation Theory of Transport Problems in Condensed Systems," Industrial and Engineering Chemistry, Vol. 50, No. 7, 1958, pp. 1036-1041.

47. Eberle, C. C., "A Study of the Critical Weissenberg Number in Mechanically Degrading Polymer Solutions," M.S. Thesis, Oklahoma State University, 1984.

48. Virk, P. S., "Drag Reduction Fundamental," AIChE J., Vol. 21, 1975, pp. 625-656.

49. Gupta, M. K., Metzner, A. B., and Hartnett, J. P., "Turbulent Heat-Transfer Characteristics of Viscoelastic Fluids," Int. J. Heat Mass Transfer, Vol. 10, 1967, pp. 1211-1224.

50. McNally, "Transport in Dilute Polymer Solutions," Ph.D. Thesis, University of Rhode Island, 1968.

51. Smith, K. A., Keuroghlian, G. H., Virk, P. S., and Merrill, E. W., "Heat Transfer to Drag-Reducing Polymer Solutions," AIChE J., Vol. 15, No. 2, 1969, pp. 294-297.

52. Sidahmed, G. H., and Griskey, R. G., "Mass Transfer in Drag Reducing Fluid Systems," AIChE J. Vol. 18, No. 1, 1972, pp. 138-141.

53. Ng, K. S., Hartnett, J. P., and Tung, T. T., "Heat Transfer of Concentrated Drag Reducing Viscoelastic Polyacrylamide Solutions," Heat Transfer in Non-Newtonian Systems, 1977, pp. 74-84.

54. Virk, P. S., and Suraiya, T., Proc. Second Int'l Conference on Drag Reduction, G3-41, BHRA Fluid Eng., Cranfield, U.K. 1977.

55. Kwack, E. Y., Cho, Y. I., and Hartnett, J. P., "Heat Transfer to Polyacrylamide Solutions in Turbulent Pipe Flow: The Once-Through Mode," AIChE Symposium Series Heat Transfer-Milwaukee, Vol. 77, No. 208, 1981, pp. 123-130.

56. Rodriquez, J. M., Zakin, J. L., and Patterson, G. K., "Correlation of Drag Reduction with Modified Deborah Number for Dilute Polymer Solutions," Society of Petroleum Engineers J., 1967, pp. 325-332.

57. Seyer, F. A., and Metzner, A. B., "Turbulence Phenomenon in Drag Reducing Systems," AIChE J., Vol. 15, No. 3, 1969, pp. 426-434.

58. Darby, R., and Chang, H. D., "Generalized Correlation for Friction Loss in Drag Reducing Polymer Solutions," AIChE J., Vol. 30, 1984, pp. 274-280.

59. Deissler, R. G., "Analysis of Heat Transfer, Mass Transfer and Friction in Smooth Tube at High Prandtl and Schmidt Numbers," N.A.C.A. TN3145, 1954.

60. Elata, C., Lehrer, J., and Kahanovitz, A., "Turbulent Shear Flow of Polymer Solutions," Israel J. Technol., Vol. 4, 1966, pp. 87-95.

61. Meyer, W. A., "A Correlation of the Frictional Characteristics for Turbulent Flow of Dilute Viscoelastic Non-Newtonian Fluids in Pipe," AIChE J., Vol. 12, 1966, pp. 522-529.

62. Dimant, Y., and Poreh, M., "Momentum and Heat Transfer in Flows with Drag Reductin," Technion - Israel Institute of Technology, Faculty of Civil Engieering, Publ. No. 203, 1974.

63. van Driest, E. R., "On Turbulent Flow Near a Wall, "Journal of Aero. Sciences, Vol. 23, 1956, p. 1007-1011.

64. Cess, R. D., "A Survey of the Literature in Heat Transfer in Turbulent Tube Flows," Westinghouse Research Report 8-0529,R24, Philadelphia, Westinghouse Corp., 1958.

65. Tiederman, W. G., and Reischman, M. M., "Calculations of Velocity Profiles in Drag-Reducing Flows," J. Fluids Engineering, Trans. ASME, September, 1976, pp. 563-566.

66. James, D. F., and Acosta, A. J., "The Laminar Flow of Dilute Polymer Solutions Around Circular Cylinders," J. Fluid Mech., Vol. 42, 1970, pp. 269-288.

67. Spalding, D. B., "A Single Formula for the Law of the Wall," Trans. ASME, Vol. 28, 1961, pp. 2329-2351.

68. Wasan, D. T., Tien, C. L., and Wilke, C. R., "Theoretical Correlation of Velocity and Eddy Viscosity for Flow Close to a Pipe Wall," AIChE J., Vol. 9, 1963, pp. 567-569.

69. Mizushina, T., and Ogino, F., "Eddy Viscosity and Universal Velocity Profile in Turbulent Flow in a Straight Pipe," J. Chem. Eng. Japan, Vol. 3, 1970, pp. 163-170.

70. Gupta, M. K., "Turbulent Heat Transfer Characteristics of Viscoelastic Fluids," M.S. Thesis, University of Delaware, 1966.

71. Arpaci, V. S., Conduction Heat Transfer, Addison-Wesley Publishing Company, 1966.

72. The Operation Manual for IDEALARC DC-600, The Lincoln Electric Company.

73. Ellison, B. A., "Turbine Meters for Liquid Measurement," Mechanical Engineering, Vol. 105, No. 2, 1983, pp. 52-56.

74. The Manual for Separan Polymers, the Dow Chemical Company, 1981.

75. The Manual for Polyox, the Union Carbide Corporation, 1982.

76. Conte, S. D., and de Boor, C., Elementary Numerical Analysis - An Algorithmic Approach, McGraw-Hill Book Company, 1980.

77. Holman, J. P., Experimental Methods for Engineers, McGraw-Hill Book Company, 1978.

78. Kays, W. M., Convective Heat and Mass Transfer, McGraw-Hill Book Company, 1960.

79. McAdams, W. H., Heat Transmission, McGraw-Hill Book Company, 1954.

80. Allen, R. W., and Eckert, E. R. G., "Friction and Heat Transfer Measurements to Turbulent Pipe Flow of Water (Pr=7 and 8) of Uniform Wall Heat Flux," J. Heat Transfer, Vol. 86, 1964, p. 301.

81. Dittus, F. W., and Boelter, L. M. K., "Heat Transfer in Automobile Radiators of the Tubular Type," U. of California Publication in Engineering, Vol. 2, 1930, p. 443.

82. Virk, P. S., Mickley, H. S., and Smith, K. A., "The Ultimate Asymptote and Mean Flow Structure in Toms' Phenomenon," Trans, ASME, Vol. 37, Sect. 3, June 1970, pp. 488-493.

83. Ghajar, A. J., "Prediction of Heat Transfer Coefficients in Drag Reducing Turbulent Pipe Flows," M.S. Thesis, Oklahoma State University, Stillwater, Oklahoma, 1975.

84. Reichardt, H., "Vollständige Darstellung der Turbulenten Geschwindigkeitsverteilung in Glatten Leitungen," ZAMM, Vol. 31, 1951, p. 208.

85. Stokes, G. G., "On the Effect of the Internal Friction of Fluids on the Motion of Pendulums," Trans. Camb. Phil. Soc., Vol. 9, 1851, p. 8.

86. Elrod, Jr., H. G., "Note on the Turbulent Shear Stress Near a Wall," J. Aero. Sci., Vol. 24, 1957, pp. 468-469.

87. Hughmark, G. A., "Heat Transfer with Viscoelastic Fluids in Turbulent Flow," AIChE J., Vol. 30, 1984, p. 1033.

88. Metzner, A. B., and Friend, P. S., "Heat Transfer to Turbulent Non-Newtonian Fluids," Industrial and Engineering Chemistry, Vol. 51, No. 7, 1959, pp. 879-882.

89. von Karman, T., "The Analogy Between Fluid Friction and Heat Transfer," Trans. ASME, Vol. 61, 1939, pp. 705-710.

90. Virk, P. S., "An Elastic Sublayer Model for Drag Reduction by Dilute Polymer Solutions of Linear Macromolecules," J. Fluid Mechanics, Part 3, 1971, pp. 417-440.

91. Pugh, E. M., and Winslow, G. H., The Analysis of Physical Measurements, Addison-Wesley Book Company, 1966.

92. Kline, S. J., and McClintock, F. A., "Describing Uncertainties in Single-Sample Experiments," Mechanical Engineering, p. 75, 1, 1953, pp. 3-9.

93. Doebelin, E. O., Measurement Systems: Analysis and Design, McGraw-Hill Book Company, 1969.

94. Young, H. D., Statistical Treatment of Experimental Data, McGraw-Hill Book Company, 1962.

95. Zimm, B. H., Roe, G. H., and Epstein, L. F., "Solution of a Characteristic Value Problem from the Theory of Chain Molecules," Chem. Phys. J., Vol. 24, 1956, pp. 279-292.

APPENDIX A

DATA REDUCTION PROCEDURE AND UNCERTAINTY ANALYSIS

APPENDIX A

DATA REDUCTION PROCEDURE AND UNCERTAINTY ANALYSIS

The data reduction procedure and the uncertainty analysis can be best illustrated with the presentation of results obtained for the sample cases. These were conducted for a Newtonian fluid (tap water in the 3/8" test section) and a highly viscoelastic fluid (Separan AP-273 solution of 1000 ppm in the 3/4" test section). The specifications of sample cases are tabulated in Tables A.1 and A.2.

TABLE A.1

THE EXPERIMENTAL SPECIFICATIONS FOR TAP WATER

D_i(in.)	D_o(in.)	L_h(ft)	L_p(ft)	F(Hz)	H(in.Hg)
0.436	0.682	34.0	16.0	69.2	15.3
V(volt)	T_i(°F)	T_e(°F)	T_{wo}(°F)	η_a(cps)	
12.97	69.2	73.56	76.4	0.961	

TABLE A.2

THE EXPERIMENTAL SPECIFICATIONS FOR 1000 ppm SEPARAN AP-273

D_i(in.)	D_o(in.)	L_h(ft)	L_p(ft)	F(Hz)	H(in.Hg)
0.739	1.025	31.0	14.5	102.9	1.5
V(volt)	T_i(°F)	T_e(°F)	T_{wo}(°F)	η_a (cps)	
6.756	73.673	75.158	88.181	4.891	

A.1 Data Reduction Procedure

For the sample cases specified in Tables A.1 and A.2, the numerical computations are conducted for the determination of dimensionless parameters, friction factors and heat transfer coefficients.

A.1.1 Apparent Reynolds Number and Prandtl Number

The apparent Reynolds number and Prandtl number are the key dimensionless parameters defining the state of fluid and flow. In this study, the physical fluid properties used for those numbers are evaluated at the film temperature except that the fluid thermal conductivity is given at the exit bulk temperature. The resistance and the thermal conductivity of pipe are determined at the outside wall temperature. The film temperature (T_f) is defined as

$$T_f = (T_i + T_e)/2 \tag{A.1}$$

Yoo [28] contended that the physical properties of a Newtonian fluid except the viscosity are not affected significantly by the addition of polymer and expressed them as a function of temperature. The proposed equations are as follows:

$$C_p = 1.020892 - 6.639922E{-}4 \times T_f + 7.103168E{-}6 \times T_f^2 - 3.310227E{-}8 \times T_f^3 + 6.185928E{-}10 \times T_f^4 \tag{A.2}$$

$$K_f = 0.482659 - 6.987679E{-}3 \times T_e + 1.146261E{-}4 \times T_e^2 - 7.323056E{-}7 \times T_e^3 + 1.656699E{-}9 \times T_e^4 \tag{A.3}$$

$$\rho_f = 61.95387 + 2.704542E{-}2 \times T_f - 4.901768E{-}4 \times T_f^2 + 3.114458E{-}6 \times T_f^3 - 8.743613E{-}9 \times T_f^4 \tag{A.4}$$

He also correlated the properties of tube in terms of temperature as follows:

$$K_s = 8(1 + 7.432E{-}4 \times T_{wo}) \tag{A.5}$$

$$R = 27.8142E{-}6 \times (1 + 5.826E{-}4 \times T_{wo}) \times 12L_h/[\pi/4(D_0^2 - D_i^2)] \tag{A.6}$$

Since the same type of tube was used in this study, the above equations were employed here with the proper modification through several

calibration runs. The flow rates were calculated using the calibration equation for the turbine meter:

flow rate for tap water:

$$Q = -0.00746 + 0.06748F$$

$$= -0.00746 + 0.06748 \times 69.2 = 4.662 \text{ (GPM)}$$

flow rate for 1000 ppm solution:

$$Q = 0.95 \times (-0.00746 + 0.06748F)$$

$$= 0.95 \times (-0.00746 + 0.06748 \times 120.9) = 7.743 \text{ (GPM)}$$

From the known flow rates and dimensions of tubes, the average velocity across the tube can be calculated:

$$U = Q/(\frac{\pi}{4} D_i^2) \qquad \text{(A.7)}$$

average velocity for tap water:

$$U = \frac{4.662 \text{ gal}}{\text{min}} \cdot \frac{0.1337 \text{ ft}^3}{1 \text{ gal}} \cdot \frac{1 \text{ min}}{60 \text{ sec}} \cdot \frac{1}{\frac{\pi}{4} (0.436/12 \text{ ft})^2}$$

$$= 10.02 \text{ (ft/sec)}$$

average velocity for 1000 ppm solution:

$$U = 7.743 \frac{\text{gal}}{\text{min}} \cdot \frac{0.1337 \text{ ft}^3}{1 \text{ gal}} \cdot \frac{1 \text{ min}}{60 \text{ sec}} \cdot \frac{1}{\frac{\pi}{4} (0.739/12 \text{ ft})^2}$$

$$= 5.793 \text{ (ft/sec)}$$

The dimensionless parameters were based on the apparent viscosity data. All the fluid properties used in the dimensionless parameters were determined using Equations (A.2), (A.3) and (A.4).

The apparent Reynolds number is defined as

$$Re_a = \frac{\rho_f U D_i}{\eta_a} \qquad \text{(A.8)}$$

Reynolds number for tap water:

$$Re_a = \frac{62.29 \text{ slug}}{32.174 \text{ ft}^3} \cdot \frac{10.02 \text{ ft}}{\text{sec}} \cdot \frac{0.436 \text{ ft}}{12} \cdot \frac{47900 \text{ cps}\cdot\text{ft}^2/\text{lb}\cdot\text{sec}}{0.961 \text{ cps}}$$

$$= 35132$$

Reynolds number for 1000 ppm solution:

$$Re_a = \frac{62.27 \text{ slug}}{32.174 \text{ ft}^3} \cdot \frac{5.793 \text{ ft}}{\text{sec}} \cdot \frac{0.739 \text{ ft}}{12} \cdot \frac{47900 \text{ cps}\cdot\text{ft}^2/\text{lb}\cdot\text{sec}}{4.891 \text{ cps}}$$

$$= 6762$$

The apparent Prandtl number is defined as

$$Pr_a = \frac{\eta_a \cdot C_p}{K_f} \tag{A.9}$$

Prandtl number for tap water:

$$Pr_a = 0.961 \text{ cps} \cdot \frac{2.42 \text{ lb/ft}\cdot\text{hr}}{1 \text{ cps}} \cdot \frac{0.9993 \text{ Btu}}{\text{lb} \cdot {}^\circ\text{F}} \cdot \frac{\text{hr}\cdot\text{ft}\cdot{}^\circ\text{F}}{0.3459 \text{ Btu}}$$

$$= 6.718$$

Prandtl number for 1000 ppm solution:

$$Pr_a = 4.891 \text{ cps} \cdot \frac{2.42 \text{ lb/ft}\cdot\text{hr}}{1 \text{ cps}} \cdot \frac{1.016 \text{ Btu}}{\text{lb} \cdot {}^\circ\text{F}} \cdot \frac{\text{hr}\cdot\text{ft}\cdot{}^\circ\text{F}}{0.3469 \text{ Btu}}$$

$$= 34.66$$

A.1.2 Friction Factor

The Fanning friction is defined as

$$f = \frac{\tau_w}{1/2\ \rho_f U^2} = \frac{D_i \Delta P / 4L_p}{1/2\ \rho_f U^2} \tag{A.10}$$

The pressure drop is calculated from the fluid mechanics with reference

to Figure A.1:

$$\Delta P = P_1 - P_3 = (\rho_{Hg} - \rho_f)gH \qquad (A.11)$$

The substitution of Equation (A.11) into Equation (A.10) results in

$$f = \left(\frac{\rho_{Hg} - \rho_f}{\rho_f}\right) \frac{gHD_i}{2L_p U^2} \qquad (A.12)$$

On the other hand,

$$\frac{\rho_{Hg} - \rho_f}{\rho_f} = 12.57 \qquad \text{for } T_f = 70 \text{ to } 80\ ^\circ F$$

friction factor for tap water:

$$f = 12.57 \cdot \frac{32.174 \text{ ft}}{\text{sec}^2} \cdot \frac{15.3}{12} \text{ ft} \cdot \frac{0.436}{12} \text{ ft} \cdot \frac{1}{2 \times 16 \text{ ft}} \cdot \frac{1}{(10.02 \text{ ft/sec})^2}$$
$$= 0.00583$$

friction factor for 1000 ppm solution:

$$f = 12.57 \cdot \frac{32.174 \text{ ft}}{\text{sec}^2} \cdot \frac{1.5}{12} \text{ ft} \cdot \frac{0.739}{12} \text{ ft} \cdot \frac{1}{2 \times 14.5 \text{ ft}} \cdot \frac{1}{(5.793 \text{ ft/sec})^2}$$
$$= 0.003199$$

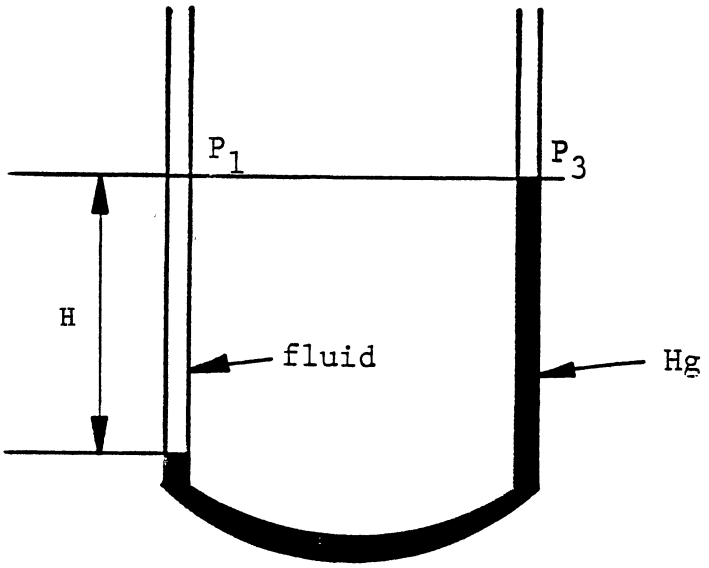

Figure A.1. Schematic of Mercury U Tube-Manometer

A.1.3 Heat Transfer Coefficients

The heat transfer coefficient is defined as

$$h = \frac{\dot{q}''}{T_{wi} - T_b} \tag{A.13}$$

The heat flux rate ($\dot{q}''$) can be determined in two ways: 1) from the enthalpy rise of the fluid, and 2) from the potential drop of electricity across the tube. The second method was used because of its good reliability. The heat flux rate calculated from the potential drop can be written as:

$$\dot{q}'' = \frac{V^2/R}{\pi D_i L_h} \tag{A.14}$$

heat flux rate for tap water:

$$\dot{q}'' = \frac{(12.97 \text{ volt})^2/0.05386\Omega}{3.14 \cdot 0.436/12 \text{ ft} \cdot 34 \text{ ft}} \cdot \frac{3.415 \text{ Btu/hr}}{1 \text{ watt}}$$
$$= 2748 \ (\text{Btu/hr}\cdot\text{ft}^2)$$

heat flux rate for 1000 ppm solution:

$$\dot{q}'' = \frac{(6.756 \text{ volt})^2/0.02471\Omega}{3.14 \cdot 0.739/12 \text{ ft} \cdot 31 \text{ ft}} \cdot \frac{3.415 \text{ Btu/hr}}{1 \text{ watt}}$$
$$= 1052 \ (\text{Btu/hr}\cdot\text{ft}^2)$$

The inside wall surface temperature (T_{wi}) can be calculated from the outside wall surface temperature (T_{wo}) using the Fourier's law of conduction:

$$T_{wi} = T_{wo} - \frac{\dot{q}}{2\pi(D_o^2 - D_i^2)K_s L_h}\left[D_o^2 \ln(D_o/D_i) - \frac{D_o^2 - D_i^2}{2}\right] \qquad (A.15)$$

inside wall temperature for tap water:

$$T_{wi} = 76.4°F - 10666\frac{\text{Btu}}{\text{hr}} \frac{[(0.682 \text{ in})^2 \ln(0.682/0.436) - (0.682^2 - 0.436^2)/2\text{in}^2]}{2\pi(0.682^2 - 0.436^2)\text{in}^2 \cdot 8.454 \text{ Btu/hr}\cdot\text{ft}\cdot°\text{F}\cdot 34 \text{ ft}}$$
$$= 74.83 \ (°F)$$

inside wall temperature for 1000 ppm solution:

$$T_{wi} = 88.181°F - 6308\frac{\text{Btu}}{\text{hr}} \frac{[(1.025 \text{ in})^2 \ln(1.025/0.739) - (1.025^2 - 0.739^2)/2\text{in}^2]}{2\pi(1.025^2 - 0.739^2)\text{ in}^2 \cdot 8.524 \text{ Btu/hr}\cdot\text{ft}\cdot°\text{F}\cdot 31 \text{ ft}}$$
$$= 87.49 \ (°F)$$

The bulk mean temperature at the desired location x is determined using

the following correlation

$$T_b = T_e - (T_e - T_i) \times (L_h - x)/L_h \qquad (A.16)$$

bulk mean temperature for tap water at x = 33 ft:

$$T_b = 73.56°F - (73.56 - 69.2)°F \times (34 - 33)\ ft/34\ ft$$

$$= 73.43\ (°F)$$

bulk mean temperature for 1000 ppm solution at x = 31 ft:

$$T_b = T_e = 75.158\ (°F)$$

Finally, the heat transfer coefficients can be obtained using Equation (A.13).

heat transfer coefficient for tap water:

$$h = \frac{2748\ Btu/hr \cdot ft^2}{(74.83 - 73.43)\ °F} = 1963\ (Btu/hr \cdot ft \cdot °F)$$

heat transfer coefficient for 1000 ppm solution:

$$h = \frac{1052\ Btu/hr \cdot ft^2}{(87.49 - 75.158)\ °F} = 85.31\ (Btu/hr \cdot ft \cdot °F)$$

The heat transfer coefficients can be nondimensionalized into the Nusselt number which is defined as

$$Nu = \frac{h\ D_i}{K_f} \qquad (A.17)$$

Nusselt number for tap water:

$$Nu = \frac{1963 \text{ Btu/hr·ft·°F} \cdot 0.436/12 \text{ ft}}{0.3459 \text{ Btu/hr·ft·°F}} = 206$$

Nusselt number for 1000 ppm solution:

$$Nu = \frac{85.31 \text{ Btu/hr·ft·°F} \cdot 0.739/12 \text{ ft}}{0.3469 \text{ Btu/hr·ft·°F}} = 15.1$$

A.2 Uncertainty Analysis

The probable error in the experimental measurements of friction factor and heat transfer coefficient are presented in this section. For a complete discussion of the theory of uncertainty analysis, refer to the literatures [91-94].

A.2.1 Friction Factor

The Fanning friction factor is defined as

$$f = \tau_w / \frac{1}{2}\rho_f U^2 = \frac{D_i \Delta p}{4L_p} / \frac{1}{2}\rho_f U^2 \qquad (A.18)$$

In terms of the measured quantity, it becomes

$$f = \left(\frac{\rho_{Hg} - \rho_f}{\rho_f}\right) \frac{g H D_i}{2L_p[(-0.00746 + 0.06748F)/\frac{\pi}{4}D_i]^2} \qquad (A.19)$$

Here, the densities of mercury and fluid and the gravitational acceleration are assumed to be accurately known. The uncertainty in friction factor may then be found from

$$\delta f = \left[\left(\frac{\partial f}{\partial D_i}\,\delta D_i\right)^2 + \left(\frac{\partial f}{\partial H}\,\delta H\right)^2 + \left(\frac{\partial f}{\partial L_p}\,\delta L_p\right)^2 + \left(\frac{\partial f}{\partial F}\,\delta F\right)^2\right]^{1/2} \qquad (A.20)$$

The percentage uncertainty, which can be obtained with the substitution of the partial derivatives of Equation (A.19) with respect to each variable into Equation (A.20) and division of its result by Equation (A.19), may be written as

$$\frac{\delta f}{f}\,(\%) = 100x\left[\left(\frac{5\delta D_i}{D_i}\right)^2+\left(\frac{\delta H}{H}\right)^2+\left(-\frac{\delta L_p}{Lp}\right)^2+\left(\frac{-0.06748\delta F}{-0.00746 + 0.06748F}\right)^2\right]^{1/2} \qquad (A.21)$$

The uncertainty of each variable was estimated as follows:

δD_i : The uncertainty for each test section was assumed to be 0.002" for 3/8" pipe and 0.003" for 3/4" pipe.

δH : The resolution of mercury manometer was ±0.1". This value was taken as the uncertainty in H.

δL_p : The pressure tap interval was measured with the accuracy of ±1/4".

δF : The reading of frequency from the turbine meter was influenced by the instantaneous change of flow rate. It was also affected by the calibration procedure. The probable error in F was assumed to be ±2.0 Hz.

The sample calculations for uncertainty analysis were conducted for the cases presented in Tables A.1 and A.2.

tap water in the 3/8" tube:

$$\frac{\delta f}{f}(\%) = 100x\left[\left(\frac{5 \times 0.002}{0.436}\right)^2 + \left(\frac{0.1}{15.3}\right)^2 + \left(-\frac{0.25}{16.0}\right)^2 + \left(\frac{-0.06748 \times 2}{-0.00746 + 0.06748 \times 69.2}\right)^2\right]^{1/2}$$

$$= 100 \times \left[(0.0229)^2 + (0.0065)^2 + (-0.0156)^2 + (-0.0289)^2\right]^{1/2}$$

$$= 4.06(\%)$$

1000 ppm solution in the 3/4" tube:

$$\frac{\delta f}{f}(\%) = 100 \times \left[\left(\frac{5 \times 0.003}{0.739}\right)^2 + \left(\frac{0.1}{1.5}\right)^2 + \left(-\frac{0.25}{14.5}\right)^2 + \left(\frac{-0.06748 \times 2}{-0.00746 + 0.06748 \times 102.9}\right)^2\right]^{1/2}$$

$$= 100 \times \left[(0.0203)^2 + (0.0667)^2 + (-0.0172)^2 + (-0.0166)^2\right]^{1/2}$$

$$= 7.37(\%)$$

From the above calculations, the following observations can be made:

1. The uncertainty from the measurement of the inside diameter is significant for both test sections.
2. For the 3/4" tube whose pressure drop is small, the uncertainty from the reading of mercury manometer is predominant.
3. For the low flow rate, the uncertainty from the turbine meter reading is considerable.

The overall uncertainty in friction factor was estimated to be 5 ~ 8%.

A.2.2 Heat Transfer Coefficient

The heat transfer coefficient is defined as

$$h = \dot{q}''/\Delta T \tag{A.22}$$

where $\Delta T = T_{wi} - T_b$

The percent probable error in h is given by

$$\frac{\delta h}{h}(\%) = \left[\left(\frac{\delta \dot{q}''}{\dot{q}''}\right)^2 + \left(-\frac{\delta \Delta T}{\Delta T}\right)^2\right]^{1/2} \times 100 \tag{A.23}$$

From Equation (A.14) for heat flux rate, the uncertainty in $\dot{q}''$ can be written as

$$\frac{\delta\dot{q}''}{\dot{q}''} = \left[\left(\frac{2\delta V}{V}\right)^2 + \left(-\frac{\delta R}{R}\right)^2 + \left(-\frac{\delta D_i}{D_i}\right)^2\right]^{1/2} \qquad (A.24)$$

where the uncertainty in L_h is neglected due to the use of extremely long heated length. The uncertainty in each variable was assumed as:

δV : The voltage fluctuation was observed to be ±0.01 volt. Therefore, δV was taken as 0.01 volt.

δR : Following Yoo's suggestion [28], $\delta R/R$ was assumed to be 0.01.

The combination of Equation (A.15) and Equation (A.16) results in the expression for ΔT in terms of the measured quantities:

$$\Delta T = T_{wo} - T_e + T_1 + T_2 \qquad (A.25)$$

where

$$T_1 = -\frac{\dot{q}}{2\pi(D_o^2 - D_i^2)K_s L_h}\left[D_o^2 \ln (D_o/D_i) - \frac{D_o^2 - D_i^2}{2}\right] \qquad (A.26)$$

and

$$T_2 = (T_e - T_i) \times (L_h - x)/L_h \qquad (A.27)$$

In the present analysis, the following uncertainty in each term was assumed:

δT_{wo} : The probable error in T_{wo} was estimated to be 0.15 °F from the thermocouple calibration.

δT_e : The probable error in T_e was estimated to be 0.15 °F from the thermocouple calibration.

δT_1 : $\delta T_1/T_1$ was assumed to be 0.05.

δT_2 : $\delta T_2/T_2$ was assumed to be 0.05.

The uncertainty in ΔT can be estimated by

$$\frac{\delta\Delta T}{\Delta T} = \left[\left(\frac{|\delta T_{wo}| + |\delta T_e| + |\delta T_1| + |\delta T_2|}{T_{wi} - T_b}\right)^2\right]^{1/2} \qquad (A.28)$$

where T_{wi} and T_b can be obtained from Equations (A.15) and (A.16).

The uncertainty analysis for heat transfer coefficients was conducted for the sample cases presented in Tables A.1 and A.2.

tap water in the 3/8" tube:

$$\frac{\delta h}{h}(\%) = 100 \times \left[\left(\frac{2 \times 0.01}{12.97}\right)^2 + (\mp 0.01)^2 + \left(\mp \frac{0.002}{0.436}\right)^2 + \left(\frac{0.15 + 0.15 + 0.05 \times 1.57 + 0.05 \times 0.13}{74.83 \mp 73.43}\right)^2\right]^{1/2}$$

$$= 100 \times \left[(0.0015)^2 + (\mp 0.01)^2 + (\mp 0.0046)^2 + (0.275)^2\right]^{1/2}$$

$$= 27.5\%$$

1000 ppm solution in the 3/4" tube:

$$\frac{\delta h}{h}(\%) = 100 \times \left[\left(\frac{2 \times 0.01}{6.756}\right)^2 + (\mp 0.01)^2 + \left(\mp \frac{0.003}{0.739}\right)^2 + \left(\frac{0.15 + 0.15 + 0.05 \times 0.691 + 0.0}{87.49 \mp 75.158}\right)^2\right]^{1/2}$$

$$= 100 \times \left[(0.0030)^2 + (\mp 0.01)^2 + (\mp 0.0041)^2 + (0.027)^2\right]^{1/2}$$

$$= 2.94(\%)$$

From the above analysis, it may be concluded that the uncertainty in h

is predominated by the probable error in the measurements of temperatures. Particularly, when Newtonian fluids or very dilute solutions are being dealt with, every precaution should be taken to raise the accuracy of temperature readings.

APPENDIX B

EXPERIMENTAL DATA

APPENDIX B

EXPERIMENTAL DATA

The experimental results are tabulated. These include the apparent viscosities, friction factors and Colburn j-factors.

TABLE B.1

APPARENT VISCOSITY DATA OF SEPARAN AP-273 SOLUTIONS IN THE 3/4" TUBE

ppm	$\dot{\gamma}$ (sec^{-1})	η_a (cps)	ppm	$\dot{\gamma}$ (sec^{-1})	η_a (cps)
10	6.876	1.051	50	6.876	1.251
	13.75	1.051		13.75	1.201
	34.38	1.031		34.38	1.181
	68.76	1.011		68.76	1.181
	542.7	1.036		543.4	1.130
	1085	0.9891		1087	1.035
	1628	0.9734		1630	1.035
	3256	0.9734		3260	0.9884
	λ = 0.435 E-2 sec			λ = 1.84 E-2 sec	
100	3.438	1.602	300	1.719	4.005
	6.876	1.602		3.438	4.005
	13.75	1.452		6.876	4.005
	34.38	1.442		13.75	3.704
	68.76	1.392		34.38	3.184
	543.4	1.316		68.76	2.813
	1087	1.100		543.4	2.067
	1630	1.065		1087	1.832
	3260	1.050		1630	1.678
				3260	1.581
	λ = 4.44 E-2 sec			λ = 6.42 E-2 sec	

TABLE B.1 (Continued)

ppm	$\dot{\gamma}$ (sec^{-1})	η_a (cps)	ppm	$\dot{\gamma}$ (sec^{-1})	η_a (cps)
500	0.6876	10.01	1000	0.3438	63.03
	1.719	8.821		0.6876	47.90
	3.438	8.210		1.719	33.96
	6.876	7.409		3.438	26.81
	13.75	6.357		6.876	21.51
	34.38	5.186		13.75	17.48
	68.76	4.405		34.38	13.48
	543.4	2.912		169.2	8.140
	1087	2.583		338.5	6.623
	1630	2.474		541.3	5.743
	3260	2.208		1083	4.547
	5009	2.123		1624	3.894
	6702	2.074		3248	2.976
				14486	2.740
	λ = 29.0 E-2 sec			λ = 78.2 E-2 sec	

TABLE B.2

APPARENT VISCOSITY DATA OF SEPARAN AP-273 SOLUTIONS IN THE 3/8" TUBE

ppm	$\dot{\gamma}$ (sec^{-1})	η_a (cps)	ppm	$\dot{\gamma}$ (sec^{-1})	η_a (cps)
50	6.876	1.907	100	3.438	2.503
	13.75	1.907		6.876	2.303
	34.38	1.768		13.75	2.303
	64.76	1.673		34.38	2.082
	543.4	1.414		68.76	2.022
	1087	1.330		543.4	1.788
	1630	1.283		1087	1.646
	3260	1.207		1630	1.631
				3260	1.505
	λ = 3.33 E-2 sec			λ = 7.90 E-2 sec	
300	3.438	6.007	500	0.3438	14.02
	6.876	5.306		0.6876	13.02
	13.75	4.705		1.719	12.81
	34.38	4.085		3.438	12.21
	68.76	3.644		6.876	11.31
	541.3	2.815		13.75	9.261
	1083	2.440		34.38	7.609
	1624	2.252		68.76	5.947
	3248	2.002		169.2	5.317
				338.5	4.229
	λ = 12.6 E-2 sec			541.3	3.815
				1083	3.305
				1624	3.179
				3248	2.865
				7461	2.506
				11868	2.389
				21605	2.161
				λ = 17.5 E-2 sec	

TABLE B.3

APPARENT VISCOSITY DATA OF WSR¬301 SOLUTION IN THE 3/4" AND 3/8" TUBE

ppm	$\dot{\gamma}$ (sec^{-1})	η_a (cps)	ppm	$\dot{\gamma}$ (sec^{-1})	η_a (cps)
50	34.38	1.001	100	3.438	1.402
	68.76	0.9811		6.876	1.352
	542.5	0.9794		13.75	1.302
	1085	0.9417		34.38	1.261
	1628	0.9103		68.76	1.246
	3255	0.8946		542.5	1.244
				1085	1.225
λ = 0.578 E¬2 sec				1628	1.212
				3255	1.194
			λ =0.500 E¬2 sec		
300	3.438	1.602	500	6.876	1.752
	6.876	1.602		13.75	1.752
	13.75	1.602		34.38	1.692
	34.38	1.602		68.76	1.682
	68.76	1.602		542.5	1.658
	542.5	1.603		1085	1.630
	1085	1.650		3255	1.570
	1628	1.603		4388	1.526
				7771	1.465
λ =0.100 E¬2 sec			λ = 0.374 E¬2 sec		
1000	3.438	3.204			
	6.876	3.204			
	13.75	3.014			
	34.38	2.923			
	68.76	2.863			
	342.9	2.684			
	514.3	2.585			
	543.5	2.446			
	1029	2.386			
	1087	2.352			
	1630	2.258			
	3261	2.148			
λ = 2.01 E¬2 sec					

TABLE B.4

APPARENT VISCOSITY DATA OF 1500 ppm SEPARAN AP-273 SOLUTIONS IN THE 3/4" TUBE

Run	$\dot{\gamma}$ (sec^{-1})	η_a (cps)	Run	$\dot{\gamma}$ (sec^{-1})	η_a (cps)
1	0.3438	216.3	4	0.3438	158.2
	0.6876	152.2		0.6876	132.2
	1.719	108.9		1.719	99.72
	3.438	81.09		3.438	75.29
	6.876	58.77		6.876	55.36
	13.75	41.95		13.75	40.15
	171.8	14.58		172.0	13.67
	343.5	9.554		344.0	10.11
	543.8	8.649		544.0	8.082
	1088	6.722		1088	6.249
	1631	5.854		1632	5.419
	3263	4.920		3264	5.479
	4973	4.518		5315	4.100
	10607	4.015		15443	3.588
	15266	3.995			
	λ = 2.348 sec			λ = 1.46 sec	
8	0.3438	170.2	13	0.3438	152.2
	0.6876	143.2		0.6876	138.2
	1.719	106.9		1.719	102.9
	3.438	81.09		3.438	77.89
	6.876	59.37		6.876	57.47
	13.75	42.55		13.75	41.70
	171.6	13.70		171.6	14.36
	343.2	10.28		343.2	10.55
	543.6	7.429		543.6	7.053
	1087	6.395		1087	5.971
	1631	5.548		1631	5.486
	3267	4.467		3262	4.448
	5718	4.075		6045	4.054
	10757	3.700		11395	3.593
	15555	3.628			
	λ = 1.46 sec			λ = 1.214 sec	

TABLE B.4 (Continued)

Run	$\dot{\gamma}$ (sec^{-1})	η_a (cps)	Run	$\dot{\gamma}$ (sec^{-1})	η_a (cps)
17	0.3438	146.2	19	0.3438	136.2
	0.6876	128.1		0.6876	117.1
	1.719	98.11		1.719	90.91
	3.438	75.89		3.438	71.88
	6.876	56.37		6.876	53.96
	13.75	40.80		13.75	39.45
	172.5	13.93		172.2	13.07
	344.9	10.23		344.3	9.799
	544.4	8.263		544.2	7.985
	1089	6.291		1088	6.154
	1633	5.415		1632	5.292
	3267	4.319		3265	4.243
	5998	4.001		8533	3.700
	11028	3.608		13828	3.640
	λ = 1.224 sec			λ = 1.214 sec	
23	0.3438	130.2	25	0.3438	124.1
	0.6876	115.1		0.6876	111.1
	1.719	89.70		1.719	86.50
	3.438	70.08		3.438	68.28
	6.876	53.26		6.876	52.06
	13.75	38.74		13.75	38.64
	172.3	13.06		172.2	13.06
	344.5	9.497		344.4	9.798
	544.3	7.796		544.2	8.079
	1089	5.965		1088	6.200
	1633	5.166		1633	5.292
	3266	4.149		3265	4.259
	5973	3.791		6104	3.777
	15999	3.439		11892	3.354
				16859	3.300
	λ = 1.127 sec			λ = 1.068 sec	

TABLE B.4 (Continued)

Run	$\dot{\gamma}$ (sec^{-1})	η_a (cps)	Run	$\dot{\gamma}$ (sec^{-1})	η_a (cps)
29	0.3438	118.1	31	0.3438	114.1
	0.6876	104.1		0.6876	94.11
	1.719	83.30		1.719	77.69
	3.438	66.68		3.438	63.27
	6.876	50.96		6.876	48.76
	13.75	37.79		13.75	36.49
	172.2	13.06		172.3	13.35
	344.4	9.649		344.6	9.793
	544.2	7.985		544.3	8.078
	1088	6.153		1089	6.152
	1633	5.292		1633	5.323
	3265	4.227		3266	4.258
	6358	3.761		6142	3.655
	11417	3.465		11997	3.241
				17386	3.173
	λ = 1.032 sec			λ = 1.113 sec	
34	0.3438	106.1	35	0.3438	90.10
	0.6876	93.11		0.6876	83.10
	1.719	76.09		1.719	69.28
	3.438	62.27		3.438	56.67
	6.876	48.36		6.876	45.45
	13.75	36.14		13.75	34.44
	172.3	13.06		171.8	12.80
	344.6	9.495		343.5	9.375
	544.3	7.702		543.8	6.863
	1089	5.917		1088	5.359
	1633	5.135		1631	5.001
	3266	4.101		3263	4.074
	6267	3.642		6644	3.599
	12052	3.232		12321	3.246
	17295	3.214		17545	3.208
	λ = 0.9479 sec			λ = 0.7605 sec	

TABLE B.4 (Continued)

Run	$\dot{\gamma}$ (sec^{-1})	η_a (cps)	Run	$\dot{\gamma}$ (sec^{-1})	η_a (cps)
40	0.3438	92.11	42	0.3438	80.09
	0.6876	83.10		0.6876	69.08
	1.719	69.28		1.719	62.87
	3.438	57.47		3.438	50.86
	6.876	45.15		6.876	40.65
	13.75	34.24		13.75	31.54
	172.1	12.48		172.0	11.89
	344.1	9.358		344.0	8.917
	544.1	7.517		544.0	7.236
	1088	5.873		1088	5.591
	1632	5.074		1632	4.887
	3264	4.056		3264	3.916
	6495	3.581		6045	3.544
	12084	3.327		12402	3.152
	16989	3.288		17716	3.088
	λ = 0.808 sec			λ = 0.7483 sec	
45	0.3438	76.09	47	0.3438	74.09
	0.6876	65.08		0.6876	71.08
	1.719	59.67		1.719	58.47
	3.438	50.86		3.438	48.86
	6.876	40.85		6.876	39.15
	13.75	31.44		13.75	30.44
	172.0	11.89		171.4	11.63
	344.0	8.918		342.8	8.650
	544.0	7.048		543.4	6.679
	1088	5.498		1087	5.644
	1632	4.793		1630	4.923
	3264	3.884		3261	3.998
	6356	3.482		7277	3.350
	12540	3.122		12401	3.246
	18127	3.007		17887	3.136
	λ = 0.6746 sec			λ = 0.6726 sec	

TABLE B.5

APPARENT VISCOSITY DATA OF SEPARAN AP-30 SOLUTIONS IN THE 3/4" TUBE

ppm	$\dot{\gamma}$ (sec^{-1})	η_a (cps)	ppm	$\dot{\gamma}$ (sec^{-1})	η_a (cps)
3000	0.3438	328.4	2450	0.3438	235.3
	0.6876	299.3		0.6876	200.6
	1.719	215.9		1.719	155.8
	3.438	165.8		3.438	126.1
	179.8	26.45		6.876	95.15
	359.5	18.91		179.6	22.20
	539.3	15.45		359.2	16.08
	551.4	14.83		538.8	13.28
	1079	10.90		551.3	13.08
	1654	9.302		1078	9.298
	3309	6.876		1654	8.130
	8840	4.764		3308	6.059
	12568	4.378		9184	4.595
				11957	4.547
	λ = 133.3 E-2 sec			λ = 123.7 E-2 sec	
2025	0.3438	144.2	1840	0.3438	105.1
	0.6876	127.1		0.6876	98.11
	1.719	108.1		1.719	84.90
	3.438	89.10		3.438	71.08
	6.876	70.08		6.876	57.77
	178.9	18.28		13.75	44.95
	357.9	13.43		178.1	16.08
	536.8	11.14		356.1	11.91
	550.7	11.05		534.2	9.953
	1074	7.856		549.8	9.670
	1652	7.087		1100	7.392
	3304	5.307		1649	6.354
	6099	4.931		3299	4.912
	12034	4.184		6903	4.372
	14298	3.876		11308	3.733
				15370	3.585
	λ = 87.42 E-2 sec			λ = 60.82 E-2 sec	

TABLE B.5 (Continued)

ppm	$\dot{\gamma}$ (sec^{-1})	η_a (cps)	ppm	$\dot{\gamma}$ (sec^{-1})	η_a (cps)
1640	0.3438	91.11	1500	0.3438	56.07
	0.6876	77.09		0.6876	52.06
	1.719	66.88		1.719	48.86
	3.438	58.27		3.438	43.45
	6.876	48.06		6.876	37.04
	13.75	38.14		13.75	29.98
	176.3	14.21		177.4	12.39
	352.6	10.73		354.7	9.080
	528.9	8.988		532.1	7.687
	548.2	7.368		549.1	7.541
	1058	6.524		1064	5.669
	1096	6.202		1647	5.123
	1644	5.754		3295	4.034
	3289	4.461		5822	3.857
	7111	4.210		11293	3.430
	11701	3.604		15733	3.460
	λ = 74.94 E-2 sec			λ = 38.40 E-2 sec	
1360	0.3438	38.04	1100	0.3438	22.03
	0.6876	34.04		1.719	20.42
	1.719	36.12		3.438	17.02
	3.438	31.64		13.75	15.47
	6.876	27.63		34.38	12.25
	13.75	23.28		68.76	9.962
	34.38	17.32		175.2	7.586
	176.2	10.45		350.4	5.981
	352.3	7.980		525.7	5.252
	528.5	6.868		547.1	4.952
	548.0	6.437		1051	4.133
	1057	5.127		1094	4.065
	1644	4.667		1641	3.613
	3288	3.747		6786	3.276
	12011	3.357		18754	2.796
	16673	3.353			
	λ = 16.92 E-2 sec			λ = 22.82 E-2 sec	

TABLE B.5 (Continued)

ppm	$\dot{\gamma}$ (sec^{-1})	η_a (cps)	ppm	$\dot{\gamma}$ (sec^{-1})	η_a (cps)
990	0.3438	20.20	800	1.719	10.01
	1.719	16.42		3.438	9.811
	6.876	14.72		13.75	8.335
	13.75	13.22		34.38	7.178
	34.38	10.71		68.76	6.267
	68.76	8.910		174.6	5.564
	175.1	7.007		349.2	4.539
	350.2	5.402		523.7	4.002
	525.3	4.769		546.5	3.742
	547.0	4.580		1047	3.172
	1051	3.796		1093	3.134
	1094	3.785		1639	2.806
	1641	3.552		12280	2.426
	3282	2.788			
	14787	2.784			
	λ = 8.672 E-2 sec			λb = 5.607 E-2 sec	
385	3.438	3.704	277	3.438	2.403
	6.876	3.604		6.876	2.403
	13.75	3.304		13.75	2.303
	68.76	2.853		34.38	2.183
	345.5	2.516		68.76	2.102
	518.2	2.269		344.9	1.927
	544.7	2.252		544.5	1.784
	1089	2.112		1089	1.643
	1634	2.033		1633	1.565
	14377	1.942		3267	1.455
	λ = 6.289 E-2 sec			λ = 1.98 E-2 sec	
152	6.876	1.502			
	13.75	1.502			
	34.38	1.482			
	68.76	1.482			
	339.1	1.507			
	508.7	1.507			
	1017	1.306			
	1083	1.274			
	1625	1.227			
	3250	1.196			
	λ = 0.494 E-2 sec				

TABLE B.6

FRICTION FACTORS AND COLBURN j-FACTORS OF SEPARAN AP-273 SOLUTIONS IN THE 3/4" TUBE

ppm	$Re_a \times 10^{-4}$	Pr_a	$f \times 10^3$	$j_h \times 10^3$
10	2.247	7.126	5.832	2.957
	2.732	7.064	5.294	2.614
	3.509	6.960	4.662	2.333
	4.333	6.872	4.111	2.163
	4.984	6.824	3.715	1.920
50	2.511	7.619	3.632	1.888
	3.302	7.363	2.976	1.460
	4.313	7.174	2.437	1.144
	5.472	7.121	2.013	0.8792
	6.182	7.136	1.743	0.7322
100	1.419	9.375	4.642	2.354
	2.231	8.643	3.495	1.682
	3.109	8.038	2.713	1.356
	4.487	7.534	2.131	0.9585
	5.507	7.391	1.747	0.7421
300	1.522	13.74	1.926	0.6964
	2.228	12.98	1.521	0.4947
	2.999	12.33	1.335	0.3841
	3.599	11.93	1.229	0.3277
	4.245	11.60	1.163	0.2742
500	1.182	18.92	2.029	0.5338
	1.689	18.03	1.678	0.4415
	2.143	17.63	1.660	0.3871
	3.154	16.90	1.355	0.3215
1000	0.6758	34.09	3.199	0.6908
	0.9034	31.76	2.774	0.6137
	1.146	29.97	2.424	0.5698
	1.496	28.08	2.264	0.5425

TABLE B.7

FRICTION FACTORS AND COLBURN j-FACTORS OF SEPARAN AP-273 SOLUTIONS IN THE 3/8" TUBE

ppm	$Re_a \times 10^{-4}$	Pr_a	$f \times 10^3$	$j_h \times 10^3$
10	2.719	7.113	4.776	3.251
	4.003	7.113	3.143	2.185
	4.616	7.127	2.889	1.789
	5.866	7.113	2.089	1.081
50	2.586	9.333	2.197	0.8028
	3.481	9.283	1.640	0.5693
	4.568	9.264	1.165	0.4113
	5.300	9.271	0.9793	0.2600
100	1.939	11.45	1.889	0.7873
	2.626	11.11	1.477	0.5096
	3.421	10.68	1.236	0.3799
	4.271	10.68	1.036	0.2985
300	1.311	15.49	2.129	0.4980
	1.735	14.88	1.600	0.3994
	2.147	14.45	1.520	0.3625
	2.444	14.24	1.430	0.3323
	2.879	14.25	1.349	0.2970
500	0.9682	21.82	2.462	0.5597
	1.176	21.25	2.139	0.4963
	1.297	20.96	2.106	0.4695
	1.459	20.60	2.102	0.4357
	1.717	20.11	1.849	0.4048
	1.866	19.86	1.962	0.3802

TABLE B.8

FRICTION FACTORS AND COLBURN j-FACTORS OF WSR-301
SOLUTIONS IN THE 3/4" TUBE

ppm	$Re_a \times 10^{-4}$	Pr_a	$f \times 10^3$	$j_h \times 10^3$
50	2.722	6.693	5.512	3.140
	3.786	6.569	4.770	2.781
	4.654	6.484	4.331	2.425
	5.655	6.394	3.910	2.254
	6.788	6.302	3.452	1.885
100	2.039	8.827	5.341	3.314
	2.658	8.781	4.487	2.904
	3.196	8.742	3.926	2.327
	3.902	8.695	3.374	2.007
	4.823	8.646	2.855	1.401
300	1.906	11.53	3.646	1.859
	2.263	11.64	3.189	1.609
	2.608	11.69	2.863	1.417
	3.284	11.67	2.480	1.132
500	1.902	11.76	3.626	1.639
	2.384	11.70	3.021	1.284
	2.888	11.63	2.682	1.151
	3.832	11.49	2.143	0.8418
1000	1.637	16.71	2.008	0.6827
	2.220	16.18	1.646	0.5093
	2.842	15.85	1.529	0.4266

TABLE B.9

FRICTION FACTORS AND COLBURN j-FACTORS OF WSR-301
SOLUTIONS IN THE 3/8" TUBE

ppm	$Re_a \times 10^{-4}$	Pr_a	$f \times 10^3$	$j_h \times 10^3$
50	3.236	6.165	5.889	3.763
	3.764	6.105	5.353	3.309
	4.699	6.076	4.460	3.262
	5.276	6.098	4.105	2.902
	5.901	6.109	3.766	2.758
100	2.946	8.527	2.862	1.504
	3.567	8.500	2.467	1.206
	4.202	8.475	2.103	1.009
	5.125	8.482	1.752	0.7083
300	1.831	11.37	2.197	0.9741
	2.282	11.37	1.755	0.7355
	2.731	11.38	1.544	0.6403
	3.153	11.36	1.391	0.5875
	3.769	11.37	1.228	0.4589
500	1.792	11.36	2.118	0.9027
	2.247	11.33	1.793	0.6890
	2.661	11.28	1.553	0.5769
	3.157	11.19	1.428	0.4845
	3.797	11.02	1.285	0.5821
1000	1.698	15.81	1.831	0.3904
	2.248	15.12	1.569	0.3604
	2.265	15.06	1.421	0.3221
	2.983	15.07	1.346	0.2925

TABLE B.10

FRICTION FACTORS AND COLBURN j-FACTORS OF 1500 ppm SEPARAN AP-273 SOLUTIONS IN THE 3/4" TUBE

Run	$Re_a \times 10^{-4}$	Pr_a	$f \times 10^3$	$j_h \times 10^3$
1	6.796	57.65	3.320	0.6831
4	7.213	42.93	3.027	0.6217
8	6.896	44.21	3.174	0.6577
13	7.336	41.58	3.042	0.6563
17	7.147	42.92	3.016	0.7215
19	7.242	42.15	2.917	0.7486
23	7.309	41.04	2.917	0.7519
25	6.988	42.89	2.957	0.8029
29	7.178	42.29	2.900	0.8260
31	7.034	42.68	2.885	0.7950
34	7.577	40.61	2.739	0.7697
35	7.972	37.52	2.820	0.7492
40	7.310	40.84	2.852	0.8292
42	7.291	39.49	2.847	0.7754
45	7.724	38.37	2.822	0.7813
47	7.776	39.20	2.698	0.7894

TABLE B.11

FRICTION FACTORS AND COLBURN j-FACTORS OF SEPARAN AP-30 SOLUTIONS IN THE 3/4" TUBE

ppm	$Re_a \times 10^{-4}$	Pr_a	$f \times 10^3$	$j_h \times 10^3$
3000	0.6112	66.49	3.725	0.6985
	0.6962	63.78	3.515	0.6566
2450	0.6789	58.47	3.127	0.7257
	0.9619	52.95	2.444	0.5782
2025	0.7939	50.73	2.914	0.8288
	0.9102	49.24	2.613	0.7509
1840	0.8767	46.16	2.645	0.7567
	1.188	42.08	2.142	0.5906
1640	0.8392	39.21	3.033	0.8162
	1.022	39.87	2.222	0.7004
1500	0.8493	38.52	2.683	0.7666
	1.118	36.71	2.216	0.6819
	1.444	34.61	1.888	0.5302
1360	0.9227	35.78	2.323	0.7176
	1.182	34.08	1.988	0.6288
	1.649	31.24	1.602	0.5459
1100	1.176	27.27	2.049	0.6146
	1.565	25.96	1.770	0.5336
990	1.267	26.28	2.268	0.6065
	1.588	25.52	1.705	0.5573
	2.160	24.14	1.512	0.4725
800	1.125	22.21	2.502	0.8466
	1.507	21.83	1.873	0.6935
	2.051	20.40	1.521	0.5723
385	1.018	15.88	4.877	2.265
	1.595	15.23	3.344	1.845
	2.218	14.88	2.559	1.399
277	1.265	12.68	7.590	2.586
	2.059	11.66	4.402	1.750
	2.830	11.55	2.863	1.410

TABLE B.11 (Continued)

ppm	$Re_a \times 10^{-4}$	Pr_a	$f \times 10^3$	$j_h \times 10^3$
152	1.777	10.34	5.099	3.307
	2.727	9.528	4.003	2.250
	3.878	8.897	3.337	1.799

APPENDIX C

COMPUTER PROGRAMS

APPENDIX C

COMPUTER PROGRAMS

Various computer programs have been used to reduce the current experimental data. Listed are the computer programs, including viscosity, fluid time scale, data reduction and prediction.

C.1 Viscosity

The following computer programs are used to reduce viscosity data measured with the use of two Couette viscometers (Brookfield Synchro-Electric Model LVT with UL adaptor and Fann Model VG) and a capillary tube viscometer.

C.1.1 Couette Viscometers

```
C   THIS PROGRAM IS TO CALCULATE THE APPARENT VISCOSITY FROM THE
C   FLOW CURVE MEASURED BY A FANN VISCOMETER
C
C
C   --- NOTATIONS OF PARAMETERS ---
C
C   CR -- CORRECTION CONSTANT FOR SHEAR STRAIN
C   GAMMA --- SHEAR RATE (1/SEC)
C   IFLAG -- INDICATION OF THE TYPE OF VISCOMETER
C            (IFLAG=1, FANN AND IFLAG=2, BROOKFIELD VISCOMETER)
C   IRUN -- NO. OF DATA POINTS
C   K -- INTERCEPT K VALUE
C   K1 -- SPRING CONSTANT (DYNE/CM**4)
C   K2 -- BOB SURFACE AREA (CM**2)
C   LE -- EFFECTIVE BOB LENGTH (CM)
C   N -- INDEX N VALUE
C   NTWO -- SLOPE OF STRESS VS RPM ON LOGARITHMIC PLOT
C   RB -- RADIUS OF BOB (CM)
C   RC -- RADIUS OF CAP (CM)
C   RPM -- REVOLUTION / MIN.
C   T -- TEMPERATURE OF FLUID (DEG. C)
C   TAU -- SHEAR STRESS (LB/FT**2)
C   THETA -- DEFLECTION ANGLE (DEG.)
C   VISC -- APPARENT VISCOSITY (POISE)
C
C
```

```
      DIMENSION T(30), RB(30), RC(30), S(30), THETA(30), RPM(30),
     $          TAU(30), GAMMA(30), DUDR(30), CR(30), ATAU(30),
     $          ARPM(30), G(30),ADUDR(30),VISC(30)
      REAL NTWO, N,K, K1(30), K2(30), LE(30)
      PI = 3.141593
      IM=1
C
C   FANN VISCOMETER MEASUREMENT DATA
C
      READ(5,100) IRUN
      WRITE(6,99)
      WRITE(6,110)
      WRITE(6,120)
      DO 10 I=1, IRUN
      II=I
      READ(5,200)IFLAG, RPM(I), T(I), RB(I), RC(I), K1(I), K2(I),
     $           THETA(I)
      IF (IFLAG.EQ.2) GO TO 91
      S(I)=RC(I)/RB(I)
   10 WRITE(6,300)I,RPM(I),T(I),RB(I),RC(I),S(I),K1(I),K2(I),
     $           THETA(I)
   91 IN=II-1
C
C   CALCULATION OF SLOPE OF SHEAR STRESS VS ROTATIONAL SPEED
C
      DO 20 I=1, IN
      TAU(I)=0.20899E-2*K1(I)*K2(I)*THETA(I)
      ARPM(I)=ALOG(RPM(I))
   20 ATAU(I)=ALOG(TAU(I))
C
C   CALLING SUBROUTINE SQUARE WHICH SOLVES THE LEAST
C   SQUARE FITTING
C
      CALL SQUARE(1,IN,ARPM,ATAU,NTWO,AK)
      WRITE(6,400) NTWO
      WRITE(6,410)
      WRITE(6,420)
      DO 30 I=1, IN
      G(I)=(1.0/NTWO-1.0)*ALOG(S(I))
      CR(I)=1.0+(S(I)**2-1.0)/(2.0*S(I)**2)*(1.0/NTWO-1.0)
     $      *(1.0+2.0/3.0*ALOG(S(I))+1.0/3.0*G(I)-1.0/45.0
     $      *G(I)**3+2.0/945.0*G(I)**5-1.0/4725.*G(I)**7)
      DUDR(I)=4.0*PI*(RPM(I)/60.0)*CR(I)/(1.0-1.0/S(I)**2)
      ADUDR(I)=ALOG(DUDR(I))
   30 WRITE(6,500)I,G(I),CR(I),DUDR(I),TAU(I)
C
C   BROOKFIELD VISCOMETER MEASUREMENT DATA
C
      WRITE(6,1000)
      WRITE(6,1100)
      DO 11 I=II,IRUN
      READ(5,1200)IFLAG,RPM(I),T(I),RB(I),RC(I),LE(I),THETA(I)
   11 WRITE(6,1300)I,RPM(I),T(I),RB(I),RC(I),LE(I),THETA(I)
C
C   CALCULATION OF FLOW CONDITIONS
C
      WRITE(6,2000)
      WRITE(6,2100)
      DO 12 I=II,IRUN
      DUDR(I)=PI*RPM(I)/30.0*(RB(I)*RB(I)+RC(I)*RC(I))/(RC(I)*RC(I)
     $       -RB(I)*RB(I))
      TAU(I)=0.20899E-2*6.737*THETA(I)/(2.0*PI*RB(I)*RB(I)*LE(I))
      ADUDR(I)=ALOG(DUDR(I))
      ATAU(I)=ALOG(TAU(I))
   12 WRITE(6,2200)I,DUDR(I),TAU(I)
C
C   SORTING SHEAR RATE AND STRESS IN ORDER OF INCREASING VALUE.
C
      IRN1=IRUN-1
      DO 13 I=1,IRN1
       IP1=I+1
       IP=I
       AMIN=DUDR(I)
      DO 14 J=IP1,IRUN
   14 IF(DUDR(J).LT.DUDR(IP)) IP=J
       AMIN=DUDR(IP)
       DUDR(IP)=DUDR(I)
```

```
        DUDR(I)=AMIN
        AMIN=TAU(IP)
        TAU(IP)=TAU(I)
   13   TAU(I)=AMIN
       DO 15 I=1,IRUN
        ATAU(I)=ALOG(TAU(I))
   15  ADUDR(I)=ALOG(DUDR(I))
C
C    CALLING SUBROUTINE SQUARE TO CALCULATE SLOPE N AND INTERCEPT K
C
       CALL SQUARE(IM,IRUN,ADUDR,ATAU,N,AK)
       K=EXP(AK)
       WRITE(6,600)N,K
       WRITE(6,610)
       WRITE(6,620)
C
C    CALCULATION OF SHEAR RATE AND APPARENT VISCOSITY
C
       DO 40 I=1, IRUN
       GAMMA(I)=4.*N/(3.*N+1.)*DUDR(I)
       VISC(I)=TAU(I)/DUDR(I)*479.
   40  WRITE(6,700)I, GAMMA(I),DUDR(I),VISC(I)
C
C    FORMAT STATEMENTS
C
    99  FORMAT(1H1)
   100  FORMAT(I2)
   110  FORMAT(//1X,'FANN VISCOMETER MEASUREMENT DATA'/)
   120  FORMAT(12X,'RPM',14X,'T',13X,'RB',13X,'RC',14X,'S',13X,'K1',13X,
     $         'K2',10X,'THETA')
   200  FORMAT(I1,7F10.3)
   300  FORMAT(I4,8E15.4)
   400  FORMAT(/1X,'N TWO PRIME =',E14.4/)
   410  FORMAT(1X,'FLOW CONDITIONS'/)
   420  FORMAT(14X,'G',13X,'CR',11X,'DUDR',12X,'TAU')
   500  FORMAT(I4,4E15.4)
   600  FORMAT(/1X,' N= ',E12.4,' K = ',E15.4/)
   610  FORMAT(1X,'SHEAR RATE AND APPARENT VISCOSITY'/)
   620  FORMAT(11X,'STRAIN',10X,'DUDR',11X,'VISCOSITY'/)
   700  FORMAT(I4,3E15.4)
  1000  FORMAT(///1X,'BROOKFIELD VISCOMETER MEASUREMENT DATA'/)
  1100  FORMAT(12X,'RPM',14X,'T',13X,'RB',13X,'RC',13X,'LE',10X,
     $         'THETA')
  1200  FORMAT(I1,6F10.3)
  1300  FORMAT(I4,8E15.5)
  2000  FORMAT(//1X,'FLOW CONDITIONS'/)
  2100  FORMAT(11X,'DUDR',12X,'TAU')
  2200  FORMAT(I4,2E15.5)
        STOP
        END

        SUBROUTINE SQUARE(IM,M,X,Y,A,B)
        DIMENSION X(30), Y(30)
C
C    SUBROUTINE TO SOLVE THE LEAST SQUARE FITTING OF FIRST ORDER
C
C
C    A -- SLOPE OF STRAIGHT LINE
C    B -- INTERCEPT AT X = 0.0
        SXX=0.0
        SXY=0.0
        SX=0.0
        SY=0.0
        DO 10 I=IM, M
        SX=SX+X(I)
        SY=SY+Y(I)
        SXX=SXX+X(I)*X(I)
   10   SXY=SXY+X(I)*Y(I)
        IM1=M-IM+1
        SSXY=SXY-SX*SY/FLOAT(IM1)
        SSXX=SXX-SX*SX/FLOAT(IM1)
        A=SSXY/SSXX
        B=SY/FLOAT(IM1)-A*SX/FLOAT(IM1)
        RETURN
        END
```

C.1.2 Capillary Tube Viscometer

```
C    THIS PROGRAM IS TO CALCULATE THE APPARENT VISCOSITY FROM THE
C    FLOW CURVE MEASURED BY A CAPILLARY TUE VISCOMETER
C
C
C    --- NOTATIONS OF PARAMETERS ---
C
C    D -- CAPILLARY TUBE DIAMETER (IN.)
C    DELP -- PRESSURE DROP (PSI)
C    DELT -- TIME INTERVAL (SEC)
C    H -- AVERAGE FLUID HEIGHT (IN.)
C    GAMMA --- SHEAR STRAIN (1/SEC)
C    IRUN -- NO. OF DATA POINTS
C    K -- INTERCEPT K VALUE
C    L -- CAPILLARY TUBE LENGTH (IN.)
C    N -- INDEX N VALUE
C    PG -- GAUGE PRESSURE ( IN. WATER)
C    RE -- GENERALIZED REYNOLDS NUMBER
C    ROW -- DENSITY OF FLUID (SLUG/FT**3)
C    T -- TEMPERATURE OF FLUID (DEG. C)
C    TAU -- SHEAR STRESS (LB/FT**2)
C    V -- VELOCITY (FT/SEC)
C    VISC -- APPARENT VISCOSITY (POISE)
C    VOL -- VOLUME OF FLUID COLLECTED (ML)
C
C
       DIMENSION T(30),PG(30),VOL(30),DELT(30),H(30),TAU(30),GAMMA(30),
      $            V(30),DELP(30),VISC(30),RE(30),ROW(30),ATAU(30),
      $            AGAMMA(30),DUDR(30)
       REAL L,N,K
C
C     INITIALIZATION OF PARAMETERS
C
       PI=3.141593
       A1=0.0
       A2=0.0
       B1=0.0
       B2=0.0
       C1=0.0
       C2=0.0
C
C    DIMENSIONS OF VISCOMETER
C
       READ(5,100) IRUN, L, D
       WRITE(6,110)
       WRITE(6,120)
       DO 10 I=1, IRUN
C
C    MEASUREMENT DATA
C
       READ(5,200) T(I), PG(I), VOL(I), DELT(I), H(I)
   10  WRITE(6,300) I, T(I), PG(I), VOL(I), DELT(I), H(I)
       WRITE(6,310)
       WRITE(6,320)
       DO 20 I=1, IRUN
C
C    CALCULATION OF SHEAR RATE AND SHEAR STRESS
C
       T(I)=32.0+1.8*T(I)
       ROW(I)=(61.95387+2.704542E-2*T(I)-4.901768E-4*(T(I)**2)+
      $          3.114458E-6*(T(I)**3)-8.743613E-9*(T(I)**4))/32.174
       V(I)=VOL(I)/(PI/4.*(D*2.54)**2*DELT(I))/30.48
       DELP(I)=PG(I)*14.7*2.54/(76.*13.6)+ROW(I)*((L+H(I))*32.174/12.
      $          -1.12*V(I)**2)/144.
       GAMMA(I)=8.0*V(I)/(D/12.0)
       TAU(I)=D/(4.*L)*DELP(I)*144.
C
C    CALCULATION OF INDEX N AND INTERCEPT K USING THE LEAST SQUARE METHOD
C
```

```
      ATAU(I)=ALOG(TAU(I))
      AGAMMA(I)=ALOG(GAMMA(I))
      A1=A1+1.0
      B1=B1+AGAMMA(I)
      A2=B1
      B2=B2+AGAMMA(I)**2
      C1=C1+ATAU(I)
      C2=C2+ATAU(I)*AGAMMA(I)
   20 WRITE(6,400) I,V(I),DELP(I),GAMMA(I),TAU(I),AGAMMA(I),ATAU(I)
      N=(C1*A2-C2*A1)/(B1*A2-A1*B2)
      Y=(C1*B2-C2*B1)/(A1*B2-A2*B1)
      K=EXP(Y)
      WRITE(6,500) N, K
      WRITE(6,510)
      WRITE(6,520)
      DO 30 I= 1, IRUN
C
C   CALCULATION OF APPARENT VISCOSITY
C
      VISC(I)=TAU(I)*4.*N/(3.*N+1.)/GAMMA(I)*479.
      DUDR(I)=GAMMA(I)*(3.*N+1.)/(4.*N)
      RE(I)=(D/12.0)**(N)*V(I)**(2.0-N)*ROW(I)/(K*8.0**(N-1.0))
   30 WRITE(6,600)I, RE(I), GAMMA(I), VISC(I), DUDR(I)
  100 FORMAT(I2,2F10.3)
  110 FORMAT(//3X,'MEASUREMENT DATA'/)
  120 FORMAT(13X,'T',13X,'PG',14X,'VOL',11X,'DELT',12X,'H'/)
  200 FORMAT(5F10.3)
  300 FORMAT(I4,5E15.5)
  310 FORMAT(//3X,' FLOW CONDITIONS'/)
  320 FORMAT(13X,'V',12X,'DELP',10X,'GAMMA',12X,'TAU',10X,'LN(GAMMA)',
     $       8X,'LN(TAU)'/)
  400 FORMAT(I4,6E15.5)
  500 FORMAT(/2X,'INDEX N= ' ,E12.4,5X,' INTERCEPT K =' ,E12.4/)
  510 FORMAT(/3X,'APPARENT VISCOSITY'/)
  520 FORMAT(13X,'RE',12X,'STRAIN',7X,'VISCOSITY',6X,'DRDU'/)
  600 FORMAT(I4,6E15.5)
      STOP
      END
```

C.2 Fluid Time Scale

The following computer program is used to calculate the fluid time scale from viscosity data using the Powell-Eyring fluid model.

```
C     THIS PROGRAM SHOULD BE USED TO DETERMINE THE POWELL-EYRING
C     TIME CONSTANT FOR POLYMER SOLUTIONS IN PIPE FLOW.
C     THERE ARE TWO DISTINCT SECTIONS IN THE PROGRAM,
C     DESCRIBED BELOW.
C
C       1)  BEGINS AT LINE 500.  THIS SECTION OF THE PROGRAM
C           CALCULATES AND PLOTS THE SUM SQUARED ERROR VS.
C           THE POWELL-EYRING TIME CONSTANT, AND IS USED TO BE SURE
C           THE TIME BAND USED IN THE NUMERICAL SCHEME OF
C           SECTION 2 CONTAINS ONLY THE ABSOLUTE MINIMUM.  IF
C           THE REGION CONTAINS ANY OTHER LOCAL MINIMA, THE
C           TIME CONSTANT CALCULATED MAY NOT BE THE BEST VALUE
C           ACCORDING THE LEAST SQUARES METHOD.
C
C           INPUT VARIABLES ARE:
C
C             NP   THE NUMBER OF EXPERIMENTAL DATA PAIRS OF
C                  SHEAR RATE AND VISCOSITY.
```

```
C              TC   INITIAL ESTIMATE OF THE POWELL-EYRING
C                   TIME CONSTANT, IN SECONDS.
C              GAM  SHEAR RATE IN SEC**(-1)
C              VIS  EXPERIMENTAL SHEAR RATE DEPENDENT VISCOSITY
C                   IN ANY SET OF CONSISTENT UNITS.
C              H    THE STEP VALUE OF THE TIME CONSTANT.
C
C     AFTER SECTION 1 HAS BEEN EXECUTED, THE BAND MAY BE
C     NARROWED AND SECTION 1 EXECUTED AN ADDITIONAL NUMBER
C     OF TIMES UNTIL THE USER IS SATISFIED WITH THE RESULTS.
C
C       2)  SECTION 2 OF THE PROGRAM BEGINS AT LINE 1270.  IT IS
C           A NUMERICAL PROCEDURE TO CALCULATE THE POWELL-EYRING TIME
C           CONSTANT WHICH GIVES THE BEST FIT OF THE POWELL-EYRING MODEL
C           TO THE EXPERIMENTAL DATA.  THERE IS ONE NEW INPUT
C           VARIABLE FOR THIS PORTION OF THE PROGRAM.  IT IS
C
C             TOL  ACCURACY DESIRED IN THE FINAL ESTIMATE OF THE
C                  POWELL-EYRING TIME CONSTANT.
C
C           UPON COMPLETION OF SECTION 2 OF THE PROGRAM, THE
C           POWELL-EYRING TIME CONSTANT IS KNOWN AND THE USER MAY
C           RETURN TO THE TOP OF THE PROGRAM WITH NEW DATA
C           OR EXIT THE PROGRAM.
C
C
C     DEFINE AND DIMENSION THE VARIABLES.
C
      REAL LAM,LAMBDA,LAMI,LAMJ,LAMK,LAML,LAMMIN,LAMMAX
      DIMENSION GAM(100),LAMBDA(1000),SSE(1000),VIS(100)
C
C     INPUT DATA
C
1111     IFLG = 1
 1   ) WRITE(6,1902)
      READ(5,*)VINF
         IF(IFLG .EQ. 20) GO TO 28
      WRITE(6,1903)
      READ(5,*)NP
      WRITE(6,1904)
      DO 1020 IA=1,NP
      READ(5,*)VIS(IA),GAM(IA)
 1020 CONTINUE
      PAUSE
      WRITE(6,1920)
      WRITE(6,1921)
      DO 25 ISCAN=1,NP
      WRITE(6,1922)ISCAN,VIS(ISCAN),GAM(ISCAN)
    5 CONTINUE
      PAUSE
   27 WRITE(6,1925)
      READ(5,*)ICHECK
      IF(ICHECK.EQ.2) GO TO 28
      WRITE(6,1926)
      READ(5,*)ICOR
      WRITE(6,1927)
      READ(5,*)VIS(ICOR),GAM(ICOR)
      GO TO 27
   28 WRITE(6,1905)
      READ(5,*)TC
C
      LAMMIN=.5*TC
      LAMMAX=1.5*TC
      VZERO=VIS(1)
C
C     TOP OF REPLOTTING ROUTINE.
C
 1030 LAMBDA(1)=LAMMIN
      WRITE(6,1906)
      READ(5,*)H
      PTSMAX=(LAMMAX-LAMMIN)/H
      IF(PTSMAX.GE.1000.) H=(LAMMAX-LAMMIN)/998.
C
C     START THE LOOP TO INCREMENT THE TIME CONSTANT LAMBDA
C
      I=0
 1040 I=I+1
```

```
      IF (I.GT.1) LAMBDA(I)=LAMBDA(I-1)+H
C
C     LOOP TO SUM THE ERROR AND SQUARE IT.
C
      ERRSUM=0.
      DO 1050 K=1,NP
      X=LAMBDA(I)*GAM(K)
      Z=X+(X**2+1.)**0.5
      ERR=VIS(K)-(VINF+(VZERO-VINF)*ALOG(Z)/X)
 1050 ERRSUM=ERRSUM+ERR**2
C
C     SAVE THE SUM SQUARED ERROR FOR PLOTTING. TEST TO SEE
C     IF SSE HAS BEEN FOUND FOR ALL VALUES OF LAMBDA.
C
      SSE(I)=ERRSUM
      IF(LAMBDA(I).LT.LAMMAX) GO TO 1040
C
C     PLOT THE DATA USING THE QUICKPLOT SUBROUTINE.
C
      CALL QCKPLT(LAMBDA, SSE, I, 'EYRING TIME CONSTANT$',
     1 'SUM SQUARED ERROR$', 'PLOT TO EXAMINE LOCAL MINIMA$',
     2 4, 5, 0)
      PAUSE
C
C     CHOOSE THE NEXT STEP.
C
      WRITE(6,1907)
      READ(5,*)ITEST1
      IF(ITEST1.EQ.1) GO TO 1060
      WRITE(6,1908)
      IF (FJ.GT.FK) FI=FJ
      IF (FJ.GT.FK) FJ=FK
C
C     TEST TO SEE IF LAMBDA VALUES HAVE CONVERGED TO A SMALL
C     ENOUGH VALUE.
C
      DEL=LAML-LAMI
      IF (DEL.LT.TOL) GO TO 1120
      IF (N.EQ.1) GO TO 1080
      IF (N.EQ.2) GO TO 1090
C
C     PRINT FINAL ESTIMATE OF THE EYRING TIME CONSTANT.
C
 1120 LAM=0.5*(LAMI+LAML)
      WRITE(6,1900)LAM
      PAUSE
         WRITE (6,9100)
         READ (5,*) III
         IF (III .EQ. 1) THEN
            IFLG = 20
            GO TO 1010
         ENDIF
C
C
C     CHOOSE WHETHER TO EXIT PROGRAM OR TO EXECUTE AGAIN.
C
      WRITE(6,1911)
      READ(5,*)ITEST3
         IF(ITEST3.EQ.1) GO TO 1111
C
 1900 FORMAT(//10X,'LAMBDA = ',E11.4)
 1901 FORMAT(10X,I2,2(15X,E11.4))
 1902 FORMAT(//5X,'ENTER THE VISCOSITY OF WATER AT',
     1/5X,'EXPERIMENTAL TEMPERATURE.  UNITS MUST BE',
     2/5X,'CONSISTENT WITH THOSE REPORTED FROM THE',
     3/5X,'SHEAR RATE-VISCOSITY CURVE.')
 1903 FORMAT(/5X,'ENTER THE # OF DATA POINTS')
 1904 FORMAT(/5X,'ENTER VISCOSITY AND THE CORRESPONDING',/
     15X,'SHEAR RATE FOR EACH DATA POINT.  THE FIRST',
     2/5X,'DATA POINT ENTERED MUST CONTAIN THE ',
     3/5X,'MINIMUM SHEAR RATE VALUE, AND THE LAST MUST',
     4/5X,'CONTAIN THE MAXIMUM SHEAR RATE VALUE.')
 1905 FORMAT(/5X,'ENTER THE INITIAL ESTIMATE OF THE',
     1/5X,'POWELL-EYRING TIME CONSTANT, IN SECONDS.')
 1906 FORMAT(/5X,'ENTER TIME CONSTANT INCREMENT FOR',/
     15X,'PLOTTING PURPOSES')
```

```
 1907 FORMAT(/5X,'ENTER THE NUMBER CORRESPONDING TO',/
     15X,'WHAT YOU WISH TO DO.',/
     210X,'1.  CONTINUE EXECUTION',/
     310X,'2.  RESPECIFY PLOT ENDPOINTS AND PLOT AGAIN.')
 1908 FORMAT(/5X,'ENTER NEW ENDPOINTS FOR TIME CONSTANT.',
     1/5X,'ENTER THE MINIMUM VALUE FIRST.')
 1909 FORMAT(/5X,'ENTER THE ACCURACY DESIRED FOR',
     1/5X,'THE ESTIMATE OF THE EYRING TIME CONSTANT.')
 1911 FORMAT(/5X,'1.  RETURN TO TOP OF PROGRAM',
     1/5X,'2.  EXIT THE PROGRAM',
     2//5X,'ENTER THE INTEGER CORRESPONDING TO YOUR CHOICE.')
 1920 FORMAT(//5X,'PLEASE CHECK YOUR DATA FOR TYPE ERRORS')
 1921 FORMAT(//5X,'DATA #',10X,'VISCOSITY',10X,'SHEAR RATE'//)
 1   ? FORMAT(7X,I2,9X,E11.4,10X,E11.4)
 1>45 FORMAT(//5X,'DO YOU NEED TO CORRECT ANY OF THE',
     1/5X,'VISCOSITY-SHEAR RATE DATA?',//10X,
     2'1.  YES',/10X,'2.  NO')
 1926 FORMAT(//5X,'ENTER THE DATA #')
 1927 FORMAT(//5X,'ENTER VISCOSITY & SHEAR RATE')
9100     FORMAT(//'TRY A NEW VINF?:Y=1,N=2')
      READ(5,*)LAMMIN,LAMMAX
      GO TO 1030
C
C     SECTION 2
C
C     NEW INPUT DATA
C
 1   ) WRITE(6,1909)
      READ(5,*)TOL
      J=1
C
C     DEFINE THE FIRST FOUR VALUES OF LAMBDA
C
      LAMI=LAMMIN
      LAML=LAMMAX
      LAMJ=LAMI+0.3819660115*(LAML-LAMI)
      LAMK=LAMI+0.6180339885*(LAML-LAMI)
C
 1070 IF (J.EQ.1) LAM=LAMI
      IF (J.EQ.2) LAM=LAMJ
      IF (J.EQ.3) LAM=LAMK
      IF (J.EQ.4) LAM=LAML
      GO TO 1100
C
C     RECALCULATE LAMJ FOR THE CASE WHERE REGION K-L IS
C     DISCARDED.
C
 1080 LAMJ=LAMI+0.3819660115*(LAML-LAMI)
      LAM=LAMJ
      GO TO 1100
C
C     RECALCULATE LAMK FOR I-J BEING DISCARDED.
C
 1   ) LAMK=LAMI+0.6180339885*(LAML-LAMI)
      LAM=LAMK
C
C     LOOP TO FIND SUM SQUARED ERROR.
C
 1100 ERRSUM=0.
      DO 1110 L=1,NP
      X=LAM*GAM(L)
      Z=X+(X**2+1.)**0.5
      ERR=VIS(L)-(VINF+(VZERO-VINF)*ALOG(Z)/X)
 1110 ERRSUM=ERRSUM+ERR**2
      J=J+1
C
C     DETERMINE FUNCTION VALUES
C
      IF (LAM.EQ.LAMI) FI=ERRSUM
      IF (LAM.EQ.LAMJ) FJ=ERRSUM
      IF (LAM.EQ.LAMK) FK=ERRSUM
      IF (LAM.EQ.LAML) FL=ERRSUM
```

```
C
      IF (J.LE.4) GO TO 1070
C
C     REDEFINE POINTS AS NEEDED.
C
      IF (FJ.LE.FK) N=1
      IF (FJ.LE.FK) LAML=LAMK
      IF (FJ.LE.FK) LAMK=LAMJ
      IF (FJ.LE.FK) FL=FK
      IF (FJ.LE.FK) FK=FJ
C
      IF (FJ.GT.FK) N=2
      IF (FJ.GT.FK) LAMI=LAMJ
      IF (FJ.GT.FK) LAMJ=LAMK
```

C.3 Data Reduction

The following computer program is used to determine dimensionless parameters, friction factors and heat transfer coefficients from the measurements of fluid properties, pressure drops and heat transfer rates.

```
C THIS IS THE DATA REDUCTION PROGRAM FOR TURBULENT VISCOELASTIC
C FLOWS IN A PIPE.
C AI --- TEST SECTION AREA BASED ON INSIDE DIAMETER(IN**2)
C AO --- TEST SECTION AREA BASED ON OUTSIDE DIAMETER(IN**2)
C CP --- SPECIFIC HEAT OF FLUID(BTU/LB-F)
C DELH --- PRESSURE DROP(IN-MERCURY)
C DELV --- VOLTAGE DROP(VOLTS)
C DI --- INSIDE DIAMETER OF TEST SECTION(IN)
C DO --- OUTSIDE DIAMETER OF TEST SECTION(IN)
C F --- FANNING FRICTION FACTOR
C FC --- TURBINE METER FREQUENCY(HZ)
C GAM --- SHEAR STRAIN OF INTERPOLATION DATA(1./SEC), GAM=8*V/D
C H --- FILM HEAT TRANSFER COEFFICIENT(BTU/HR-FT**2-F)
C JH --- COLBURN J-FACTOR
C KF --- FLUID THERMAL CONDUCTIVITY(BTU/HR-FT-F)
C KS --- STEEL PIPE THERMAL CONDUCTIVITY(BTU/HR-FT-F)
C LH --- HEATED TUBE LENGTH(FT)
C LP --- INTERVAL BETWEEN TWO PRESSURE TAPS(FT)
C M --- NUMBER OF VISCOSITY INTERPOLATION DATA
C MU --- APPARENT VISCOSITY(CENTIPOISE)
C N --- NUMBER OF TEST RUN
C NU --- NUSSELT NUMBER
C PF --- POWER FACTOR, PF=QF/QP
C PPM --- CONCENTRATION OF POLYMER SOLUTION(PPM)
C PR --- APPARENT PRANDTL NUMBER
C R --- RESISTANCE OF TEST SECTION(OHM)
C ROW --- FLUID DENSITY(LBM/FT**3)
C Q --- HEAT FLUX(BTU/HR-FT**2)
C QF --- HEAT FLOW RATE BASED ON ENERGY BALANCE(BTU/HR)
C QP --- HEAT FLOW RATE BASED ON VOLTAGE DROP(BTU/HR)
```

```
C RE --- APPARENT REYNOLDS NUMBER
C SR --- SHEAR RATE OF FLUID(1./SEC)
C T --- AVERAGE TEMPERATURE OF INLET AND OUTLET TEMPERATURES(F)
C TIN --- INLET BULK TEMPERATURE(F)
C TOUT --- OUTLET BULK TEMPERATURE(F)
C TWI --- LOCAL INSIDE WALL TEMPERATURE OF TEST SECTION(F)
C TWO --- LOCAL OUTSIDE WALL TEMPERATURE OF TEST SECTION(F)
C ST --- STANTON NUMBER
C VIS --- VISCOSITY OF CALIBRATION DATA(CENTIPOISE)
C VQ --- VOLUME FLOW RATE(GPM)
C V --- FLOW VELOCITY(FT/S)
C UTAU --- SHEAR VELOCITY(FT/SEC)
C
C
C
C DIMENSION STATEMENT
C
      DIMENSION CP(20),DELH(20),DELV(20),F(20),FC(20),H(20),PR(20),
     $          ROW(20),R(20),Q(20),QF(20),QP(20),RE(20),TIN(20),
     $          TOUT(20),TWI(20),TWO(20),ST(20),VQ(20),PF(20),V(20),
     $          GAM(20),VIS(20),SR(20),UTAU(20)
      REAL LH,LP,JH(20),KF(20),KS(20),MU(20),NU(20)
C
C READ STATEMENT FOR SPECIFING  TEST SECTION GEOMETRIES
C AND SOLUTION PROPERTIES
C
      PI = 3.14159
      M = 17
      WRITE(6,550)
      WRITE(6,560)
C
C READ STATEMENT FOR VISCOSITY INTERPOLATION DATA
C
      DO 9 I=1,M
      READ(5,600)GAM(I),VIS(I)
    9 WRITE(6,610)I,GAM(I),VIS(I)
      READ(5,100)N,DI,DO,LH,LP,PPM
      WRITE(6,99)
      WRITE(6,101)
      WRITE(6,102)N,DI,DO,LH,LP,PPM
C
C READ STATEMENT FOR INPUTTING MEASUREMENT DATA FOR EACH RUN
C
      WRITE(6,199)
      WRITE(6,201)
      DO 10 I = 1 , N
       READ(5,200)DELH(I),DELV(I),FC(I),TIN(I),TOUT(I),TWO(I)
      TOUT(I)=TOUT(I)-2.0/LH*(TOUT(I)-TIN(I))
 10   WRITE(6,202)I,DELH(I),DELV(I),FC(I),TIN(I),TOUT(I),TWO(I)
C
C CALCULATION OF TEST SECTION AREAS
C
      AI = PI/4.*(DI*DI)
      AO = PI/4.*(DO*DO)
C
C DATA REDUCTION PROCEDURES
C
      DO 20 I = 1 , N
C
C CALCULATION OF FLUID AND TEST SECTION PROPERTIES
C
      T = (TIN(I)+TOUT(I))/2.
      CP(I) = 1.020892 -6.639922E-4*T + 7.103168E-6*(T**2)
     $        -3.310227E-8*(T**3) + 6.185928E-11*(T**4)
      KF(I) = 4.826587E-1 - 6.987679E-3*TOUT(I) + 1.146261E-4
     $       *(TOUT(I)**2) - 7.323056E-7*(TOUT(I)**3)
     $       +1.656699E-9*(TOUT(I)**4)
      KS(I) = 8.0*(1.+7.432E-4*TWO(I))
      R(I) = 27.8142E-6*(1.+5.826E-4*TWO(I))*LH*12./(AO-AI)
      ROW(I) = 61.95387 + 2.704542E-2*T - 4.901768E-4*(T**2)
     $         +3.114458E-6*(T**3) - 8.743613E-9*(T**4)
C
C CALCULATION OF FANNING FRICTION FACTOR
C
      VQ(I) =0.95*(-.00746+.06748*FC(I))
      V(I) = 0.32088*VQ(I)/AI
```

```
C
C INTERPOLATION OF VISCOSITY DATA USING THE CUBIC SPLINE
C INTERPOLATION METHOD
C
   20  SR(I)=8.0*V(I)/(DI/12.0)
       CALL CUBIC(N,M,GAM,VIS,SR,MU)
       DO  21 I=1,N
       RE(I) = 1.24016E2*ROW(I)*V(I)*DI/MU(I)
       F(I) = 1.40426*DELH(I)*DI/(LP*V(I)**2)
       UTAU(I)=V(I)*SQRT(F(I)/2.0)
       RO = DO/2.
       RI = DI/2.
C
C CALCULATION OF HEAT TRANSFER J FACTOR
C
       QF(I) = 8.02139*ROW(I)*VQ(I)*CP(I)*(TOUT(I)-TIN(I))
       QP(I) = 3.415*DELV(I)*DELV(I)/R(I)
       TOUT(I) = TIN(I)+QP(I)/(8.02139*ROW(I)*VQ(I)*CP(I))
       PF(I) = QF(I)/QP(I)
       TWI(I) = TWO(I)-QP(I)/(2.*PI*(RO*RO-RI*RI)*KS(I)*LH)
     $          *(RO*RO*ALOG(RO/RI)-(RO*RO-RI*RI)/2.)
       Q(I) = 12.*QP(I)/(PI*DI*LH)
       H(I) = Q(I)/(TWI(I)-TOUT(I))
       NU(I) = H(I)*(DI/12.)/KF(I)
       PR(I) = 2.42*MU(I)*CP(I)/KF(I)
       ST(I) = NU(I)/(RE(I)*PR(I))
   21  JH(I) = ST(I)*(PR(I)**(2./3.))
C
C WRITE STATEMENT
C
       WRITE(6,399)
       WRITE(6,401)
       DO 40 I =1, N
   40  WRITE(6,402)I,V(I),KF(I),UTAU(I),SR(I),MU(I),QF(I),TWI(I),Q(I)
       WRITE(6,501)
       DO 30 I =1 , N
   30  WRITE(6,502)I,RE(I),F(I),PF(I),PR(I),H(I),NU(I),ST(I),JH(I)
C
C FORMAT STATEMENT
C
    99  FORMAT(//1X,'THE SPECIFICATIONS OF EXPERIMENTAL CONDITIONS :')
   100  FORMAT(I3,5F10.3)
   101  FORMAT(//1X,'RUN',8X,'DI',8X,'DO',8X,'LH',8X,'LP',7X,'PPM'/ )
   102  FORMAT(1X,I3,5F10.3)
   199  FORMAT(//1X,'THE EXPERIMENTAL MEASUREMENT DATA :')
   200  FORMAT(7F10.3)
   201  FORMAT(//1X,'RUN',6X,'DELH',6X,'DELV',8X,'FC',7X,'TIN',
     $         6X,'TOUT',7X,'TWO'/)
   202  FORMAT(1X,I3,7F10.3)
   399  FORMAT(//1X,'THE REDUCED DATA :')
   401  FORMAT(//1X,'RUN',8X,'UAV',10X,'KF',8X,'UTAU',9X,'SR',9X,'MU',
     $         10X,'QF',9X,'TWI',11X,'Q'/)
   402  FORMAT(1X,I3,8E12.4)
   501  FORMAT(//1X,'RUN',8X,'RE',9X,'F',10X,'PF',10X,'PR',11X,'H',
     $         10X,'NU',10X,'ST',10X,'JH'/)
   502  FORMAT(I3,8E12.4)
   550  FORMAT(//1X,'THE CALIBRATION DATA FOR APPARENT VISCOSITIES'/)
   560 FORMAT(2X,'I',8X,'GAM',12X,'VIS')
   600  FORMAT(2F15.2)
   610  FORMAT(I3,2E15.5)
        STOP
        END

        SUBROUTINE CUBIC(N,M,X,Y,SR,MU)
C THE CUBIC SPLINE IS A SET OF THIRD-ORDER POLYNOMIALS, ONE FOR EACH
C INTERVAL BETWEEN THE KNOWN POINTS, WHOSE CONSTANTS ARE ADJUSTED
C TO MAKE THE SLOPES OF ADJOINING INTERVALS EQUAL.
C ESPECIALLY, THIS ROUTINE IS WRITTEN FOR SMALL Y COORD. VARIATION
C VERSUS LARGE X COORD. VARIATION.
C
        DIMENSION X(20),Y(20),D(20),A(20,20),B(20),C(20,4),SR(20)
        REAL MU(20)
C
C INITIALIZATIONS OF VARIABLES
        MM1=M-1
        MM2=M-2
        MP1=M+1
```

```
      DO 10 I=1,20
      B(I)=0.0
      D(I)=0.0
      DO 20 J=1,20
   20 A(I,J)=0.0
   10 CONTINUE
C
C CHANGES OF PLAIN COORD. TO CORRESPONDING LOG-LOG COORD.
C
      DO 21 I=1,M
      X(I)=ALOG10(X(I))
   21 Y(I)=ALOG10(Y(I))
      DO 31 I=1,N
   31 SR(I)=ALOG10(SR(I))
      DO 30 I=2,M
      IM1=I-1
   30 D(IM1)=X(I)-X(IM1)
C
C CALCULATIONS OF COEFFICIENT MATRIX FOR M=2 THROUGH M-1
C
      DO 40 I=2,MM1
      IM1=I-1
      IP1=I+1
      A(I,IM1)=D(IM1)
      A(I,I)=2.0*(D(IM1)+D(I))
      A(I,IP1)=D(I)
   40 B(I)=6.0*((Y(IP1)-Y(I))/D(I)-(Y(I)-Y(IM1))/D(IM1))
C
C CALCULATIONS OF COEFFICIENT MATRIX FOR I=1 AND M USING THE
C CONSTRAINTS THAT THE THIRD DERIVATIVE BE CONTINUOUS AT I=2 AND M-1
C
      A(1,1)=-1.0/D(1)
      A(1,2)=1.0/D(1)+1.0/D(2)
      A(1,3)=-1.0/D(2)
      A(M,MM2)=-1.0/D(MM2)
      A(M,MM1)=1.0/D(MM2)+1.0/D(MM1)
      A(M,M)=-1.0/D(MM1)
C
C CALL SUBROUTINE YSOLV TO SOLVE M SIMULTANEOUS EQUATIONS
C
      CALL YSOLV(A,B,M,20,NRANK)
C
C CALCULATIONS OF M-4 COEFFICIENT CONSTANTS FOR A CUBIC SPLINE
C
      DO 50 I=1,MM1
      IP1=I+1
      C(I,1)=B(I)/(6.0*D(I))
      C(I,2)=B(IP1)/(6.0*D(I))
      C(I,3)=Y(I)/D(I)-B(I)*D(I)/6.0
   50 C(I,4)=Y(IP1)/D(I)-B(IP1)*D(I)/6.0
      DO 60 I=1,N
      IF(SR(I).LT.X(1) .OR. SR(I).GT.X(M)) WRITE(6,1000) I
      IF(SR(I).LT.X(1)) STOP
      IF(SR(I).GE.X(M)) MU(I) = 10.0**Y(M)
      IF(SR(I).GE.X(M)) GO TO 60
      DO 70 J=1,MM1
      JP1=J+1
   70 IF(SR(I).GE.X(J) .AND. SR(I).LT.X(JP1)) K=J
      MU(I)=C(K,1)*(X(K+1)-SR(I))**3+C(K,2)*(SR(I)-X(K))**3
     $     +C(K,3)*(X(K+1)-SR(I))+C(K,4)*(SR(I)-X(K))
      SR(I)=10.0**SR(I)
      MU(I)=10.0**MU(I)
   60 CONTINUE
 1000 FORMAT(//1X,'THE SHEAR RATE IS OUT OF INTERPOLATION
     $  CALIBRATION DATA RANGE : CASE = ',I2/)
      RETURN
      END

      SUBROUTINE YSOLV (A,BX,N,LDIM,NRANK)
C
C YSOLV SOLVES A SYSTEM OF LINEAR EQUATIONS USING GAUSSIAN ELIMINATION
C WITH PARTIAL PIVOTING.
C IF THE MATRIX OF COEFFICIENTS IS SINGULAR, YSOLV COMPUTES THE
C SOLUTION THAT WOULD RESULT FROM MULTIPLYING A RAO PSEUDO-INVERSE
C OF THE COEFFICIENT MATRIX BY THE VECTOR OF CONSTANTS.
C C. R. RAO AND S. K. MITRA, -GENERALIZED INVERSE OF MATRICES AND
C ITS APPLICATIONS - (WILEY, 1971), PAGE 212. THIS SUBROUTINE WAS
```

```
C WRITTEN BY DR. J. P. CHANDLER, COMSC DEPT., OKLAHOMA STATE
C UNIVERSITY, IN NOVEMBER 1981.
C
C N IS THE NUMBER OF EQUATIONS IN THE LINEAR SYSTEM.
C ON INPUT, A(*,*) CONTAINS THE MATRIX OF COEFFICIENTS ABD BX(*)
C CONTAINS THE VECTOR OF CONSTANTS (THE RIGHT HAND SIDES).
C ON OUTPUT, BX(*) CONTAINS THE SOLUTION VECTOR AND A(*,*) CONTAINS
C GARBAGE.
C LDIM IS THE VALUE OF THE DIMENSIONS OF THE ARRAYS A AND BX.
C THE VALUE OF N MUST NOT EXCEED THE VALUE OF LDIM.
C NRANK RETURNS THE RANK OF THE MATRIX A. IF NRANK .LT. N THEN
C THE MATRIX A IS SINGULAR.
C
C
C CHECK FOR AN INVALID VALUE OF N OR LDIM.
C
      DIMENSION A(LDIM,LDIM),BX(LDIM)
      NRANK = -1
      IF(N)210,210,10
   10 IF(N-LDIM)20,20,210
C
C TRIANGULARIZE THE MATRIX A.
C
   20 NRANK =0
      NMU = N-1
      IF(NMU)210,140,30
   30  DO 130 J = 1,NMU
C
C SEARCH COLUMN J FOR THE PIVOT ELEMENT.
C
      BIGA = 0.
      DO 50 K =J,N
       TEMP=ABS(A(K,J))
       IF(TEMP-BIGA)50,50,40
   40 BIGA = TEMP
      JPIV = K
   50 CONTINUE
      IF(BIGA)130,130,60
   60 IF(JPIV-J)90,90,70
C
C INTERCHANGE EQUATION J AND JPIV.
C
   70 DO 80 L = J,N
       TEMP = A(J,L)
       A(J,L) = A(JPIV,L)
   80 A(JPIV,L) = TEMP
      TEMP = BX(J)
      BX(J) = BX(JPIV)
      BX(JPIV) = TEMP
   90 JPU = J+1
C
C PERFORM ELIMINATION ON EQUATION K.
C
      DO 120 K = JPU,N
       EM = A(K,J)/A(J,J)
       IF(EM)100,120,100
  100 DO 110 L = JPU,N
  110 A(K,L) = A(K,L)-EM*A(J,L)
      BX(K) = BX(K)-EM*BX(J)
  120 CONTINUE
  130 CONTINUE
C
C DO THE BACK SOLUTION
C
  140  DO 200 JINV = 1,N
       J = N+1-JINV
       IF(A(J,J))160,150,160
  150 BX(J) = 0.
      GO TO 200
  160 NRANK = NRANK+1
      SUM = 0.
      IF(J-N)170,190,190
  170 JPU = J+1
      DO 180 K = JPU,N
  180 SUM = SUM+A(J,K)*BX(K)
```

```
  190  BX(J) = (BX(J)-SUM)/A(J,J)
  200  CONTINUE
  210  RETURN
       END
```

C.4 Prediction

The following computer program is used to predict heat transfer coefficients using the Cess model for momentum eddy diffusivity and the proposed expression for heat eddy diffusivity.

```
C      THIS PROGRAM PREDICTS HEAT TRANSFER COEFFICIENTS IN SOLVENT AND
C      DRAG REDUCING TURBULENT PIPE FLOWS.
C      THIS PROGRAM ALSO PREDICTS VELOCITY PROFILE , EDDY DIFFUSIVITY
C      DISTRIBUTION , AND TEMPERATURE PROFILE FOR SOLVENT  AND DRAG
C      REDUCING TURBULENT PIPE FLOWS
C      CESS EDDY DIFFUSIVITY PROGRAM FOR MOMENTUM TRANSPORT IN TUBES
C
C
       REAL K, JH
       DIMENSION ED(410), DU(410),YPLUS(410),Y(410),U(410),UPLUS(410),
      $YD(410), DUM(410),DA(410),A(410),DB(410),T(410),S(410),C(410),
      $DC(410),TM(410),UC(410), ENEWD(500),FN(500)
     1 READ (5,100,END=1000)UAVG,RO,VISC,UTAU,APLUS,TK,PR
C      UAVG IS THE AVERAGE VELOCITY IN FT/SEC ,
C      RO IS THE TUBE RADIUS IN FT
C      VISC IS THE KINEMATIC VISCOSITY IN FT**2/SEC
C      UTAU IS THE SHEAR VELOCITY IN FT/SEC
C      APLUS CONSTANT THAT CHARACTERIZES THICKNESS OF WALL LAYER
C      K IS VON KARMAN CONSTANT
C      TK IS THE THERMAL CONDUCTIVITY IN BTU/(HR-FT-F)
C      PR IS THE PRANDTL NUMBER
       K=0.4
       RE=UAVG*RO/VISC
        RD=2.0*RE
C      RE IS THE REYNOLDS NUMBER
       B=2.0*(UTAU/UAVG)**2.0
C      B IS THE FANNING FRICTION FACTOR
       ROP=RO*UTAU/VISC
       RPLUS=RO*UTAU/VISC
C      ROP NON-DIMENSIONAL PIPE RADIUS
       N=401
        RANDA=1.84E-2
        FF=(UTAU**2)*2./(UAVG**2)
        FS=0.0014+0.1250*RD**(-0.32)
        FR=(FS-FF)/FS
        WS=RANDA*UAVG/(2.*RO)
       IF(WS.GT.205.) WS=205.
       G=0.0025
       DAPLUS=10.0
       C12=G/12.0
       C3=G/3.0
C      C12,C3  CONSTANTS OF SIMPSONS RULE
       NP=0
       MP=0
     2 IND=0
       Y(1)=0.0
       ED(1)=0.0
       DU(1)=RE*B/2.0
```

```
      YD(1)=0.0
      YPLUS(1)=0.0
      UPLUS(1)=0.0
      FN(1)=0.
      DO 10 I=2,N
      IND=IND+1
      X=IND*G
C     X IS THE NON-DIMENSIONAL DIRECTION NORMAL TO WALL
      R=1.0-X
C     R IS THE NON-DIMENSIONAL RADIAL COORDINATE
      ED(I)=0.5*SQRT(1.+((K*K*ROP*ROP)/9.)*((1.-(R*R))**2)*((1.+2.*R*R)*
     $*2)*((1.-EXP((-X)/(APLUS/ROP)))**2))-0.5
C     ED IS THE NON-DIMENSIONAL EDDY DIFFUSIVITY
      DU(I)=0.5*(RE*B)*(1.0-X)/(1.0+ED(I))
      YPLUS(I)=(X*UTAU*RO)/VISC
C     YPLUS IS THE NON-DIMENSIONAL DISTANCE NORMAL TO WALL
      Y(I)=X*RO
C     Y IS THE COORDINATE DIRECTION NORMAL TO WALL
      YD(I)=X
C     YD IS THE NON-DIMENSIONAL DIRECTION NORMAL TO WALL
   10 CONTINUE
      U(1)=0.0
      UM=0.0
      DUM(1)=0.0
      DA(1)=0.0
      A(1)=0.0
      M=N-2
      DO 25 I=1,M,2
      U(I+1)=U(I)+C12*(5.0*DU(I)+8.0*DU(I+1)-DU(I+2))
      U(I+2)=U(I)+C3*(DU(I)+4.0*DU(I+1)+DU(I+2))
      DUM(I)=2.0*U(I)*(1.0-YD(I))
      DUM(I+1)=2.0*U(I+1)*(1.0-YD(I))
      DUM(I+2)=2.0*U(I+2)*(1.0-YD(I))
      UM=UM+C3*(DUM(I)+4.0*DUM(I+1)+DUM(I+2))
      DO 20 J=1,2
   20 DA(I+J)=(1.0-YD(I+J))*U(I+J)
      IP1=I+1
      IP2=IP1+1
      A(IP1)=A(I)+C12*(5.0*DA(I)+8.0*DA(IP1)-DA(IP2))
      A(IP2)=A(I)+C3*(DA(I)+4.0*DA(IP1)+DA(IP2))
   25 CONTINUE
      BM=B/UM
C     BM NON-DIMENSIONAL PRESSURE DROP FROM NORMALIZATION CONDITIONS
C     UM NON-DIMENSIONAL VELOCITY FROM NORMALIZATION CONDITION
      WRITE (6,240) APLUS,BM,B,UM
      IF((ABS(BM-B)/B).LE.0.001)  GOTO40
      IF((BM-B).LT.0.000) GOTO400
      APLUS=APLUS+DAPLUS
      GOTO2
  400 IF(MP.EQ.5.0) GOTO 1000
      MP=1
       APLUS=APLUS-DAPLUS
       DAPLUS=DAPLUS/10.0
      NP=1
      GO TO 2
   40 CONTINUE
      DO 45 I=1,N,1
      UPLUS(I)=U(I)/SQRT(B/2.0)
C     UPLUS IS THE NON-DIMENSIONAL VELOCITY
   45 CONTINUE
      DO 46 I=1,N
      UC(I)=U(I)/U(N)
C     UC IS THE NORMALIZED VELOCITY
   46 CONTINUE
       DO 323 I=1,N
  323   ED(I)=0.37*ED(I)*(1.-FR)**(.75)*EXP((1.-WS/200.)**3)
      ALFA=A(401)
      S(1)=0.0
      DB(1)=-ALFA*PR
      DC(1)=0.0
      C(1)=0.0
      DO 35 I=1,M,2
      DO 30 J=1,2
   30 DB(I+J)=(-ALFA+A(I+J))/((1.0-YD(I+J))*(ED(I+J)+1.0/PR))
```

```
      IP1=I+1
      IP2=I+2
      S(I+1)=S(I)+C12*(5.0*DB(I)+8.0*DB(IP1)-DB(IP2))
      S(I+2)=S(I)+C3*(DB(I)+4.0*DB(IP1)+DB(IP2))
      DC(I)=DA(I)*S(I)
      DC(I+1)=DA(I+1)*S(I+1)
      DC(I+2)=DA(I+2)*S(I+2)
      C(I+1)=C(I)+C12*(5.0*DC(I)+8.0*DC(I+1)-DC(I+2))
      C(I+2)=C(I)+C3*(DC(I)+4.0*DC(I+1)+DC(I+2))
   35 CONTINUE
      H=-(TK*ALFA*PR)/(2.0*RO*C(I))
C     H IS THE HEAT TRANSFER COEFFICIENT IN BTU/(HR-FT**2-F)
      TN=(H*2.0*RO)/TK
C     TN IS THE NUSSELT NUMBER
      F=TN/(RE*PR)
      ST=0.5*F
C     ST IS THE STANTON NUMBER
      TM(N)=-(F*UAVG*RO*S(I)/VISC)
C     TM IS THE NON-DIMENSIONAL TEMPERATURE
      DO 37 I=1,N
      TM(I)=-(F*UAVG*RO*S(I)/VISC)
      T(I)=TM(I)/TM(N)
C     T IS THE NORMALIZED TEMPERATURE
   37 CONTINUE
       JH = ST*PR**(2./3.)
      WRITE (6,200) UAVG
      WRITE(6,210) RO
      WRITE (6,211) B
      WRITE (6,213) BM
      WRITE (6,212) RE
      WRITE (6,220) VISC
      WRITE (6,230) K
      WRITE (6,250) UTAU
      WRITE(6,270) TK
      WRITE(6,280) PR
      WRITE(6,290) H
      WRITE(6,310) TN
      WRITE(6,320) ST
       WRITE(6,321) JH
      WRITE (6,260)
      WRITE(6,300) (YD(I),Y(I),YPLUS(I),UC(I),ED(I),UPLUS(I),T(I),I=1,10
     $,1)
       WRITE(6,300) (YD(I),Y(I),YPLUS(I),UC(I),ED(I),UPLUS(I),T(I),I=11,3
     $0,2)
       WRITE(6,300) (YD(I),Y(I),YPLUS(I),UC(I),ED(I),UPLUS(I),T(I),I=31,9
     $0,4)
       WRITE(6,300) (YD(I),Y(I),YPLUS(I),UC(I),ED(I),UPLUS(I),T(I),I=91,4
     $01,31)
       WRITE(6,3)
       GO TO 1
  100 FORMAT(4F10.7,F10.6,3F10.7)
  200 FORMAT (1H0,7HUAVG = ,F10.5)
  210 FORMAT (1H0,6HRO  = ,F6.4)
  211 FORMAT (1H0,4HB=  ,F10.8)
  212 FORMAT (1H0,6HRE =  ,F10.2)
  213 FORMAT (1H0,5HBM=  ,F10.8)
  220 FORMAT (1H0,22HKINEMATIC VISCOSITY = ,F10.8)
  230 FORMAT (1H0,4HK = ,F6.4)
  240 FORMAT (1X ,8HAPLUS = ,F5.1,7X,5HBM = ,F6.4,7X,4HB = ,F6.4,7X,5HUM
     * = ,F6.4)
  250 FORMAT (1H0,7HUTAU = ,F6.4)
  260 FORMAT (1H1,5X,1HX,10X,4HX*RO,9X,5HYPLUS,16X,6HU/UCEN,13X,9HEDDY D
     *IFF,14X,5HUPLUS,17X,1HT)
  270 FORMAT(1H0,23HTHERMAL CONDUCTIVITY = ,F6.4)
  280 FORMAT(1H0,17HPRANDTL NUMBER = ,F6.2)
  290 FORMAT(1H0,23HHEAT TRANSFER COEFF. = , F7.2)
  300 FORMAT(1H0,2X,F6.4,7X,F6.4,7X,F8.3,14X,F6.4,14X,F7.3,13X,F9.4,11X,
     $F8.3)
  310 FORMAT(1H0,17HNUSSELT NUMBER = , F7.3)
  320 FORMAT(1H0,17HSTANTON NUMBER = , F9.7)
  321  FORMAT(/1X,'JH = ',E12.5,/)
    3 FORMAT(1H1)
 1000 STOP
      END
```

VITA

Hyung Kee Yoon

Candidate for the Degree of

Doctor of Philosophy

Thesis: AN EXPERIMENTAL AND ANALYTICAL STUDY OF HEAT TRANSFER TO POLYMER SOLUTIONS IN TURBULENT PIPE FLOWS UNDER CONSTANT WALL HEAT FLUX.

Major Field: Mechanical Engineering

Biographical:

Personal Data: Born in Hampyeong, Korea, March 15, 1954, the son of Mr. and Mrs. In Shik Yoon.

Education: Graduated from Sung Nam High School, Seoul, Korea, in February, 1972; received the Bachelor of Engineering degree in Mechanical Engineering from Korea University in February, 1980; received the Master of Science degree in Mechanical Engineering from Oklahoma State University in July, 1982; completed the requirements for the Doctor of Philosophy degree at Oklahoma State University in December, 1986.

Professional Experience: Graduate Research Assistant, School of Mechanical and Aerospace Engineering, Oklahoma State University, 1981-1982; Graduate Research Associate, School of Mechanical and Aerospace Engineering, Oklahoma State University, 1983-1986.